https://doi.org/10.1016/j.geomorph.2021.108066

Geomorphology

Holocene eolian dunes in the National and Natural Parks of Doñana (SW Iberia): Mapping, Geomorphology, Genesis and Chronology.

--Manuscript Draft--

Manuscript Number:	GEOMOR-10516
Article Type:	Research Paper
Keywords:	Geomorphological analysis; Coastal dunes; Holocene Chronology; Guadalquivir Basin- Spain
Corresponding Author:	A.M. Martinez-Graña, Dr. University of Salamanca Salamanca, SPAIN
First Author:	J.L. Goy, Dr.
Order of Authors:	J.L. Goy, Dr.
	C. Zazo, Dr.
	C.J. Dabrio, Dr.
	A.M. Martinez-Graña, Dr.
	J. Lario, Dr.
	F. Borja, Dr.
	T. Bardají, Dr.
	C. Borja, Dr.
	F. Díaz del Olmo, Dr.
Abstract:	The dune fields of the National and Natural Park of Doñana Dunes are considered one of the most outstanding dune fields in Western Europe. They are located at the west margin of the Guadalquivir river estuary. The accumulation of aeolian, and in less proportion marine and fluviatile, sands partly block the communication with the Gulf of Cadiz, in the Atlantic Ocean. The sand units form a large oval dome, the “Abalario Dome” which connects with the large Doñana Spit Bar where dune systems accumulated as well, coeval with the spit growth. The aim of this paper is to map, date and set a robust chronological sequence, and describe these Holocene Dune Systems paying special attention to the dune types present and genesis related to the paleo winds blowing at the time of accumulation, and degree of activity past in recent times. The most frequent dune morphologies are parabolic or transverse. The degree of activity was classified as stable, semi-stable and active. Most stable dunes concentrate on the Abalario Dome, whereas active dunes occur mainly on the Doñana spit bar. Relative chronology was erected from the superposition of dune Systems and Subsystems deduced from photogeology coupled with field surveys, orthophotos, and oblique and 3D images. Sampling and radiogenic dating (Optically Stimulated Luminescence-OSL) allowed to assign “numeric” ages to the aeolian units. Eight dune Systems have been defined: Systems I to VII, plus the CS, which is a lateral equivalent of part of SIV, V and VI The discussion, presented as a chronological synthetic chart, compares the dune Systems of Doñana with other examples in the Iberian Peninsula and southwestern France (Aquitaine) and allows to correlate the genesis of dunes with arid climatic periods and events (warm and cold), thus refining the deduced chronology. Additional help came from superposition of dunes on the actively prograding Doñana spit bar. As a conclusion, besides the much refined maps, this paper offers the ages assigned to the Holocene dune Systems and Subsystems. System I, age 11.1 to 9.5 ky BP, perhaps extending to 8.5 ky BP. System II, 8.2 to 6.1 ky BP. System III, 5.9 to 2.6 ky BP. System IV, 2.6 to 1.6 ky BP. System V, 1.6 to 1.3 ky BP. System VI, 1.2 to 0.7 ky BP. System VII, 0.7 to 0.15 ky BP. The age of the Complex System is 2.2 to 0.15 ky BP. Dune System were accumulated with two cyclicities: millennial for the older, stable, Systems and centennial for the younger, semi-stable and active ones. The origin of the

Highlights

- Geomorphological characterization of the aeolian dunes of Doñana Natural Park and surroundings
- Geomorphological mapping of Holocene systems, subsystems and dune units
- Correlation with similar deposits and arid events in Iberian Peninsula
- Chronology of the Holocene dune subsystems and significant cyclicities
- Neotectonic origin of the complex system of El Asperillo and correlation with the Holocene dune systems

Holocene eolian dunes in the National and Natural Parks of Doñana (SW Iberia): Mapping, Geomorphology, Genesis and Chronology.

J. L. Goy [a], C. Zazo[b], C. J. Dabrio[c], A.M. Martínez-Graña[a,*], J. Lario[d], F. Borja[e], T. Bardají[f], C. Borja[g], F. Díaz del Olmo[h]

[a] Departamento de Geología, Universidad de Salamanca, 37008, Salamanca, Spain.
[b] Departamento de Geología, Museo Nacional de Ciencias Naturales (CSIC), 28006, Madrid, Spain.
[c, *] Departamento de Geomorfología, Estratigrafía y Paleontología, Universidad Complutense, 28040, Madrid, Spain.
[d] Departamento de Ciencias Analíticas, UNED, 28040, Madrid, Spain.
[e] Departamento de Historia, Geografía y Antropología. Facultad de Humanidades. Universidad de Huelva, 21007, Huelva, Spain.
[f] Departamento de Geología, Geografía y Medio Ambiente, Universidad de Alcalá, 28871, Alcalá de Henares, Spain.
[g, h] Departamento de Geografía Física y A.G.R. Facultad de Geografía e Historia. Universidad de Sevilla. 41004 Sevilla, Spain.

* Corresponding author. Tel: +34 923 294496; Fax: +34 923 294514.
E-mail address: amgranna@usal.es (Antonio Martínez-Graña)

Abstract.

The dune fields of the National and Natural Park of Doñana Dunes are considered one of the most outstanding dune fields in Western Europe. They are located at the west margin of the Guadalquivir river estuary. The accumulation of aeolian, and in less proportion marine and fluviatile, sands partly block the communication with the Gulf of Cadiz, in the Atlantic Ocean. The sand units form a large oval dome, the "Abalario Dome" which connects with the large Doñana Spit Bar where dune systems accumulated as well, coeval with the spit growth.

The aim of this paper is to map, date and set a robust chronological sequence, and describe these Holocene Dune Systems paying special attention to the dune types present and genesis related to the paleo winds blowing at the time of accumulation, and degree of activity past in recent times. The most frequent dune morphologies are parabolic or transverse. The degree of activity was classified as stable, semi-stable and active. Most stable dunes concentrate on the Abalario Dome, whereas active dunes

occur mainly on the Doñana spit bar. Relative chronology was erected from the superposition of dune Systems and Subsystems deduced from photogeology coupled with field surveys, orthophotos, and oblique and 3D images. Sampling and radiogenic dating (Optically Stimulated Luminescence-OSL) allowed to assign “numeric” ages to the aeolian units. Eight dune Systems have been defined: Systems I to VII, plus the CS, which is a lateral equivalent of part of SIV, V and VI

The discussion, presented as a chronological synthetic chart, compares the dune Systems of Doñana with other examples in the Iberian Peninsula and southwestern France (Aquitaine) and allows to correlate the genesis of dunes with arid climatic periods and events (warm and cold), thus refining the deduced chronology. Additional help came from superposition of dunes on the actively prograding Doñana spit bar.

As a conclusion, besides the much refined maps, this paper offers the ages assigned to the Holocene dune Systems and Subsystems. System I, age 11.1 to 9.5 ky BP, perhaps extending to 8.5 ky BP. System II, 8.2 to 6.1 ky BP. System III, 5.9 to 2.6 ky BP. System IV, 2.6 to 1.6 ky BP. System V, 1.6 to 1.3 ky BP. System VI, 1.2 to 0.7 ky BP. System VII, 0.7 to 0.15 ky BP. The age of the Complex System is 2.2 to 0.15 ky BP.

Dune System were accumulated with two cyclicities: millennial for the older, stable, Systems and centennial for the younger, semi-stable and active ones. The origin of the Complex Systems is related to activity of Mazagón and Torre del Loro faults caused by regional seismic activity.

Keywords: Geomorphological analysis, Coastal dunes, Holocene, Chronology, Guadalquivir Basin, Spain

Holocene eolian dunes in the National and Natural Parks of Doñana (SW Iberia): Mapping, Geomorphology, Genesis and Chronology.

J. L. Goy [a], C. Zazo[b], C. J. Dabrio[c], A.M. Martínez-Graña[a,*], J. Lario[d], F. Borja[e], T. Bardají[f], C. Borja[g], F. Díaz del Olmo[h]

[a] Departamento de Geología, Universidad de Salamanca, 37008, Salamanca, Spain.
[b] Departamento de Geología, Museo Nacional de Ciencias Naturales (CSIC), 28006, Madrid, Spain.
[c, *] Departamento de Geomorfología, Estratigrafía y Paleontología, Universidad Complutense, 28040, Madrid, Spain.
[d] Departamento de Ciencias Analíticas, UNED, 28040, Madrid, Spain.
[e] Departamento de Historia, Geografía y Antropología. Facultad de Humanidades. Universidad de Huelva, 21007, Huelva, Spain.
[f] Departamento de Geología, Geografía y Medio Ambiente, Universidad de Alcalá, 28871, Alcalá de Henares, Spain.
[g, h] Departamento de Geografía Física y A.G.R. Facultad de Geografía e Historia. Universidad de Sevilla. 41004 Sevilla, Spain.

* Corresponding author. Tel: +34 923 294496; Fax: +34 923 294514.
E-mail address: amgranna@usal.es (Antonio Martínez-Graña)

Abstract.

The dune fields of the National and Natural Park of Doñana Dunes are considered one of the most outstanding dune fields in Western Europe. They are located at the west margin of the Guadalquivir river estuary. The accumulation of aeolian, and in less proportion marine and fluviatile, sands partly block the communication with the Gulf of Cadiz, in the Atlantic Ocean. The sand units form a large oval dome, the "Abalario Dome" which connects with the large Doñana Spit Bar where dune systems accumulated as well, coeval with the spit growth.

The aim of this paper is to map, date and set a robust chronological sequence, and describe these Holocene Dune Systems paying special attention to the dune types present and genesis related to the paleo winds blowing at the time of accumulation, and degree of activity past in recent times. The most frequent dune morphologies are parabolic or transverse. The degree of activity was classified as stable, semi-stable and active. Most stable dunes concentrate on the Abalario Dome, whereas active dunes

occur mainly on the Doñana spit bar. Relative chronology was erected from the superposition of dune Systems and Subsystems deduced from photogeology coupled with field surveys, orthophotos, and oblique and 3D images. Sampling and radiogenic dating (Optically Stimulated Luminescence-OSL) allowed to assign "numeric" ages to the aeolian units. Eight dune Systems have been defined: Systems I to VII, plus the CS, which is a lateral equivalent of part of SIV, V and VI

The discussion, presented as a chronological synthetic chart, compares the dune Systems of Doñana with other examples in the Iberian Peninsula and southwestern France (Aquitaine) and allows to correlate the genesis of dunes with arid climatic periods and events (warm and cold), thus refining the deduced chronology. Additional help came from superposition of dunes on the actively prograding Doñana spit bar.

As a conclusion, besides the much refined maps, this paper offers the ages assigned to the Holocene dune Systems and Subsystems. System I, age 11.1 to 9.5 ky BP, perhaps extending to 8.5 ky BP. System II, 8.2 to 6.1 ky BP. System III, 5.9 to 2.6 ky BP. System IV, 2.6 to 1.6 ky BP. System V, 1.6 to 1.3 ky BP. System VI, 1.2 to 0.7 ky BP. System VII, 0.7 to 0.15 ky BP. The age of the Complex System is 2.2 to 0.15 ky BP.

Dune System were accumulated with two cyclicities: millennial for the older, stable, Systems and centennial for the younger, semi-stable and active ones. The origin of the Complex Systems is related to activity of Mazagón and Torre del Loro faults caused by regional seismic activity.

Keywords: Geomorphological analysis, Coastal dunes, Holocene, Chronology, Guadalquivir Basin, Spain.

1. Introduction

Studies of coastal processes and their evolution usually face the problem of stablishing a precise chronology of depositional events, an issue particularly difficult in the case of the coastal aeolian systems. In the study case addressed in this paper, the aeolian complex includes two natural Spaces. a) The Doñana National Park,

a Biosphere Reserve (UNESCO 1980) and World Heritage (UNESCO 1994), and b) the littoral fringe of Doñana Natural Park.

The dune complex occupies an area of 420 square kilometers, approx. 62 km in length by 16 km maximum width, (Fig. 1), reaching elevations of 106 m near the sea cliff. This, and Les Landes (Gascogne-Aquitaine, France), are the largest aeolian systems in Western Europe. The area has attracted numerous scientists since the middle 1970s who generated a copious flow of papers. Geomorphological/neotectonic analysis of sedimentary units coupled with isotopic and luminescence dating allowed reconstructing the general evolution of paleoenvironments during the Pleistocene epoch, as most of sampling and analyses were carried out along the wall of the coastal cliff (Zazo et al., 2005).

According to this, the main aim of this paper is to present the space-temporal evolution of the Holocene dune field systems that, as top-cliff dunes, extend several kilometers inland. Our goal is to recognize the main phases of sedimentary activity and erect a robust hierarchical stratigraphic framework closely attached to climate and the degree of “tectonic activity” of the Abalario Dome (Fig. 1) upon which the aeolian sand unit rests.

We intended to separate the events of sedimentary activity at a millennial/sub-millennial scale between the mouths of the Odiel-Tinto and Guadalquivir rivers (Fig. 1). This required to elaborate a thorough geomorphological cartography which begun with detail photointerpretation with field surveys prior any sampling, to implement GIS and, finally, build a DTM. An essential addition was to obtain a reliable chronostratigraphy by refining the ages of some of the units distinguished by Zazo et al. (2005) with new surveys. A crucial point is that, besides refining the Pleistocene-Holocene limit, the aim of this research is to analyze the degree of “tectonic stability” of the Abalario Dome. This new focus required resampling and dating by means of luminescence, radiocarbon, lithic industries and archaeological data. Last, but not least, the study required a careful survey of the close inter-relation between aeolian and beach-barriers deposits.

2. Geological and geomorphological setting

The study area is placed in SW Iberian Peninsula at the mouth of the Guadalquivir River, in the Cenozoic Basin of Guadalquivir, the northern foreland basin of the Betic Cordillera, the passive margin of which is the Iberian Massif located to the north. The Guadalquivir basin was progressively filled with marine sediments of Miocene and Pliocene ages and, towards the Pleistocene, it was reduced to an estuary where the Guadalquivir River debouched. An aeolian dune complex accumulated at the distal seaward part of the estuary, resting upon the Holocene estuarine and Doñana spit bar to shallow-marine deposits

The mapped area includes two realms: the Abalario dome and the Doñana spit bar being limited by the Rocina creek (East), the present coastline (West), Mazagón (North) and the Guadalquivir River (South-east), (Fig. 1). Here, dune systems reach variable elevations, with a maximum at 106 m near the Asperillo coast. The drainage pattern is asymmetrical, with plenty, relatively long, creeks in the eastern side and few, short, creeks in the western side. For this reason, the dune systems in the eastern flank are more degraded. Between the localities of Mazagón and Matalascañas, the coastal side of the dome is a 28 km-long marine cliff, 16 to 20 m high (Fig. 2).

Numerous gravitational faults affect the estuary, largely controlling the accumulation of dune systems, allowing Zazo et al. (2005) to separate the coastal cliff in two paleogeographical realms: an uplifted one to the NW (from Mazagón to Torre del Loro) and a subsiding one to the SE (between Torre del Loro and Matalascañas).

Further neotectonic activity controls not only the general morphology but also the repartition of dune systems: the area is limited by extensional Quaternary faults running NE-SW, NW-SE and E-W, which delineate the El Abalario Dome (EAD) and the Doñana spit bar (DS). Some of these faults generated gravitational sliding (e.g. TLF: Torre del Loro Fault (Fig. 1). (Flores, 1993; Goy et al, 1994, 1996; Rodríguez-Ramírez et al., 2012, 2014)

In previous papers dealing with the aeolian deposits, most of the research was focused on the Pleistocene deposits exposed along the sea cliff wall. In contrast, the top-cliff dunes received only a marginal attention (Dabrio et al., 1996; Zazo et al., 1999, Zazo et al., 2005, and Zazo et al., 2008).

As one of the main aims of this paper is to study the Holocene aeolian systems and their space-temporal distribution, we refer below only to papers related to cartographic representations.

Geology: Geological Maps of Spain (MAGNA) scaled 1:50,000 Sheets of Moguer (Pastor and Zazo, 1976), El Abalario (Pastor, Leyva and Zazo, 1976), El Rocío (Leyva, Pastor and Goy, 1976) and Palacio de Doñana (Leyva, Pastor, Zazo and Goy, 1975). The dune systems are represented in a general way, with the main interest in sedimentology.

Physiography: "Mapa Fisiográfico del litoral atlántico de Andalucía (1:50,000): Punta Umbría-Matalascañas and Matalascañas-Chipiona" (Vanney and Menanteau, 1985, with geology by Zazo and Goy). Here landforms are mapped according to the various systems that generated them: submarine and coastal, aeolian, humid and terrestrial systems.

Ecology: "Mapa Ecológico de Doñana" scaled 1:40,000 (Montes et al., 1998) focused on ecotopes with a geomorphological base, including the dune systems. "Map of the marsh complex of Doñana" (Ruiz-Labourdette et al., 2004), with representation of aeolian, coastal and marsh ecosystems.

Borja (1992) and Borja and Díaz del Olmo (1996) presented a cartographic scheme including superposition of dunes, wind directions, sand sedimentology and approximate ages. They named the accumulations of sand as Aeolian Sheets (Mantos Eólicos), distinguishing five of such sand sheets. The oldest accumulation is the Lower Aeolian Sheet (LAS), a bimodal grainsized unit, with approximate age 15-14 Ka BP, and paleo-winds from WNW. The overlying Humid High Aeolian Sand sheet (HASS) consists of parabolic and transverse dunes of well sorted unimodal sand deposited around 11 ka BP under winds from the SW. The overlying Dry High Aeolian Sand Sheet (DHASS) include dunes of the same type deposited under winds from the W between 11

and 5.4 ka BP. Resting on these sediments there are Neolithic-Chalcolithic remains/artifacts. Above these, the Semi-stable Dunes Aeolian Sand Sheet of (SSD) with parabolic dunes accumulated by winds from the WSW in an estimated time span from late Middle Age to late 18th Century. The younger aeolian unit includes the active transverse dunes (AD) accumulated by SW winds in the two last centuries. These dunes are semi-active in El Asperillo, because they are disconnected from the beach and have been reforested in recent times.

Geomorphology: Zazo (1980) and Zazo et al., (1981), based on the cartography made (1:50,000) on the southern part of the study zone, differentiate five large dune systems: 1st: Aeolian sheet with degraded parabolic dunes; 2nd Barchans, at the beginning of the spit bar; 3rd: Parabolic dunes at the base of El Asperillo system and W of Palacio de Doñana; 4th: Transverse dunes, closing the barrier of the paleocoast between Torre del Loro and Matalascañas; and 5th: Transverse and longitudinal mobile dunes, over the littoral spit bar.

A 1:50.000 map accompanied the monography “Geomorfología del Parque Nacional de Doñana y su entorno” (Rodríguez Ramírez, 1998). This is the most significant analysis of the dune systems in Doñana, including the dunes of the Médano Littoral. Besides the structural, slope, fluvial and fluvio-littoral morphologies, the author distinguished five dune systems, called I, II, III, IV, and V, in stratigraphically ascending order.

Rodríguez-Vidal et al. (2014) used the cartography by Rodríguez Ramírez (1998) and correlated the deposits described by him with the seven dune units (U1 to U7) distinguished and dated by Zazo et al. (2005) in the downthrown block of the TLF. These authors distinguished five aeolian Dune Systems (I to V):

System I: parabolic dunes, winds from WSW, aged 31 to 18 ka BP, correlated with U-2.

System II: elongated parabolic dunes; winds from the W, age 14-11 ka, correlated with U-3.

System III, parabolic dunes, winds from WSW, age 11-5.4 ka, correlated with U-4.

148 System IV: active parabolic dunes, winds from the SW. Chronology based on archaeological remains: late
149 Neolithic-Chalcolithic-Roman (age 2.7 ka cal BP) and correlated this system with U-6. These authors include
150 in this same system, younger parabolic dunes coeval of the watch towers built in late 16th to early 17th
151 centuries.

152 System V: migrating transverse dunes, winds from the SW. Early 17th Century to present.

153

154 **3. Materials and methods**

155 The elaboration of geomorphological and geological maps of the Holocene dune systems required working
156 at a variety of scales. (Fig. 2 and 3)

157

158 Photointerpretation of the whole study area used the aerial photographs scaled ~1:33,000 (Flight 1956,
159 Ministry of the Army) with the help of the national survey scaled 1:18.000 (1980-1986) for specific areas.
160 Orthophotographs of the National Plan for Aerial Orthophotography (PNOA) of the National Geographic
161 Institute (IGN), shot in 2002, 2007 and 2009 (resolution 25 cm/pixel), scaled 1:10.000 were used for
162 comparison with the older 1956 aerial photographs. Comparison of the orthophotographs of 2009 and the
163 1956 flight with geo-positioning of the various advance fronts revealed changes of the dunes in the last 53
164 years, and the activity degree of the dune systems was evaluated (Fig. 4). These interpretations were checked
165 along several fieldwork surveys both for mapping and sampling for dating. This generated a vector layer of
166 points based on GPS data.

167 Topographic maps in raster format scaled 1:50.000 (MTN50) and 1:25.000 (MTN25), the last one
168 georeferenced. The geological base was the Plan Magna geological map, scaled 1:50.000, sheets: Moguer
169 (1000). El Abalario (1017). El Rocío (1018), Palacio de Doñana (1033) and Sanlúcar de Barrameda (1047). In
170 addition the geological map of the GEODE Project of the Geological and Mining Institute of Spain (IGME). The

resulting map was reduced to a 1:100,000 scale for a working document and, later, it was reduced to publication format (approx. 1:250.000).

The virtual 3D analysis was processed using the ArcScene and ArcGlobe of the GIS (ArcGis v10.8), to obtain views of the terrain or the virtual scenes from several orientations, such as in Figures 4 and 5.

The digital elevation model (DEM) based on the Digital Terrain Model (DTM) with 5m resolution or pixel size obtained with LIDAR data, improving the triangle irregular networks (TIN), allowed to draw contour curves at an appropriate scale (1.5 and 10 m intervals). Using scrips of flow accumulation with GIS techniques, the network of drainage pattern was reconstructed.

GIS techniques allowed calculations of the areas occupied by every dune system and subsystem, distances, profiles, volumes, advances of dunes, and generation of models of evolution of Holocene dunes.

In this study eight aeolian systems (SI to SVII, plus a Complex System, CS) have been recognized (Fig. 2) on the basis of prevailing wind directions at the time of accumulation, morphological type, degree of stability and relative stratigraphic age, taking into account the inter-relation between systems, their relationships with the Pleistocene paleo-dunes exposed in the cliff, and, in some cases, the position of the dune systems and beach ridges in the Doñana spit, at the right, western, margin of the Guadalquivir river mouth.

The chronology of the system CS, placed along the littoral from Torre del Loro to Torre de la Higuera, is more difficult to stablish because it is not connected to the other systems.

Dune systems (recognized by different colours), were subdivided in subsystems (SS) (different shades of colours). Subsystems are composed of dune units, and have been conveniently separated with dotted lines in the map (Figs. 2 and 3).

All these divisions and subdivisions are based upon the following criteria (Fig. 6): 1. Morphological type of dunes (transverse, parallel, etc.); 2. Position and geometry of dune systems and subsystems (basal parabolic,

193 transverse, imbricate, etc.); 3. Paleo wind directions (measured in degrees); 4. Aeolian activity; 5. Size of dune
194 units and their progression (migration) fronts; 6. Degree of conservation; 7. Relations between systems,
195 subsystems and dune units (deduced from air photographs, and 2D and 3D images, (Figs. 4 and 5). Using
196 these criteria we deduced a first relative chronology that narrowed the areas to be sampled for laboratory
197 techniques such as optically stimulated luminescence (OSL), aimed at obtaining a more precise chronology
198 (Table I, Figs. 1 and 6). Aeolian activity was deduced from comparison of air photographs taken in 1956 and
199 2009, and additional criteria, viz. antiquity, position of water table, dune morphology, and so on. Three main
200 groups of dunes were separated: stable (no changes observed), semi-active (small, metric-sized
201 displacements) and active (decametric migrations).

202 The first resulting map (Fig. 2) presents the Holocene aeolian dune systems with a geomorphological
203 emphasis, indicated by different colours (I to VII, plus the CS, Complex System) and superimposed
204 geomorphological symbols. The second resulting map (Fig. 3) includes the Holocene subsystems that are
205 represented with a more chronological emphasis, as indicated by shades in the colours (increasing darkness
206 with older relative age). A total of 25 subsystems have been described for the general sequence, plus 7 for
207 the CS. This implies, obviously, a proposal of correlation between the CS and the other aeolian units.

208 **4. Results**

209 *4.1. Pleistocene dune systems of Doñana*

210 They crop out in the sea cliff between the localities of Mazagón and Matalascañas, forming the substratum
211 of the Holocene dunes. They have been repeatedly studied but, here, we refer only to the paper by Zazo et
212 al. (2005) because new radiogenic dating (OSL) and archaeological findings (lithic workshops) allow to refine
213 the limits separating the Pleistocene and Holocene dune sequences and also the activity of the gravitational
214 Torre del Loro Fault (TLF), both of which are closely related to the cartography of aeolian systems and their
215 distribution, and the succession of depositional events after the late Pleistocene. The upthrown (Poblado
216 Forestal) and downthrown (south of Torre del Loro) blocks of the TLF (Fig 7) were resampled and dated.

Downthrown block: In ascending order, the lower part of the cliff (0.5 m above the high tide mark) has been dated as ~82 ky BP. Previous data from the top part of this unit (~50 ky BP and 32 ky BP) point to a U-2 age for this unit. Just below a super-surface marked by a relatively-thick layer rich in organic matter aged 21 ky BP (Fig. 7), a splinter with pseudolevallois shapes was found, the morphotechnological characteristics of which are compatible with the typical middle Pleistocene cultures. The organic-rich layer marks the limit between U-2 and U-3.

Unit 3 includes two erosional surfaces enriched in iron, including the occurrence of goethite, the oldest of which (SsFe 1 in Fig. 7) is dated between 16 and 13 ky BP.

The last, uppermost, paleodune in the section (~9.9 ky BP in age) corresponds to the System I in this paper, and it is topped by an mud-cracked, organic matter-rich layer. The sequence in the cliff ends with a degraded layer rich in fragments of ferralithic crust, which corresponds to the erosional super-surface (SsFe2) at the top of Unit 3 of Zazo et al. (2005).

Upthrown block: New sampling near the Poblado Forestal of Mazagón (Fig. 7) was aimed to refine the age of the top-cliff supersurface SsFe2, on top of which layers with lithic workshops of a post-Paleolithic context, mode 4, are found. The thickness of the ferralithic crust associated to this SsFe is 1.5 m, and the sample was taken 0.30 m below the top. The supersurface is covered by non-cemented aeolian dunes with OSL age 5.5 ky BP. In conclusion, and given de age of underlying S.I Unit, the age of the top-cliff supersurface SsFe2 is bracketed between 9.5 and 5.5 ky BP.

4.2. Holocene dune systems

The Holocene systems are mainly made up of transverse and parabolic dunes (Fig.2) accumulated in the last 11.7 ky. Eight of them have been defined: Systems I to VII, plus the CS, which is a lateral equivalent of part of SIV, V and VI. The big accumulation of sand in CS reaches locally 106 m in elevation. The restricted, narrow area that occupies this Complex System results from large scale gravitational sliding related to the uplift of El

240 Abalario Dome; in fact, the conspicuous tectonic lineaments visible near the coast are slide scars. Sliding
241 produced a void which was filled by the successive dune units forming the CS (Fig.1)

242 To interpret morphologically the parabolic dunes, we consider that they need an certain supply of sand,
243 moderate to strong unidirectional winds and moderate vegetal cover. With increased sand supply, or reduced
244 vegetal cover, parabolic dunes tend to evolve into the more mobile, transverse dunes. On the other hand,
245 parabolic dunes can derive from transverse (stabilized or not), coastal foredunes, blowouts, transgressive
246 dunes, etc. (Yan and Bear, 2015).

247 In some cases (Ardon et al., 2009) transverse dunes can evolve into parabolic, with not well-defined drag
248 arms; this is rather usual in the study area. The occurrence of blowouts in the highest parts of transverse
249 dunes is thought to indicate a deficit of sand (Pusty, 1988). This happens in the CS because the sea cliff
250 separates the dunes from the active beaches nearby which supply sand. For this reason, parabolic dunes
251 occur in the lee of system SS-C7 (Fig. 3). This is also the cause of the relatively high variability of dune
252 morphologies (Fig. 6).

253 *4.2.1. Stable dune systems*

254 System I. It crops out in the north and northeast part of the study area. The main feature is the absence of
255 dune morphologies; for which reason it was named “aeolian sheet” by Leyva et al. (1975). Sand was supplied
256 by the Early Pleistocene Bonares Sands, a fluvial-deltaic deposit at the mouth of the Odiel and Tinto rivers,
257 that crop-out not far to the north, and transported by NW winds and former longshore drift. Two dune
258 subsystems (SS-I1, the older, and SS-I2, the younger) have been differentiated within this system. The first
259 one (SS-I1) occupies the largest area and it does not show any clear dune morphology because it is
260 crisscrossed by many creeks generated by the uplift of the Abalario Dome, and floods in these creeks
261 destroyed the dune fronts (Fig. 1 and 2). However, the distribution of some outcrops suggest that this
262 subsystem accumulated under winds blowing from the SW (Sheet 1 b).

263 The Subsystem I2 (SS-I2) is present only in the northern sector. It includes relatively well-preserved parabolic
264 dunes accumulated under NW winds and climbing over the degraded dunes of SS-I1 (Figs. 2 and 3, Sheet 1a
265 and b).

266 System II. This system partly covers S-I from the south, with a well-preserved dune front (Fig. 2, Sheet 1 a and
267 b). According with the prevailing winds that generated them (ranging from SW to NW), up to 11 dune units
268 have been distinguished and grouped into four subsystems (Fig. 3 and 6), very easy to separate thanks to
269 obvious superposition and neat, well exposed advance fronts.

270 SS-II1 and SS-II2 directly overlap SS-I1 and SS-I2 (Sheet 1a and b) while the younger subsystems (SS-II3 and
271 SS-II4) cover the older ones, with neat advance fronts and significant changes in wind directions (Figs. 2, 3
272 and 6).

273 System III. It is the most significant of the stable systems owing to its location and state of preservation. It
274 crops out in the central and north-western parts of the study area (Figs. 1, 2 and 3). In the central part it steps
275 on System II with two well marked, well preserved dune fronts (Fig. 2).

276 Five subsystems have been differentiated according to directions of prevailing winds and the superposition
277 of the transverse (with a slight parabolic component) dune fronts (Figs. 2, 3 and 6; Sheet 1c and 1d).

278 In the central zone (El Acebuche area, Figs. 2 and 3), dunes of SS-III1, migrating under winds from the W, step
279 on SS-II1 and SS-II2, that accumulated under winds from the SW. No direct relations between SS-III1 and SS-
280 II4 were observed in any of the two sectors, but there is a significant difference of ages measured in both
281 subsystems: SS-II4, sample 12, age 6966 y BP, SS-III1, sample 11, age 5848 y BP (Table I).

282 SS-III2, with winds from the SW (dune migration towards N60-70˚E), overlies SS-III1 in the north and NW of
283 Laguna de Santa Olalla (Fig.2 and Fig. 3), while SS-III3 steps on SS-III2 east of Matalascañas, under winds from
284 the west (dune migration towards N95-100˚E). SS-III4 is distinguished by a new change in wind direction,
285 from the SW (dune migration towards N75˚E), and SS-III5 outcrops only in the northern zone resting on SS-

III4 and SS-III3, with variable wind directions from SW (migration towards N45˚E) to the NW (migration to N135˚E), what points to rapid changes in wind directions or seasonal winds (Fig. 8).

4.2.2. Semistable dune systems

System IV. It crops only in the area occupied by the Doñana Spit (DS), from the south of Palacio de Doñana to Lucio del Membrillo where it covers partially the sectors 1 and 2 of the spit, which are separated by the tidal channel of Vetacarrizosa and limited to the south by the tidal channel of Vetalengua (Figs. 2 and 3).

A most relevant feature of System IV is that it is partly stabilized. It consists of three subsystems characterized by their different dune morphology (Fig. 6) and their position on top of the Doñana spit, as long as wind directions are quite constant in the three subsystems.

SS-IV1 rests on the older visible part of the Doñana spit (sector 1), south of Laguna de Santa Olalla (Fig. 3). Its morphology is a rather flat sedimentary body made up of alternating clear and darker sandy strips which curve convexly towards the direction of the prevailing winds. García Novo et al. (1975) referred to these strips as “worms” and related their origin to fixation of the rear part of dune fronts by vegetation (Sheet 1c, 1e and Sheet 2b), what evidences a very limited migration during the studied period. The resemblance of this system of stripes with those of SS-V1 (irregular transverse to barchanoid) allows interpreting them as similar systems that do no preserve the dune bodies (Sheet 3 a1 and a2).

SS-IV2 crops out to the NW of Lucio del Membrillo, on top of sector 2 of the Doñana spit (Fig.3), resting upon an interdune depression (Corral de la Punta del Caño). It consists of rather low parabolic dunes with little migration (Sheet 1f).

SS-IV3 is made up of transverse-parabolic dunes and covers the former SS-IV2 (Sheet 1f, Sheet 2a).

4.2.3. Active dune systems

System V. It is the first, older active dune system. It lays on top of sector 2 of the DS marked by large, extensive transverse dune units, with various morphologies (Figs. 2 and 6). This system overlies System IV to the south of Laguna de Santa Olalla and near Cerro del Trigo; it is overlain by the younger System VI north and south of the DS, (Fig. 3). It is differentiated from the older System IV because an increased mobility and larger size of dune units. Three subsystems (SS) have been distinguished: SS-V1 with transverse, barchanoid dunes having lobate fronts that overly the oldest zone of the sector 2 of the dune sheet (DS) (Sheets 2a and 3a2). SS-V2 consists of large transverse dunes that reach up to 35m in elevation and 3x5 km in plant (Cerro de los Ánsares). It is followed in the southern part by a large interdune through, up to 1.5 km wide (Fig. 3, Sheet 2a) separating it from SS-V3.

In general, the mobility of these large dunes is smaller in the central parts as compared with the margins. Vallejo and García (2013) estimated a displacement of 2 m/a in the last half century.

SS-V3 includes three parabolic, transverse dune units separated in a north-south direction. The oldest one develops in the central sector, hence located more to the inner part of sector 2 of the Doñana spit, with a well-developed advance front covering the previous SS (Fig. 3, Sheet 2a).

System VI. Includes the most characteristic parabolic dunes in the studied area, with various morphologies (typical parabolic, hackle, cliff, and asymmetrical, (Figs. 2, 3 and 6). These are active dunes that have migrated in the studied timespan. Rates of movement and dune sizes depend on the type of dunes. Six subsystems and fifteen dune units have been identified within this System.

SS-VI1: well preserved, symmetrical parabolic dunes, with arms 1.5 to 2.5 km long. They show a low relief ranging from 5 m (the oldest) to 15 m (the younger ones), and migration rates between 0.7 and 1.5 m/a respectively. They step upon the SS-V3 and SS-IV1 to the south of Laguna de Santa Olalla (Sheet 1c and 1d, Sheet 2b, Sheet 3a1).

330 SS-VI2: hackle parabolic dunes found west of Matalascañas. Dune bodies and arms are narrow, likely owing
331 to a deficit of sediment supply, as far as they accumulated in the transition zone from the retrograding to the
332 prograding areas of the coastline (Fig. 1). The aeolian activity is therefore smaller (migration rates between
333 0.2 and 0.5m/a) than in the former subsystem (Sheet 2c).

334 SS-VI3: located at the northern part of the study area, it is found on top of the present sea-cliff between Torre
335 del Loro and Mazagón; the rest on the stable dunes of Systems II and III, and aeolian sand cover (Fig. 3). This
336 subsystem consists of parabolic dunes that, at present, migrate landwards very slowly, and have their arms
337 cut off by the sea cliff as a consequence of the coastal retreat since the time of accumulation (Sheet 2d).
338 Rates of cliff retreat to the south of Torre de la Higuera have been estimated as 0.7-0.8 m/a, which means a
339 cliff retreat of 700-800 m in the last thousand years (Rodriguez Ramirez et al., 2014, 2019).

340 SS-VI4: it crops out in a small area to the west of Lucio del Membrillo. These are well-preserved barchanoid
341 dunes, quite similar to those of SS-VI.1, that occur sandwiched between SS-VI.3 (below) and SS-VI.5 (above),
342 (Figs. 3, 5, and Sheet 2e).

343 SS-VI5: parabolic dunes with better-developed arms and higher elevation and thickness towards the right-
344 hand side (SE). It includes six dune units with decreasing dimensions in stratigraphically ascending order. The
345 relatively larger size of the older dune systems seems to be related to an increased sediment supply in the
346 northern area of the outcrop (Figs. 3, 5, and sheet 2e).

347 System VII. It consists of large, active transverse dunes with several advance fronts separated by interdune
348 troughs (locally referred to as 'corrales'), which accumulated under intense, maintained southwestern winds.
349 Migration rates exceed 200 m for the considered half century time span. Some dunes exhibit a certain
350 parabolic trend (Sheet 2 a, b, c, and e).

351 The dunes of System VII are best developed in the area between Torre de la Higuera and Torre del Zalabar
352 (Figs. 2 and 3), with deflation surfaces and well-marked advance fronts separated by wide interdune troughs.

353 Up to fourteen superposed dune units can be distinguished, with a slight onlap towards the SW. These were
354 grouped into three subsystems, according to variable wind directions, degree of activity, size and
355 superpositions (Figs. 3 and 6, Sheet 2a and e, Sheet 3 a1 and a2).

356 Subsystem SS-VII1 is the most important according to its extension and number of units (6), but also for the
357 mobility (ca 200m in 53 years) and size of the dune units. The first four units are transverse, the fifth one is a
358 small-sized parabolic dune, and the sixth is a transverse dune. The size of the four transverse dune units
359 decrease towards the south. The first of them lays on top of the SS-VI.1 and 2 (Fig 3, Sheet 2b and c) and the
360 youngest upon the barchanoid dunes of SS-VI4 (Sheet 2e). The wide interdune troughs include counter-dunes
361 that look as elongate, narrow, flat-topped, sandy ridges related to the advance of the dune units (Sheet 2a
362 and 3 a.1) over areas of very shallow water table where vegetation partly traps the moving sand.

363 Dunes in this Subsystem migrate actively under strong south-westerly winds which moved the abundant
364 sediment constantly supplied by the Odiel and Tinto river mouths to the beach to be incorporated later to
365 the aeolian dunes, promoting advance rates in the central sector ranging from 2.4 to 3.8 m/y.

366 Subsystem SS-VII2 is similar to the previous one but with less extensive and lower dune units. It consists of
367 four dune units migrating towards N65˚E under winds from WSW (Fig. 6), clearly differentiating it from SS-
368 VII1. It consists of transverse dunes parallel to the dunes of SS-VII1 to which they overly (Sheet 3 a.2) both
369 north and south of Doñana spit (Fig.3). It is best represented to the south of the study area from Torre de
370 Zalabar to the extremity of the spit.

371 To the north of Torre de la Higuera this subsystem bypasses the former and advances downwind of it (Sheet
372 3 e).

373 Subsystem SS-VII3 consists of four dune units that overly the former subsystems. They are smaller than the
374 dune units of SS-VII2 and extend parallel to them all along the prograding sector of the DS, but with migrating
375 direction towards N45˚E (southwestern winds).

376 To the south of DS, the limit with the former subsystem is the dune where the Torre de San Jacinto was built,
377 which means an age around late 16th to early 17th century (De Mora Figueroa, 1981).

378 Complex System (CS) is the most important dune complex of the study area and, consequently, of the Iberian
379 Peninsula littoral. The CS crops out between Torre del Loro (SE from Mazagón) and Torre de la Higuera (NW
380 of Matalascañas) along the erosional sea cliff cut in sediments from the Last Interglacial to the recent
381 Holocene (Zazo et al., 1999, 2005,2011).

382 The CS was first referred to as "coarse sands" (arenas gordas) by Pastor et al. (1976), Vanney and Menanteau
383 (1979),and Vanney et al. (1979). It was also named "stable dunes of the External System", (Rodríguez Vidal
384 et al. (1993), which Borja and Díaz del Olmo (1987, 1994) included in the Aeolian Mantle of Active Dunes
385 (AMAC). Rodríguez Ramírez (1998), on his turn, considered the CS as an active system in the recessing
386 (erosional) sector and included it in his systems IV and V.

387 We consider the CS as a part of the semi-stable (semi-mobile) aeolian dunes owing to their modest migration
388 rates in recent times. It is formed by a vertical stack of partly vegetated dune units (SS-C1 to C7) that, locally
389 (to the SE of El Asperillo), reaches elevations in excess of 100 m (Fig. 2). The system is being reworked at
390 present, as evidenced by numerous blowouts, because it is disconnected from the source area, the beach,
391 fed by the longshore drift. In some localities, to the lee of the complex, the blown sand feeds new dune units
392 (SS-C7) (Sheet 3, b and c). The transverse dunes of subsystems SS-C2 to SS-C6 moved under SW winds with
393 variable directions, and imbricate or step differently in each sector (Fig. 3)

394 The CS steps on fixed sands of Systems II and III (Fig. 2), but it is covered by System VII in both NW and SE
395 extremities of the outcrop (Torre del Loro and Matalascañas respectively, (Figs. 2 and 3).

396 *4.2.4. Chronology*

397 The chronological model is based on 29 OSL samples (Table 1), four of which corresponds to Late
398 Pleistocene dune units outcropping in the Asperillo cliff (Fig. 7), supporting previous chronologies assigned

399 to these aeolian dunes (Zazo et al., 2005), refining their ages and narrowing the age-intervals calculated for
400 the Super-surfaces. One of the samples (sample 20 in Table 1 and Fig. 10A, D09-20 in Fig. 7) gave an age
401 compatible with the Younger Dryas allowing us to mark more precisely the Late Pleistocene – Holocene
402 Boundary (Hb in Fig. 7).

403 The other 25 samples have been plotted (Fig. 9) giving key clues for the Holocene climatic evolution of the
404 area. Most Bond Events coincide with changes in prevailing winds and/or changes in the type of dunes (Fig.
405 6) remarked by changes in successive Systems/Subsystems. The chronology of the dune systems and
406 subsystems accumulated during the Greenlandian, Northgrippian and early Meghalayan (Systems I to III)
407 reveals a millennial cyclicity. In contrast, the more recent dune systems and subsystems (S.IV, V, VI and VII)
408 exhibit a centennial cyclicity. Bond Events BE-5 (8.2ky BP), BE-4 (5.9 ky BP) and BE-1 (1.4 ky BP) have been
409 reported to be the most prominent in the Iberian Peninsula (Cacho et al., 2010). In our case the change
410 between System I and II (coincident with BE-5) is accompanied by a marked change in the direction of
411 prevailing winds (Fig. 6). BE-4 marks the change between System II and III which is the most significant of
412 the stable dune systems. Within system III, BE-3 and BE-2 are represented by changes in wind direction (Fig.
413 6). Finally, BE-1 marks the limit between System V and System VI, with a marked change in type of dune
414 and sand supply.

415

416 **5. Discussion**

417 A general chart has been prepared to present the results of this study and to extend the findings to other
418 parts of Western Europe (Fig.10). The chart compares the aeolian dune sequence of Doñana (Fig.10 A) with
419 aeolian deposits in the Iberian Peninsula and southern France (Fig.10 B) studied by a panoply of authors:
420 Garcia-Hidalgo et al. (2007) in the Duero basin; Bernat and Pérez-González (2005 and 2008), Bernat et al.
421 (2011) in Duero basin and La Mancha; Costas et al. (2012) in south Portugal; Clarke and Rendell (2006) in
422 central and northern Portugal and, finally, Clarke et al. (2002) yielded numerical data about dunes in

Aquitaine (southern France). Figure 10 C includes general papers dealing with Holocene climate changes deduced from lacustrine, estuarine, aeolian, marine and terrestrial (pollen) sedimentary records aimed to separate arid and humid periods, more or less prone to dune accumulation respectively, and to further refine the age of some of the recent subsystems. Remarkable selected papers are: Cacho et al. (2010) for the Iberian Peninsula; Schneider et al. (2016) for the coast of Algarve in southern Portugal; Martín-Puertas et al. (2008) in lake Zoñar (Córdoba, Southern Spain) who proposed a complete climatic sequence, particularly for the last 2000 years; Fletcher et al. (2007) and Fletcher and Zielhofer (2013), in southern Portugal; and, Jalut et al. (2000) for SE Spain and France. Figure 10 D presents the data from the two most significant areas with interconnected spit bar and dune deposits in Spain. In the study area, Zazo et al. (1994) and Borja et al. (1999) cited several aeolian systems (Systems IV, V, VI, and VII) related to the spit bar of Doñana. In the coast of Almería (SE Spain), the most complete and well dated coastal plain of the Iberian Peninsula has been described (12 in Fig. 10 D). The depositional history of these coastal deposits offers valuable information concerning the coastal dynamics, viz. phases of progradation and gaps in the systems related to climatic parameters and aridity vs. humidity.

The Bond Events (BE 1 to 9) (Bond et al., 1997, 2001) included in Fig. 10 A represent rapid (lasting from some decades to a couple of hundred years) oscillations which altered the climatic conditions during the Holocene (last 11.7 ky) with the exception of BE-9 which is older. Important regional differences have been described for most Bond Events (Mayewsky et al., 2004) and, according to Cacho et al. (2010), the most significant ones are BE-5 (8.2 ky BP), BE-4 (5.9 ky BP) and BE-1 (1.4 ky BP).

The sequence studied (Fig. 10 A) starts with the paleodunes outcropping below the SSFe1 in the downthrown block of TLF along the coastal cliff (Fig. 7). The age of the dune immediately overlying this supersurface, is 13.2 ky BP (sample 20 in Table I; Figs. 7, and 10A), thus probably representing the aridity and cooling of the Younger Dryas (YD) caused by a reorganization of the circulation pattern of the North Atlantic (Hughen et al., 2000).

After the YD, the seven Holocene dune systems (SI to SVII, Fig. 10A) have been included in strips with the same colours than in the general map (Fig. 2), separated by void spaces that represent moments of reduced or null aeolian sedimentation. The age of dune systems and subsystems is stablished by our own chronological data (Table I). A good correspondence comes out when comparing our results from Doñana (Fig. 10A) with other dune systems of the Iberian Peninsula and southern France (Fig. 10B), the Holocene climate data of Iberia and southern France (Fig. 10C), and the genetic relationships between spit bars and associated dune systems, both in Atlantic and Mediterranean coasts of Spain (Fig. 10D).

Pre-Holocene dunes. There is good correspondence between our ages (13.2 ky BP, Fig.10A, OL and Sample 20 Table I) and those given for the Duero Basin and La Mancha (13.8 and 12.5 ky BP; see 1 and 2 in Fig. 10B) and South Portugal (12.6 ky BP; see 3 in Fig. 10B) where they attribute them to the Younger Dryas. The same occurs when comparing with the paleoclimate given by Cacho et al. (2010) between 13 and 11,5 ky BP (reference 6 in Fig. 10 C) and by Fletcher et al. (2007) between 12,9 and 11,7 ky BP (reference 7 in Fig. 10C). The cold and arid climate proposed by all these authors for this period fits well with the environmental requirements for the accumulation of these dune systems.

System I. Composed of two subsystems. The older SS-I1 appears very degraded and its dune units not preserving their morphology due to stream erosion (Fig. 2). An age between 11.1 ky BP (Bond Event BE-8) and 10.3 ky BP (BE-7) has been attributed to this system, based both on the age of sample 29 (10.8 ky BP), which is the oldest Holocene dating, and on the age of the next subsystem (SS-I2) (10.1 ky BP; sample 3, Table I). Subsystem SS-I2 crops out near Los Cabezudos, to the north of the surveyed area (Fig. 3). It is formed by well-preserved parabolic dunes, clearly superimposed to the previous SS (Sheet 1b). Similar chronologies have been obtained in dunes at El Asperillo cliff, on both sides of the Torre del Loro fault (Fig.7), with ages of 9.9 ky BP (sample 21), in the downthrown block and 9.5 ky BP (sample 15), in the upthrown one (Poblado Forestal = Forest Village). This latter sample has been collected at the base of the degraded iron supersurface SsFe2, represented as a ferralithic crust marking a period of non-deposition. These chronologies allow us to

bracket the age of SS-I2 between 10.3 ky BP (BE-7) and 9.5 ky BP (BE-6), since at this age no dunes but only soil formation took place.

A maximum age range between 11.1 ky BP (BE-8) and 8.2 ky BP (BE-5) has been assigned to this System I. Nevertheless (Fig. 10A) we have considered as probable the age of 8.5 ky BP, which is the age of the youngest sample from this system, and 9.5 ky BP (BE-6) as a fixed limit (upper limit of the SS-I2), obtained from the sample of the cliff of El Asperillo (Forest Village) at the base of the degraded iron crust. The age of sample 22 (8.5 ky BP), could correspond to a new System I subsystem or to the beginning of the SS-II1.

These values correlate well with the Aeolian Phase 2, age 11.5 - 9.5 ky BP in the Duero basin (1 in Fig. 10B), and the long-lasting period of dune accumulation (13.5 to 7 ky BP) in Duero basin and La Mancha (2 in Fig. 10B), however punctuated by two periods of dune stabilization and soil formation at 11.8 and 10.2 ky BP. These authors correlate the first one with a climatic warming by the end of YD and the second may be equivalent to the limit between subsystems SS-I1 and SS-I2. Some dune units in the western Portuguese coast aged 9.7 ky BP (4 in Fig. 10B) are coeval to those of SS-I2.

The time span assigned to System I coincides with arid conditions in SE France and Spain (10 in Fig. 10C). In Southern Portugal the warm and rather dry climate period between 11.7 and 9.0 ky BP was interrupted by a rapid/short episode of extreme aridity around ca. 10.2 ky BP (9 in Fig. 10B).

System II. This system is clearly on top of S-I in El Asperillo cliff (Fig. 7) and covered by S-III in El Acebuche and El Abalario areas (Fig. 3). OSL ages obtained for this unit (samples 2, 5, 12 and 17 in Table I and Fig. 10A) are compatible with the interval between Bond Events BE5 and BE4 (Fig. 10A).

its age must be younger than 9.5 ky BP. It was assigned the interval between Bond Events 5 and 4, with approximate age between 8.2 and 5.9 ky BP.

Chronologically, this system correlates well with the final part of the dune sequence of Tierra de Pinares in Duero basin and La Mancha described by Bernat and Pérez-González (2008) and Bernat et al. (2011), (13.5 –

494 7 kyBP; 2 in Fig. 10 B) and the beginning (at 6.8 a 3 ky BP) of the Aeolian Phase 3 of García-Hidalgo et al.
495 (2007), (in Fig. 10B). In addition, the beginning of this system coincides approximately with the dunes
496 accumulated on the northwestern Portuguese coast dated at ca. 8.15 ky BP (4 in Fig. 10B).

497 Some periods of arid climate have been identified in SE France and Iberia between 8.4-7.6 ky (10 in Fig. 10C)
498 and also in the coast of Algarve (7 in Fig. 10C) at 8.2-7.7 kyBP, 7-7.1 kyBP and 6.4-6.15 kyBP. The changes in
499 wind directions that characterize the four subsystems differentiated within this System (Fig. 6) can be
500 correlated to these arid periods.

501 These can be used to date the subsystems distinguished inside System II by changes in wind directions and
502 superposition criteria (Fig. 6).

503 SS-II1 can be attributed to Bond Event BE-5 (ca. 8.2 ky BP) and correlated with dunes in northwestern Portugal
504 (4 in Fig. 10B) and Duero basin and La Mancha (2 in Fig. 10B). The overlying SS-II2 was dated at 8.0 ky BP
505 (sample 5 in Table 1 and Fig. 10A). Two samples collected from SS-II3 (samples 2 and 12 in Table I and Fig.
506 10A) were dated at ca. 7 ka, coeval with the final episodes of dune development in Duero basin and La
507 Mancha (2 in Fig. 10B), and the beginning of the Aeolian Phase 3 of Duero basin (1 in Fig. 10B). Cacho et al.
508 (2010) (6 in Fig. 10C) and Schneider et al. (2016) (7 in Fig. 10C) recognized an arid phase at ca.7 ky BP. The
509 scarcely-represented SS-II4 couldn't be sampled, but its geomorphological and stratigraphic position, allowed
510 us to we consider that it may be coeval to the arid period recorded in the Algarve coast (S Portugal) between
511 6.4 and 6.1 ky BP (7 in Fig. 10C).

512 System III. We estimate its age between 5.9 and 2.6 ky, so including Bond Events BE-4, BE-3 and BE-2 (Fig.
513 10A). Luminescence dating and morpho-stratigraphy suggest a correlation with the most recent part of the
514 aeolian phase PH3 of García-Hidalgo et al. (2007), between 6.8 and 3 ky BP, and probably including paleosol-
515 c dated at ca. 2.5 ky BP (1 in Fig. 10B). It correlates well also with the period of maximum aeolian activity
516 recorded in La Mancha between 5 and 2 ky BP (2 in Fig. 10B). Likewise, coeval dunes have been described in
517 southern Portugal at 5.6 ka BP (3 in Fig. 10B) and in Aquitaine between 3.64 and 3.55 ky BP (5 in Fig. 10B).

From the climate point of view, several arid episodes prone to dune generation have been recognized between 5.6 and 5.2 ky BP (6 in Fig. 10C), 5.1 and 3.3 ky BP (7 in Fig. 10C), 5-1.7 ky BP (9 in Fig. 10C), and 5.3-3.4 and 2.8-1.7 ky BP (10 in Fig. 10C). The beach ridges of Doñana spit also record two phases of reduced coastal accretion (gaps) at 4.7-4.4 ky and 2.7-2.4 ky BP, interpreted as caused by reduced rainfall (Zazo et al., 1994, Borja et al., 1999; 11 in Fig. 10C).

Five subsystems have been identified within this system:

Subsystem SS-III1, accumulated under westerly winds, was dated with two luminescence samples (samples 11: 5.8 kyBP and 16: 5.4 ky BP; Table I; Figs. 6 and 10A). It is correlated with the phase PH-3 of Duero basin-Tierra de Pinares, 6.8 to 3 ky BP in age (García-Hidalgo et al., 2007), and southern Portugal with age 5.6 ky according to Costas et al., 2012. This is a time of regional arid conditions, dated in the Iberian Peninsula between 5.6 and 5.2 ky BP (Cacho et al., 2010); between 5.3 and 4.3 ky BP in SE France and SE Spain (Jalut et al 2000); between 5.8 and 5.0 ky BP in western Portugal (Queiroz and Mathius, 2004 in Schneider et al. 2016); between 5.9 and 4.8 ky BP in NE Iberia (Morellón et al., 2008), 5.2 and 5.0 ky BP in SW Iberia (Santos et al., 2003), and between 5.5 and 5.0 ky BP in SE Iberia (Carrión et al., 2002). According to all these data, a chronology for this subsystem between 5.9 and 5.2/5.0 ky BP is proposed here.

Subsystem SS-III2 overlies the former one, e.g. in Laguna de Santa Olalla, and accumulated under winds from the SW (Fig. 2 and 6). OSL ages (samples 10: 4.8 ky BP, and 4: 4.6 ky BP; Fig. 10A, Table 1) make this subsystem coeval with the middle part of aeolian phase PH-3 of Duero basin (1 in Fig. 10B) and the beginning of the maximum aeolian activity in La Mancha (2 in Fig. 10B).

From a climate point of view, it coincides chronologically with the beginning of an arid phase that lasted from 5.1 to 3 ky BP in Algarve (7 in Fig. 10C), a period of aridity (4 to 2.8 cal kyr BP) in south Spain (lake Zóñar, Córdoba, 8 in Fig. 10C), a dry-warm phase in southern Portugal that lasted from 4.8 to 1.7 ky BP (9 in. Fig 10C), the arid phase lasting from 5.3 to 4.3 ky BP in SE France and Spain (Jalut et al., 2000) and, finally, with the oldest exposed sedimentary gap recorded in Doñana spit between 4.7 and 4.4 ky BP (11 in Fig. 10D).

542 According to all these criteria, and considering also the age of the overlying subsystem, we place
543 chronologically subsystem SS-III2 between ca. 5.0 and 4.3 ky BP.

544 Subsystem SS-III3 overlies the precedent, as observed NE from Matalascañas (Fig.2). OSL ages suggest a
545 duration between ca. 4.3 ky (more or less coincident with BE-4) and ca. 3.3 ky BP (samples 7, age 3.8 ky BP;
546 25, age 3.7 ky BP, and 26, age 3.8 ky BP; Table I and Fig. 10A). This time span coincides with moments of dune
547 accumulation in southern Duero basin, Aquitaine and maximum wind activity in La Mancha (1, 2 and 5 in Fig.
548 10B). We consider likely that the younger limit of this system coincides with an arid event at 3.3 ka BP (6 in
549 Fig. 10C) and with the final stages of the arid episode that lasted from 5.1 to 3.3 ky BP in El Algarve (7 in Fig.
550 10C). It is chronologically included in the period of aridity that extended from 4 to 2.9 cal kyr BP recorded in
551 lake Zóñar, Córdoba (8 in Fig. 10C); in the warm-dry period (3.5 to 2,5 ky BP) recorded in south Portugal (9 in
552 Fig. 10C), and in the final part of the arid period recorded in SE France and SE Spain (10 in Fig. 10C). The
553 system of beach ridges in Almería (SE Spain) also records a gap in sedimentation between 4.2 and 3.9 ky BP
554 (12 in Fig. 10D). At a supra-regional scale, a big drought affected the low latitudes between 4.2 and 3.8 ka BP,
555 when the Acadian Empire in Mesopotamia collapsed (Mayewski et al., 2004).

556 Subsystem SS-III4. This subsystem accumulated under southwestern winds and OSL age date it at ca. 2.85 ky
557 BP (Fig. 6; sample 1 in Table 1 and Fig.10A). This age makes it almost coeval to the end of PH-3 in Duero basin
558 (1 in Fig. 10B), coinciding partially with the phase of maximum wind activity recorded in La Mancha. SS-III4
559 can be climatically correlated also with an arid period recorded in the Algarve at 2.8-2.55 ky BP (7 in Fig. 10C);
560 a warm-dry phase recorded in the Western Mediterranean between 3.5 and 2.5 ky BP, peaked at 3.1 ky BP
561 (9 in Fig. 10C), and a large sedimentary gap in the coastal plain of Roquetas, Almería (12 in Fig. 10D). According
562 to all these data, we assign SS-III4 to an age between 3.3 and 2.8 ky BP, coincident with BE-2.

563 Subsystem SS-III5 includes dunes with not well-defined wind directions (from SW to NW, Fig. 6) which overly
564 the previous unit, as observed near the Poblado Forestal (Figs. 2, 3 and 8). No OSL data are available, but this
565 system is younger than 2.8 ky BP (SS-III4, sample 1 in Fig. 10A), well inside the period of maximum aeolian

566 activity in La Mancha (2 in Fig. 10B). Regarding climate, Schneider et al. (2016) record an arid climate, prone
567 to aeolian dune accumulation, between 2.8 and 2.55 ky BP in Southern Portugal (7 in Fig. 10C). Also, a humid
568 phase is recorded in Iberia between 2.5 and 2.1 ky BP, after a long-lasting period of aridity (6 in Fig. 10C);
569 and an arid phase between 2.8 and 1.7 ky has been recognized in SE Spain and France (10 in Fig. 10C).
570 Concerning the coastal environment, a sedimentary gap in the system of beach ridges in Doñana separates
571 the prograding spit units H3 and H4 between 2.7 and 2.4 ky BP (11 in Fig. 10D) with dune accumulation
572 between ca. 2.8 and 2.6 ky BP (Borja et al., 1999).

573 System IV. It is made up of almost-immobile, semi-stable dunes. Three subsystems have been distinguished
574 according to dune morphology (Fig. 6, Sheet 1e and 1f, Sheet 2a). Age assignations between 2.6 and 1.6 ky
575 BP are estimative, since it is younger than the youngest System III unit and covers the archaeological site of
576 Cerro del Trigo, ca. 1.8 ky, in the Imperial Roman Period (ca. 2.4 to ca. 1.8 ky BP).

577 Subsystem SSIV-1 consists of barchanoid dunes resting on top of the H1 (6.9-4.4 ky BP) prograding unit (not
578 exposed) of the Doñana spit, covering partially the younger part of prograding unit H2 (4.4-2.4 ky BP). For
579 this reason, it is assigned an age 2.6-2.5 ky BP, lying within the period of maximum aeolian activity in La
580 Mancha (5.0 to 2.0 ky BP; 2 in Fig. 10B). It is also coeval with a period of regional aridity recorded in the
581 Iberian Peninsula (2.6-2.45 ky BP; 6 in Fig. 10C) and in South Portugal (2.8-2.55kyBP; 7 in Fig. 10C) as well as
582 with a phase of rapid change to dry conditions recorded in El Algarve between 3.5 and 2.5 ky BP (Fletcher
583 and Zielhofer, 2013). In the beach ridge system of Doñana spit the period between 2.7 and 2.4 ky shows a
584 gap due to reduced sediment supply and no progradation (11 in Fig. 10C).

585 Subsystem SSIV-2 consists of parabolic dunes resting on the prograding unit H2 of Doñana spit, i.e., it is
586 younger than 2.4 ky BP, and they fossilize the Roman site of Cerro del Trigo with age 4th Century (ca. 1700
587 to 1600 y BP; Menanteau, 1979). Two tombs separated by interstratified dune deposits fix the age of the
588 lower dune as older than 1700 y BP, whereas the overlying dune must be younger than 1600 y BP. Similar
589 ages have been attributed to dunes in South and North of Portugal (2.1 and 2.2ky BP; 3 and 4 in in Fig. 10B),

590 and they can be correlated to the climatic maximum of the Imperial Roman Time, between 2.14 and 1.8 ky
591 BP (IRT in Fig. 10C). This subsystem is assimilated chronologically to the lower dune recorded in lake Zóñar (8
592 in Fig. 10C) most likely accumulated during the arid period between 2.1 and 1.8 ky BP. All these data lead us
593 to suggest and estimated age between 2.15 and 1.8 ky BP for this subsystem.

594 Subsystem SSIV-3 covers the former (Fig. 2, Sheet 1f) including dunes that fossilize the Cerro del Trigo
595 archaeological site (estimated age ca.1.7-1.6 ky BP), so we assume an age of 1.6 ky BP for this subsystem
596 following the humid period between 1.8-1.6 ky BP) recorded in the Iberian Peninsula (6 in in Fig. 10C) and
597 lake Zóñar, Córdoba (8 in Fig. 10C).

598 System V. It is made up mostly of transverse dunes that rest on the H2 prograding unit of Doñana spit (4.4-
599 2.4 ky BP; 11 in Fig. 10D). In the absence of any isotopic or luminescence dating, its stratigraphic position
600 sandwiched between Subsystems IV-3 and VI-1 (Fig. 2, Sheet 2a), points to an age between 1.6 and 1.3 ka
601 BP.

602 Subsystem SSV-1 rests upon the tidal channel of Vetalengua dated as 2.1 ka (sample VL-15.01) and 1.6 ka
603 (sample 9; Table 1, Fig. 10 A), the latter collected some 500 m away from the spit, may be the age of these
604 dunes. Similar ages have been recognized in dunes from the western coast of Portugal (1.485 ky BP; 5 in Fig.
605 10B), so we propose an age between 1.6 and 1.5 ky BP for this subsystem.

606 Subsystem SSV-2 includes two very large, active, transverse dune units (Cerro de los Ánsares) younger than
607 the previously described subsystem. Considering these data and the record of an arid episode between 1.4
608 and 1.05 ky BP in the coast of Algarve (7 in Fig. 10C) and between 1.6 and 0.8 ky BP in lake Zóñar (8 in Fig.
609 10C, we propose an age of ca. 1.4 ky BP for this subsystem, coincident with BE-1.

610 Subsystem SSV-3 includes three dune units, smaller than the former ones, and locally resting on top of them
611 (Fig. 2, Sheet 2a, Sheet 3a2). Its age is bracketed between the previous subsystem (SSV-2, 1.4 ky BP) and the
612 following one (SSVI-1, 1.2 Ky BP), so we estimate an age of ca 1.3 Ky BP for this subsystem. Dunes of similar

613 ages have been described in the Duero basin (PH4, 1.4-1.0 ky BP; 1 in Fig. 10B), and Aquitaine (1.28-0.92 ky;
614 5 in Fig. 10B). Likewise, there is a record of arid periods prone to dune accumulation between 1.4 and 1.05
615 ky BP in the Algarve (7 in Fig. 10C), between 1.6 and 0.8 ky BP in lake Zóñar (8 in Fig. 10C) and between 1.8
616 and 0.7 ky BP in SE France and Spain (10 in Fig. 10C).

617 The ages estimated for these three subsystems of System V point to the occurrence of a centennial cyclicity
618 of dune development along this time span.

619 System VI. It includes several subsystems which extend N-S along the littoral, with assigned ages between
620 1.3 and 0.7 ky. Two OSL samples were dated as 1.2 and 1.1 ka (samples 6 and 24 respectively; Table I, Fig.
621 10A).

622 Subsystems SSVI-1 and VI-2 occupy the central littoral area. They are well preserved, active, parabolic (SSVI-
623 1) and parabolic-hackle (SSVI-2) dunes, the latter related to reduced sediment supply owing to its location
624 close to a retrograding sea cliff (Sheet 2 b and c). Migration rates have been calculated in 2m/yr and 0.5 m/yr
625 respectively.

626 Correlation with dune development and aeolian activity in Duero Basin (PH4, 1.65-1 ky BP; 1 in Fig. 10B),
627 southern Portugal (1.2 to 0.98 ky BP; 3 in Fig. 10B) and Aquitaine-France (1.28-0.92 ky BP; 5 in Fig. 10B), lead
628 us to estimate an age between ca. 1.2 and 1.0 ky BP or this subsystem.

629 Increased temperatures and aridity reigned in the Iberian Peninsula during the Medieval Climatic Anomaly
630 (MCA in Fig. 10C) between 1.4 to 0.7 ky BP. This was also recorded in Algarve (1.4 -1.05 ky BP; 7 in Fig. 10C),
631 in southern Spain (1.8-1.05 ky BP; 8 in Fig. 10C), in the Iberian Peninsula (1.25-0.99 ky BP; 6 in Fig. 10C) and
632 in SE France and SE Spain (1.3 – 0.75 ky BP; 10 in Fig. 10C).

633 Subsystem SSVI-3 consists of parabolic dunes along the upper line of the sea cliff which cover stable dunes
634 from System III (SSIII-5) between Mazagón and Torre del Loro, (Fig.3, Sheet 2d). The suggested age, ca. 1.2
635 ka, is the same as other parabolic dunes elsewhere in the Iberian Peninsula (1 and 3 in Fig. 10B).

636 Subsystems SSVI-4 and VI-5 cover the sector 3 of Doñana spit and we consider them younger than the
637 subsystems just described above, i.e. younger than 1.2 ky BP. SSVI-4 includes only a single transverse to
638 barchanoid dune unit whereas SSVI-5 consists of six asymmetric, parabolic dune units, (Fig. 3, Sheet 2e).
639 Assuming that they are younger than 1.2 ky BP, they must be coeval with the arid period and dune
640 stabilization recorded in Duero basin and La Mancha at ca. 1.0 ky BP (2 in Fig. 10B) as well as with the dune
641 development occurred in south Portugal and Aquitaine (0.98 ky BP and 0,92 ky BP; 3 and 5 in Fig. 10B).
642 Additionally, an arid episode has been recognized in SE France and SE Spain between 1.3 and 0.7 ky BP (10 in
643 Fig. 10C) and in south Spain between and 1.6 and 0.8 ky BP (8 in Fig. 10C). Having all these data into
644 consideration, and also taking into account that these units rest on top of the oldest part of the prograding
645 unit H6 of Doñana spit (11 in Fig. 10D), the time span for accumulation of these subsystems can be narrowed
646 to 1.0 to 0.7 ky BP.

647 System VII. It includes large transverse dunes with several advance fronts that moved up to 200 m in the
648 surveyed period of 53 yr. They are separated by interdune depressions, locally called “corrales”. Some units
649 show certain parabolic trend (Figs. 2 and 3, Sheet 2a, b and e, Sheet 3 a1 and a2). There are at least fourteen
650 superimposed dune units that tend to onlap south-westwards. They can be grouped into three subsystems
651 according to wind directions, activity and dune size (Figs. 3 and 6). System VII rests on System VI (SS VI-5 and
652 6, attributed age between 1 and 0.7 ky BP) and is genetically related to the prograding units H5 and H6 of
653 Doñana spit (Table 1).

654 Subsystem SSVII-1. One OSL sample yielded an age of 0.66±0.73 ky BP (sample 23, Table 1, Fig. 10A). Dunes
655 of similar age (0.61 and 0.58 ky BP; 3 in Fig. 10B) occur in southern Portugal, while arid periods have been
656 also recorded in the Iberian Peninsula between 0.68 and 0.62 ky BP (6 in Fig. 10C), 0.75 and 0.55 ky (7 in Fig.
657 10C) and 0.65 and 0.40 ky BP (8 in Fig. 10C). Additionally, three erosional episodes at 675-600 yr BP, 500-450
658 yr BP and 400 yr BP (Zazo et al. 2008) have been recognized in de Doñana spit bar. With all these data, it is
659 proposed here that the age of this subsystem ranges between 700 and 600 yr BP.

660 Subsystem SSVII-2. It presents similar characteristics to the previous, underlying SSVII-1 and extends parallel
661 to it (Fig. 3, Sheet 2e and 3a1). Thus, it is younger than 700-600 ky BP but older than Torre de San Jacinto
662 (late 16th – early 17th century; de Mora Figueroa, 1989). Dunes of similar ages have been described in the
663 Duero Basin and La Mancha (500-150 y BP, 2 in Fig. 10B), and Southern Portugal (580-400 y BP; 3 in Fig. 10B).
664 This episode of dune development coincides roughly with an arid phase recorded in the Iberian Peninsula
665 between 570-530 y BP (6 in Fig. 10C), in South Portugal between 750 and 550 y BP(7 in Fig. 10C) and in South
666 Spain between 650 and 400 y BP (8 in Fig. 10C). An erosional phase is also recorded at 500-450 y BP in the
667 spit bar of Doñana Spit (11 in Fig. 10D). Consequently, and according to all these data we propose an age of
668 ca. 500-400 y BP for tis subsystem.

669 Subsystem SSVII-3. Smaller in extension and dune height than the previous subsystems, this one accumulated
670 closer to the coast along the Doñana Spit (Figs. 3 and 6; Sheet 2e and 3a3). In Duero Basin and La Mancha (2
671 in Fig. 10B) a phase of dune formation occurred between 500 and 150 y BP, as well as in South Portugal (400-
672 300 y BP; 3 in Fig. 10B), North Portugal (230-100 y BP; 4 in Fig. 10B) and Aquitaine (330-290 y BP; 5 in Fig.
673 10B). Climatically arid episodes of similar ages have been reported in the Iberian Peninsula between 330 and
674 150 y BP (6 in Fig. 10C), or between 250 and 75 y BP (8 in Fig. 10C). Thus, the age proposed for this subsystem
675 ranges from 350 to 150 y BP.

676 During the last 150 y, active foredunes accumulated to the south of Mazagón and along the present-day
677 beaches.

678 Complex System (CS). The chronology of this system is based on its morphological position with respect to
679 Systems III and VII: it overlies SS-III.4 (age ca 3.3- 2.8 ka BP) but is covered by SS-VII.1 (age ca 0.7-0.6 ka BP),
680 both in the northern (Torre del Loro) and southern (NW Matalascañas) sectors. We relate the origin of this
681 system to the occurrence of two fractures (Mazagón Fault and Torre del Loro Fault; MF and TLF respectively
682 in Fig. 1) generated as a result of a gravitational, rotational slide which supplied a large amount of sediment
683 to the shore that was redistributed by the dominant SE longshore drift to the beaches in this sector. Much

684 sand was later taken by the prevailing southwesterly winds and accumulated as an extraordinary dune that
685 reached some 100 m in elevation south of El Asperillo (Fig 2 and 3).

686 The active phase of these faults can be placed between SSIV-1 (2.6-2.5 ky BP) and SS IV-2 (2.15-1.8 ky BP),
687 coincident with the 8.0 magnitude seismic event located SW of Cabo San Vicente in 218 BC (2218 y BP),
688 (Campos, 1991; Lario et al.,2011) which affected the whole coast of the Gulf of Cadiz, including the present
689 study zone, and the human settlements prior to the 3rd Century BC. Some of these settlements were
690 abandoned (according to Rodríguez-Vidal et al., 2011; Rodríguez Ramírez et al, 2014) e.g. La Algaida spit in
691 the old Roman Lake Ligustinus, the present Marismas (marshlands) de Doñana. This earthquake provoked
692 large submarine slides in the vicinity of the Gorringe Bank (Atlantic Ocean), the probable epicenter of the
693 event, according to the Catalogue of the Geological Effects of Earthquakes in Spain (Silva et al., 2014).

694 The age of the first six SS of the Complex System can be encompassed between SSIV-2 and SSVI-5 (ca 2.2 ka
695 BP and 0.7 ka BP). The lower limit is assigned to the age of the seismic event whereas the upper limit coincides
696 with the oldest age of SVII which, as said before, fossilizes it towards the north and south.

697 SS-C.7 accumulated following the partial erosion of the oldest dunes of the Complex System, which implies
698 an age coeval, at least in part, to SVII.

699 **6. Conclusions**

700 This paper presents a geomorphological map of the Holocene dune systems that gathers information about
701 aeolian activity, morphology of the various dune types, directions of prevailing winds during the
702 accumulation of each system, and spatial arrangement and relative ages of these systems.

703 The map of the Holocene dune subsystems, actually a map of the Quaternary, represents chronologically the
704 main aeolian subsystems (25), and the correlation with the Complex System.

705 Regarding the Pleistocene dunes in the Asperillo sea cliff, the ages of the iron-enriched paleosurfaces (SsFe1
706 and SsFe2) have been adjusted according to the available data. The older one has been assigned an age
707 between 16 and 13 ky BP, whereas the younger one is ca. 9.5 ky BP in age.

708 A detailed chronology of the dune subsystems is also offered, based on an initial chrono-stratigraphy, OSL
709 age measurements, correlation with other dune systems in the Iberian Peninsula, Holocene climate events
710 and stratigraphic relations with the growing Doñana spit.

711 The age of Systems and Subsystems is presented graphically (Figs. 9 and 10 A). System I is Early Holocene
712 (Greenlandian) in age, System II and half of System III (SSIII-1 and SSIII-2) accumulated during the Middle
713 Holocene (Northgrippian), and the remaining SSIII-3, SS-III.4, SSIII-5 and Systems IV to VII are of Late Holocene
714 (Meghalayan) age.

715 The chronological sequence of the dune subsystems reveals a double cyclicity: a millennial one for the
716 subsystems of Early, Middle and early Late Holocene (S-I to S-III) and a centennial cyclicity for the younger
717 ones (S-IV to S-VII).

718 The origin of the Complex System is related to neotectonics. The activity of Mazagón (MF) and Torre del Loro
719 (TLF) gravitational faults generated a rotational slide which supplied large amounts of sediment to the coast,
720 that were subsequently removed by longshore currents towards the E-SE.

721 The movement of Mazagón and Torre del Loro faults has been dated as 2.2 ky BP, the age of a magnitude 8.0
722 earthquake with epicenter SW off Cape San Vicente, which shook the whole Gulf of Cádiz including the area
723 of Doñana. The Complex System has been assigned an age between 2.2 ky, coeval to S-VII, and 0.7 ky,
724 equivalent to SSIV-2 to SS-VII-1, as the latter covers partially SS-C.6 near Matalascañas. SS-C.7 is equivalent
725 to System VII.

726

727 **Acknowledgements**. Supported by Spanish FEDER-MINECO projects CGL15-69919-R and CGL2015-67169-P.

728

729 **References**

730 Ardon, K., Tsoar, H., Blumberg, D.G. 2009. Dynamics of nebkhas superimposed on a parabolic dune and their
731 effect on the dune dynamics. Journal of Arid Environments, 73: 1014-1022.

732 Bernat Rebollal, M., Pérez-González, A. 2005. Campos de dunas y mantos eólicos de Tierra de Pinares (sureste
733 de la Cuenca del Duero, España). Boletín Geológico y Minero, 116,23-38

734 Bernat Rebollal, M., Pérez-González A. 2008. Inland aeolian deposits of the Iberian Peninsula: Sand dunes
735 and clay dunes of the Duero Basin and the Manchega Plain. Palaeoclimatic considerations. Geomorphology,
736 102, 207–220.

737 Bernat Rebollar, M., Peréz_González, A., Rodríguez García, J., Bateman, M. D. 2011. Los sistemas eólicos del
738 interior de España: geomorfología eólica del Pleistoceno superior y del Holoceno de Tierra de Pinares y de la
739 Llanura Manchega (Capitulo 20). In: Las Dunas en España. Sanjaume, E., Gracia, F. J (Eds. Sociedad Española
740 de Geomorfología. 747 p

741 Bond, G., Shower, W., Cheseby, M., Lotti, R., Almasi, P., de Menocal, P., Priore, P., Cullen, H., Hajdas, I.,
742 Bonani, G. 1997. A pervasive millennial-scale cycle in North Atlantic Holocene and Glacial climates. Science
743 258, 1257–1266.

744 Bond, G., Kromer, B., Beer, J., Muscheler, R., Evans, M.N., Showers, W., Hoffmann, S., Lotti-Bond, R., Hajdas,
745 I., Bonani, G. 2001. Persistent solar influence on North Atlantic climate during the Holocene. Science 294,
746 2130–2136.

747 Borja, F. 1992. Cuaternario reciente, Holoceno y periodos históricos del SW de Andalucía. Paleogeografía de
748 medios litorales y fluvio-litorales de los últimos 30.000 años. Tesis Doctoral. Universidad de Sevilla, 520 pp.,
749 inédita

750 Borja, F., Díaz del Olmo, F. 1987. Complejos húmedos del Abalario (entorno de Doñana, Huelva). Oxyura 4
751 (1), 27-44

752 Borja, F., Díaz del Olmo, F. 1994. El acantilado del Asperillo: Cuaternario reciente y fases históricas en el litoral
753 de Huelva. Geogaceta, 15, 94-97

754 Borja, F., Díaz del Olmo, F. 1996. Manto eólico litoral (MEL) del Abalario (Huelva, España): Episodios
755 morfogenéticos posteriores al 22.000 BP. En: Dinámica y Evolución de Medios Cuaternarios (Pérez Alberdi,
756 A., Martini, A.P., Chessworth, W., Martínez Cortizas, A. (Eds.) Xunta de Galicia, Santiago de Compostela,
757 Spain, 375 – 390.,

758 Borja, F., Zazo, C., Dabrio, C.J., Diaz del Olmo, F., Goy, J.L., Lario, J. 1999. Holocene aeolian phases and human
759 settlements along the Atlantic coast of southern Spain. The Holocene, 9, 333 – 339.

760 Cacho I., Valero Garcés B., González Sampériz, P. 2010 . Revisión de las reconstrucciones paleoclimáticas en
761 la Península Ibérica desde el último periodo glacial, In Clima en España: pasado presente y futuro. Pérez F.
762 Fiz, Boscolo R. (Edit) 9-24 pp.

763 Campos, M.L. 1991. Tsunami hazard on the Spanish coasts of the Iberian Peninsula. Science of Tsunami
764 Hazards 9, 83-90

765 Carrión, J. S. 2002. Patterns and processes of Late Quaternary environmental change in a montane region of
766 southwestern Europe, Quaternary Science Reviews, 21, 2047-2066

767 Clarke, M. L., Rendell, H. M. 2006. Effects of storminess, sand supply and the North Atlantic Oscillation on
768 sand invasion and coastal dune accretion in western Portugal, The Holocene 16,3, 341-355

769 Clarke, M. L., Rendell, H. M., Tastet, J.P., Clave, B., Masse L. 2002. Late-Holocene sand invasion and North
770 Atlantic storminess along the Aquitaine Coast, southwest France (2002). The Holocene, 12,2, 231-238

771 Costas, S., Jerez, S., Trigo, R. M., Goble, R. Rebelo, L. 2012. Sand invasion along the Portuguese coast forced
772 by westerly shifts during cold-climate events. Quaternary Science Reviews, 42, 15-28

773 Dabrio, C.J., Borja, F., Zazo, C., Boersma, R.J., Lario, J., Goy, J.L., Polo, M.D. 1996. Dunas eólicas y facies
774 asociadas pleistocenas y holocenas en el acantilado de El Asperillo (Huelva). Geogaceta, 20, 1089 – 1092.

775 De Mora Figueroa, L. 1981. Torres de Almenara de la costa de Huelva. Excma. Diputación Provincial de Huelva.
776 Instituto Padre Marchena, 19 pp.

777 Fletcher, W.J., Boski, T., Moura, D. 2007. Palynological evidence for environmental and climatic change in the
778 lower Guadiana valley, Portugal, during the last 13000 years. The Holocene, 17 (4): 481-494.

779 Fletcher, W.J., Zielhofer, C. 2013. Fragility of Western Mediterranean landscapes during Holocene rapid
780 climate changes. Catena, 103: 16-29.

781 Flores, E. 1993. Tectónica reciente en el margen ibérico suroccidental. Tesis Doctoral. Universidad de Huelva,
782 458 pp. Inédita.

783 García Novo, F, Ramírez, L. & Torres, A. 1975. El sistema de dunas de Doñana. Naturalia Hispánica, 5, 56 pp.

784 García-Hidalgo J. F., Temiño, J., Segura, M. 2007. Holocene aeolian development in Central Spain; chronology,
785 regional correlations and causal processes Quaternary Science Reviews 26, 2661–2673

786 Goy, J.L., Zazo, C., Dabrio, C.J., Lario, J. 1994. Fault-controlled shifting shorelines in the Gulf of Cadiz since 20
787 Ky BP. Abstract Volume, 1st symposium Atlantic Iberian Continental Margin, Lisbon, p. 24.

788 Goy, J.L., Zazo, C., Dabrio, C.J., Lario, J., Borja, F., Sierro, F.J., Flores, J.A. 1996. Global and regional factors
789 controlling changes of coastlines in southern Iberia (Spain) during the Holocene. Quat. Sci. Rev. 15, 773–780.

790 Goy, J.L., Zazo, C., Dabrio, C.J., 2003. A beach-ridge progradation complex reflecting periodical sea-level and
791 climate variability during the Holocene (Gulf of Almeria, Western Mediterranean). Geomorphology 50, 251–
792 268

793 Hughen K. A., Southon, J., Lehman, S. J., Overpeck, J. T. 2000. Synchronous radiocarbon and climate shifts
794 during the last deglaciation, Science, 290, 1951-1954.

795 Jalut, G., Esteban, A., Bonnet, L., Gauquelin, T., Fontugne, M. 2000. Holocene climatic changes in the Western
796 Mediterranean, from south-east France to south-east Spain. Palaeogeography, Palaeoclimatology,
797 Palaeoecology, 160, 255-290

798 Lario, J., Zazo, C., Goy, J.L., Silva, P.G., Bardají, T., Cabero, A., Dabrio, C.J., 2011. Holocene palaeotsunami
799 catalogue of SW Iberia. Quat. Int. 242, 196–200.

800 Leyva, F., Pastor, F., Goy, J.L. 1976. Mapa Geológico de España 1:50.000 (2ª serie). El Rocio (1018). Cartografía
801 1974. Instituto Geológico y Minero de España.

802 Leyva, F., Pastor, F., Zazo, C.; Goy, J.L. 1975. Mapa Geológico de España 1:50.000 (2ª serie). Palacio de Doñana
803 (1033). Cartografía 1973. Instituto Geológico y Minero de España.

804 Martín-Puertas, C., Valero-Garces, B. L., Mata, M. Pilar, Gonzalez-Sampériz, P., Bao, R., A. Moreno, Stefanova,
805 V. 2008. Arid and humid phases in southern Spain during the last 4000 years: the Zonar Lake record, Cordoba,
806 The Holocene, 18, 907-921.

807 Mayewski, P. A., Rohling, E. E., Curt Stager, J., Karlen, W., Maasch, K. A., David Meeker, L., Meyerson, E. A.,
808 Gasse, F., Van Kreveld, S., Holmgren, K. 2004. Holocene climate variability, Quaternary Research, 62, 243.

809 Menanteau, L., 1979. Les Marismas du Guadalquivir: Exemple de transformation d'un paysage alluvial au
810 cours du Quaternaire récent. (Thèse 3e cycle) , Université de Paris-Sorbonne, 252 pp.

811 Montes, C., Borja, F., Bravo, M.A., Moreira, J.M. 1998. Reconocimiento Biofísico de Espacios Naturales
812 Protegidos. Doñana: una aproximación ecosistémica. Consejería de Medio Ambiente, Junta de Andalucía, 311
813 pp.

814 Morellón, M., B. Valero-Garcés, T. Vegas, P. González-Sampériz, A. Delgado-Huertas, P. Mata, A. Moreno, M.
815 Rico, Corella J. P. 2009. Late glacial and Holocene palaeohydrology in the western Mediterranean region: the
816 Lake Estanya record (NE Spain), Quaternary Science Reviews, 28, 2582–2599

817 Pastor, F., Leyva, F., Zazo, C. (1976). Mapa Geológico de España 1:50.000 (2ª serie). El Abalario (1017).
818 Cartografía 1973. Instituto Geológico y Minero de España.

819 Pastor, F., Zazo, C. 1976. Mapa Geológico de España 1:50.000 (2ª serie). Moguer (1001). Cartografía 1973.
820 Instituto Geológico y Minero de España.

821 Psuty, N.P. 1988. Dune/beach interaction. J Coastal Res Special Issue No 3

822 Rodríguez-Ramírez, A., 1998. Geomorfología del Parque Nacional de Doñana y su entorno. Organismo
823 Autónomo Parques Nacionales del Ministerio de Medio Ambiente, Madrid (146 pp.).

824 Rodríguez-Ramírez, A., Flores, E., Contreras, C., Villarías-Robles, J.J.R., Celestino-Pérez, S., León, A., 2012.
825 Indicadores de actividad neotectónica durante el Holoceno reciente en el P. N. de Doñana (SO, España). In:
826 González-Díez, A., González-Díez, A., et al. (Eds.), Avances de la geomorfología en España, 2010-2012: Actas
827 de la XII Reunión Nacional de Geomorfología, Santander, 17-20 septiembre 2012. Publican, Ediciones de la
828 Universidad de Cantabria, Santander, pp. 289–292.

829 Rodríguez-Ramírez, A., Flores-Hurtado, E., Contreras, C., Villarías-Robles, J.J.R., Jiménez-Moreno, G., Pérez-
830 Asensio, J.N., López-Sáez, J.A., Celestino-Pérez, S., Cerrillo-Cuenca, E., León, Á., 2014. The role of neotectonics
831 in the sedimentary infilling and geomorphological evolution of the Guadalquivir estuary (Gulf of Cadiz, SW
832 Spain) during the Holocene. Geomorphology 219, pp. 126–140.

833 Rodríguez-Ramírez A., Villarías-Robles J.J.R., Pérez-Asensio J.N., Celestino-Pérez S. 2019. The Guadalquivir
834 Estuary: Spits and Marshes. In: Morales J. (eds.) The Spanish Coastal Systems, Dynamic Processes, Sediments
835 and Management. Springer, 517-541

836 Rodríguez-Vidal J, Rodríguez-Ramírez A, Cáceres LM, Clemente L (1993) Coastal dunes and post-Flandrian
837 shoreline changes. Gulf of Cádiz (SW Spain). INQUA Mediterr Black Sea Shoreline Subcomm News 15:12–15

838 Rodríguez-Vidal, J.; Bardají, T.; Zazo, C.; Goy, J.L.; Borja, F.; Dabrio, C.J.; Cáceres, L.; Ruiz, F.; Abad, M. 2014.
839 Coastal dunes and marshes in Doñana National Park. In: Landscapes and Landforms of Spain (F. Gutiérrez and
840 M. Gutiérrez, Eds.), World Geomorphological Landscapes, Springer Science + Business Media Dordrecht, 229-
841 238.

842 Rodríguez-Vidal, J., Ruiz, F., Cáceres, L.M., Abad, M., González-Regalado, M.L., Pozo, M., Carretero, M.I.,
843 Monge, A.M., Gómez, F. 2011. Geomarkers of the 218–209 BC Atlantic tsunami in the Roman Lacus Ligustinus
844 (SW Spain): a palaeogeographical approach.Quat. Int. 242, 201–212.

845 Ruiz-Labourdette, D., Coleto, C., Bravo, M. A., Borja, F., Borja, C., Montes, C., 2004. Complejo Palustre de los
846 arenales litorales de Doñana (E. 1:60000). Consejería de Medio Ambiente. Junta de Andalucía.

847 Santos, L., Sanchez-Goñi, M.F., Freitas, M.C., Andrade, C., 2003. Climatic and environmental changes in the
848 Santo Andre´ coastal area (SW Portugal) during the last 15,000 years. Quaternary climatic changes and
849 environmental crises in the Mediterranean Region, pp. 175–179.

850 Schneider, H., Höfer, D.,Trog, C., Mäusbacher, R., 2016. Holocene landscape development along the
851 Portuguese Algarve coast- A high resolution palynological approach. Quaternary International, v 407, 47-63

852 Silva, P.G.; Rodríguez Pascua, M.A.; Giner, J.L.; Pérez López, R.; Lario, J.; Perucha, M.A.; Bardají, T.; Huerta, P.;
853 Roquero, E.; Bautista, M.B. 2014. Catálogo de Efectos Geológicos de los terremotos en España. (Silva P.G.,

854 Rodríguez-Pascua M.A. Eds.). Serie Riesgos Geológicos / Geotecnia IGME. Vol., 4. Instituto Geológico y Minero
855 de España, Madrid. 350 pp.

856 Vallejo, I., García, D. 2013. Descripción de megaformas dunares en el sistema de dunas activas del P.N. de
857 Doñana. Geotemas, 14: 103-106. VII Jornadas de Geomorfología Litoral, Oviedo.

858 Vanney, J.R., Menanteau, L. 1979. Tipes de reliefs littoraux et dunaires en Basse- Andalousie. (De Huelva à
859 l'embouchure du Guadalquivir). Mélanges de la Casa Velázquez, 15, 5 – 52.

860 Vanney, J.R., Menanteau, L. , Zazo, C. 1979. Physiographie et evolution des dunes de basse andalousie (Golfe
861 de Cádix, Espagne). Actes de Colloques, 9, 277 – 286.

862 Vanney, J.R., Menanteau, L., Zazo, C., Goy, J.L. 1985. MF02. Punta Umbría- Matalascañas. Mapa fisiográfico
863 del litoral atlántico de Andalucía, E:1/50.000. Junta de Andalucía, Consejería de Política Territorial, Agencia
864 del Medio Ambiente. Sevilla, 1 mapa, 29 pp.

865 Yan, N., Baas, A. 2015. Parabolic dunes and their transformations under environmental and climatic changes:
866 Toward a conceptual framework for understanding and prediction. Global and Planetary Change, 124: 123-
867 148.

868 Zazo, C., 1980. El Cuaternario marino-continental y el límite Plio- Pleistoceno en el litoral de Cádiz. Tesis
869 Doctoral, Universidad Complutense de Madrid. Inédita

870 Zazo, C., Dabrio, C.J., Goy, J.L., Menanteau, L. 1981. Torre del Oro. Actas V Reunión G.E.T.C., Guía de la
871 excursión: Litoral de Huelva. Sevilla, 356 – 361.

872 Zazo, C., Goy, J.L., Somoza, L., Dabrio, C.J., Belluomini, G., Improta, S., Lario, J., Bardaji, T., Silva, P.G., 1994.
873 Holocene sequence of sea-level fluctuations in relation to climatic trends in the Atlantic-Mediterranean
874 linkage coast. J. Coast. Res. 10, 933–945.

875 Zazo, C., Dabrio, C.J., Borja, J., Goy, J.L., Lézine, A.M., Lario, J., Polo,M.D., Hoyos, M., Boersma, J.R., 1999.
876 Pleistocene and Holocene aeolian facies along the Huelva coast (southern Spain): Climatic and neotectonic
877 implications. Geol. Mijnb. 77, 209–224.

878 Zazo, C., Mercier, N., Silva, P.G., Dabrio, C.J., Goy, J.L., Roquero, E., Soler, V., Borja, F., Lario, J., Polo, D., Luque,
879 L., 2005. Landscape evolution and geodynamic controls in the Gulf of Cadiz (Huelva coast, SW Spain) during
880 the Late Quaternary. Geomorphology 68, 269–290.

881 Zazo, C., Dabrio, C. J., Goy, J. L., Borja, F., Silva, P. G., Lario, J., Roquero, E., Bardají, T., Cabero, A., Polo, M. D.,
882 Borja, C. 2011. El complejo eólico de El Abalario (Huelva). (Capitulo 16). En: Las Dunas en España (Eds.
883 Sanjaume, E., Gracia, F. J.). Sociedad Española de Geomorfología. 747 p

884 Zazo, C., Dabrio, C.J., Goy, J.L., Lario, J., Cabero, A., Silva, P.G., Bardají, T., Mercier, N., Borja, F., Roquero, E.
885 2008. The coastal archives of the last 15 Ka in the Atlantic-Mediterranean Spanish linkage area: sea level and
886 climate changes. Quat. Int. 181 (1), 72–87.Bailey, G.N., Reynolds, S.C., King, C.P., 2011. Landscapes of human
887 evolution: models and methods of tectonic geomorphology and the reconstruction of hominid landscapes.
888 Journal of Human Evolution 60, 257-280. DOI: 10.1016/j.jhevol.2010.01.004.

889

890

891

892

893

894

895

896 FIGURE CAPTIONS

897 Fig. 1. Location sketch of the dune systems (grey lines) with main active faults (in red) affecting the
898 area. Location of samples for OSL (yellow dots and numbers). Fault and/or alignments represented
899 are (from north to south): Huelva Fault (HF), Tinto River Fault (TRF), Huelva-Ayamonte Fault (HAF),
900 Las Madres Fault (LMF), Arroyo Rocina Fault (ARF), Mazagón-Acebuche Fault (MAF). Torre del Loro
901 Fault (TLF), El Rocio Fault (ERF), Continental Shelf Fault (CSF), Guardamar-Matalascañas Fault (GMF),
902 Palacio de Doñana Fault (PDF), Torre Carbonero-Mari López Fault (TCMLF), Madre de las Marismas
903 Fault (MMF), Bajo Guadalquivir Fault (LGF).

904

905 Fig. 2. Map of dune systems (colour) including morphological types of dunes, main wind directions,
906 degree of aeolian activity (stable, semi-active and active dunes) and areal distribution of systems
907 and subsystems (symbols). 1, 2 and 3 are sectors of Doñana Spit.

908

909 Fig. 3. Map of dune systems and subsystems from the Doñana National Park. Each system is
910 represented by a colour and subsystems by a different tone of each colour. The sequence of systems
911 and subsystems sequence goes from older (S-I, SS-I1) to younger (S-VII, SS-VII3). CS and SSC
912 correspond to Complex System and subsystems.

913

914 Fig. 4. Overlap of vertical photographic images (orthophotos) from 1956 and 2009 showing changes
915 in dune arrangements indicative of dune activity (greenish lines) during the 53 years period.

916

Fig. 5. Spatial relationship (overlapping) of various types of dunes from 3D images. Oblique photograph.

Fig. 6. Summary of dune Systems and Subsystems with prevailing winds and directions of dune advance, morphological types, activity, preservation degree and chronology. Transv: transverse. Areas are indicated in square kilometers.

Fig. 7. Sketchy cross sections of the Asperillo Cliff between Poblado Forestal and SE Torre del Loro (TLF-Torre del Loro F; Hb-Holocene boundary). U.2, U.3 (Pleistocene aeolian units defined by Zazo et al., 2005); S. I, S.II, S.III (Holocene dune systems described in this work); DO09-19… and AP00-D1…: OSL samples

Fig. 8. Photogeological interpretation of System III between Mazagón and Poblado Forestal. Note the high variability of prevailing wind directions deduced for SSIII-5.

Fig. 9. Chronology of dune systems and subsystems based on the ages obtained from OSL dating (DS-Dune System, SS-Dune subsystem, CS-Complex system, FS-Fluvial System, CH-Tidal channel).

Fig. 10. **A)** Chronological synthesis of dune systems and subsystems (SS) included in this work. Same colors for dune Systems than in Fig. 3. PD-Paleodune, OL-Organic layer (age in Zazo et al., 1999), YD-Younger Dryas, VL-Vetalengua, VC-Vetacarrizosa, 1,2,3…sample number, CS-Complex System. **B)** Iberian dune sequences studied by authors: 1. García-Hidalgo et al. 2007; 2. Bernat and Pérez-González, 2008; Bernat et al., 2011; 3. Costas et al., 2012; 4. Clarke and

941 Rendell, 2006; 5. Clarke et al., 2008. Ps: Paleosols; (4) number of dating samples; FL-Fluvial.
942 **C)** Climatic records from different locations in the Iberian Peninsula and France; 6. Cacho et
943 al., 2010; 7. Schneider et al., 2016; 8. Martin-Puertas et al., 2008; 9. Fletcher et al., 2007,
944 Fletcher and Zielhofer, 2013; 10. Jalut et al., 2007. A: Arid, C: Cold, B: Bond, H: Humid, IRT-
945 Imperial Roman Time, MCA-Medieval Climate Anomaly, LIA-Little Ice Age. **D)** Spit bar systems
946 from the Atlantic and Mediterranean coasts of Iberian Peninsula; 11. Zazo et al., 1994, Borja
947 et al., 1999; 12. Goy et al., 2003, Zazo et al., 2008; H1, H2…prograding units, GAP-Large swale,
948 E-Erosion, D1, D2, D3-Dunes.

949

950

951 Table I. OSL ages from samples of dunes.

952

953

954 Sheet 1.: a) Ground plan distribution of dune systems I, II and III; b) Detail of the dune front
955 of S-II over S-I; SS-I1 and SS-I2 dune units and its wind directions (blue arrows); c) Relationship
956 between dune systems S-III, S-IV, S-VI and S-VII around Santa Olalla laguna (plan view, p.v.).
957 Subsystems III1 and III" show different wind directions (from N90E to N60-70E). d) oblique
958 view (o.v.) of same area facing south; overlapping of SS-VI1 over SS-III2, SS-III2 over SS-III1
959 and S-VII over all of them. e) Detail of SS-IV1 (remains of barjanoids dunes). Scarce movement
960 between 1956 and 2009. f) SS-IV2 and SS-IV3 around Cerro del Trigo and marshland (Lucio del
961 Membillo). Scarce movement during the 53 years lapse. Sources: a and b: orthophoto PNOA
962 2007; c and d: orthophoto PNOA 2009; e and f: 2009 orthophoto PNOA and 1956 aerial photo
963 overlapping. Spatial resolution MDT 5x5 m.

964

965 Sheet 2. a) Relationship between SIV, V, VI and VII. The first one (SIV) consists of semistable
966 dunes, the other three (SV, VI, AND VII) are made of mobile dunes. Overlapping of SS-IV3 and
967 SS-IV2; SS-V2 and SS-V1; SS-Vi and SS-IV3, SS-VII and SS-V2, and SS-VII1 and SS-V3. b) SS-VII1
968 parabolic dunes over SS-IV1 transverse dunes (barjanoids), SS-VII1 over two of them. c) SS-
969 VI2 parabolic dunes under SVII transverse dunes. d) SS-VI3 parabolic dunes on cliff between
970 Torre del Loro and Mazagon. e) SS-VI4 and SSVI-5 dunes over the spit bar and under SS-VII2
971 and SS-VII1. Origin of images: a: 2009 PNOA orthophoto, oblique view, and 1956 aerial photo,
972 in plan; b and c: 1956 aerial photo; d: 2009 PNOA orthophoto; e) Plan views of 2009
973 orthophoto PNOA. Spatial resolution MDT 5x5 m.

974

975 Sheet 3. Overlapping of dune subsystems. **a1**. Oblique view of the overlapping of SS-VI1, SS-
976 Vi1, SS-VII1 and SSVII-2. **a2)** Overlapping between subsystems of SV, similarity of SS-V1 forms
977 (worms), with SS-IV1 (see a1); **b)** Complex system; overlapping of dunes from SS-C3, SS-C2
978 and SS-C1. Dunes in the oldest SS are parabolic but are imbricated transverse in the others

two; **c)** Complex system, overlapping of dunes, SC-1 is under Asperillo Dunes system SC-2, SC-3, SC-5 and SC-5 and over stable dunes from SS-IV4 and SS-II3. Blowout (yellow circles) indicate erosion, **d)** Shadow dunes from Complex System over SC-1 parabolic dunes and SS-III4; e) S-VII dunes over Complex System. In this case S-VII cover the internal zone and deposited over stable systems. Origin of images: a: oblique view 1956 aerial photo; b: overlapping of 2009 PNOA orthophoto and 1956 aerial photo; c, d and e: oblique view of 1956 aerial photo from MDT. Spatial resolution MDT 5x5 m.

Holocene eolian dunes in the National and Natural Parks of Doñana (SW Iberia): Mapping, Geomorphology, Genesis and Chronology.

J. L. Goy [a], C. Zazo[b], C. J. Dabrio[c], A.M. Martínez-Graña[a,*], J. Lario[d], F. Borja[e], T. Bardají[f], C. Borja[g], F. Díaz del Olmo[h]

[a] Departamento de Geología, Universidad de Salamanca, 37008, Salamanca, Spain.
[b] Departamento de Geología, Museo Nacional de Ciencias Naturales (CSIC), 28006, Madrid, Spain.
[c, *] Departamento de Geomorfología, Estratigrafía y Paleontología, Universidad Complutense, 28040, Madrid, Spain.
[d] Departamento de Ciencias Analíticas, UNED, 28040, Madrid, Spain.
[e] Departamento de Historia, Geografía y Antropología. Facultad de Humanidades. Universidad de Huelva, 21007, Huelva, Spain.
[f] Departamento de Geología, Geografía y Medio Ambiente, Universidad de Alcalá, 28871, Alcalá de Henares, Spain.
[g, h] Departamento de Geografía Física y A.G.R. Facultad de Geografía e Historia. Universidad de Sevilla. 41004 Sevilla, Spain.

* Corresponding author. Tel: +34 923 294496; Fax: +34 923 294514.
E-mail address: amgranna@usal.es (Antonio Martínez-Graña)

Abstract.

The dune fields of the National and Natural Park of Doñana Dunes are considered one of the most outstanding dune fields in Western Europe. They are located at the west margin of the Guadalquivir river estuary. The accumulation of aeolian, and in less proportion marine and fluviatile, sands partly block the communication with the Gulf of Cadiz, in the Atlantic Ocean. The sand units form a large oval dome, the "Abalario Dome" which connects with the large Doñana Spit Bar where dune systems accumulated as well, coeval with the spit growth.

The aim of this paper is to map, date and set a robust chronological sequence, and describe these Holocene Dune Systems paying special attention to the dune types present and genesis related to the paleo winds blowing at the time of accumulation, and degree of activity past in recent times. The most frequent dune morphologies are parabolic or transverse. The degree of activity was classified as stable, semi-stable and active. Most stable dunes concentrate on the Abalario Dome, whereas active dunes

occur mainly on the Doñana spit bar. Relative chronology was erected from the superposition of dune Systems and Subsystems deduced from photogeology coupled with field surveys, orthophotos, and oblique and 3D images. Sampling and radiogenic dating (Optically Stimulated Luminescence-OSL) allowed to assign "numeric" ages to the aeolian units. Eight dune Systems have been defined: Systems I to VII, plus the CS, which is a lateral equivalent of part of SIV, V and VI

The discussion, presented as a chronological synthetic chart, compares the dune Systems of Doñana with other examples in the Iberian Peninsula and southwestern France (Aquitaine) and allows to correlate the genesis of dunes with arid climatic periods and events (warm and cold), thus refining the deduced chronology. Additional help came from superposition of dunes on the actively prograding Doñana spit bar.

As a conclusion, besides the much refined maps, this paper offers the ages assigned to the Holocene dune Systems and Subsystems. System I, age 11.1 to 9.5 ky BP, perhaps extending to 8.5 ky BP. System II, 8.2 to 6.1 ky BP. System III, 5.9 to 2.6 ky BP. System IV, 2.6 to 1.6 ky BP. System V, 1.6 to 1.3 ky BP. System VI, 1.2 to 0.7 ky BP. System VII, 0.7 to 0.15 ky BP. The age of the Complex System is 2.2 to 0.15 ky BP.

Dune System were accumulated with two cyclicities: millennial for the older, stable, Systems and centennial for the younger, semi-stable and active ones. The origin of the Complex Systems is related to activity of Mazagón and Torre del Loro faults caused by regional seismic activity.

Keywords: Geomorphological analysis, Coastal dunes, Holocene, Chronology, Guadalquivir Basin, Spain.

1. Introduction

Studies of coastal processes and their evolution usually face the problem of stablishing a precise chronology of depositional events, an issue particularly difficult in the case of the coastal aeolian systems. In the study case addressed in this paper, the aeolian complex includes two natural Spaces. a) The Doñana National Park,

a Biosphere Reserve (UNESCO 1980) and World Heritage (UNESCO 1994), and b) the littoral fringe of Doñana Natural Park.

The dune complex occupies an area of 420 square kilometers, approx. 62 km in length by 16 km maximum width, (Fig. 1), reaching elevations of 106 m near the sea cliff. This, and Les Landes (Gascogne-Aquitaine, France), are the largest aeolian systems in Western Europe. The area has attracted numerous scientists since the middle 1970s who generated a copious flow of papers. Geomorphological/neotectonic analysis of sedimentary units coupled with isotopic and luminescence dating allowed reconstructing the general evolution of paleoenvironments during the Pleistocene epoch, as most of sampling and analyses were carried out along the wall of the coastal cliff (Zazo et al., 2005).

According to this, the main aim of this paper is to present the space-temporal evolution of the Holocene dune field systems that, as top-cliff dunes, extend several kilometers inland. Our goal is to recognize the main phases of sedimentary activity and erect a robust hierarchical stratigraphic framework closely attached to climate and the degree of “tectonic activity” of the Abalario Dome (Fig. 1) upon which the aeolian sand unit rests.

We intended to separate the events of sedimentary activity at a millennial/sub-millennial scale between the mouths of the Odiel-Tinto and Guadalquivir rivers (Fig. 1). This required to elaborate a thorough geomorphological cartography which begun with detail photointerpretation with field surveys prior any sampling, to implement GIS and, finally, build a DTM. An essential addition was to obtain a reliable chronostratigraphy by refining the ages of some of the units distinguished by Zazo et al. (2005) with new surveys. A crucial point is that, besides refining the Pleistocene-Holocene limit, the aim of this research is to analyze the degree of “tectonic stability” of the Abalario Dome. This new focus required resampling and dating by means of luminescence, radiocarbon, lithic industries and archaeological data. Last, but not least, the study required a careful survey of the close inter-relation between aeolian and beach-barriers deposits.

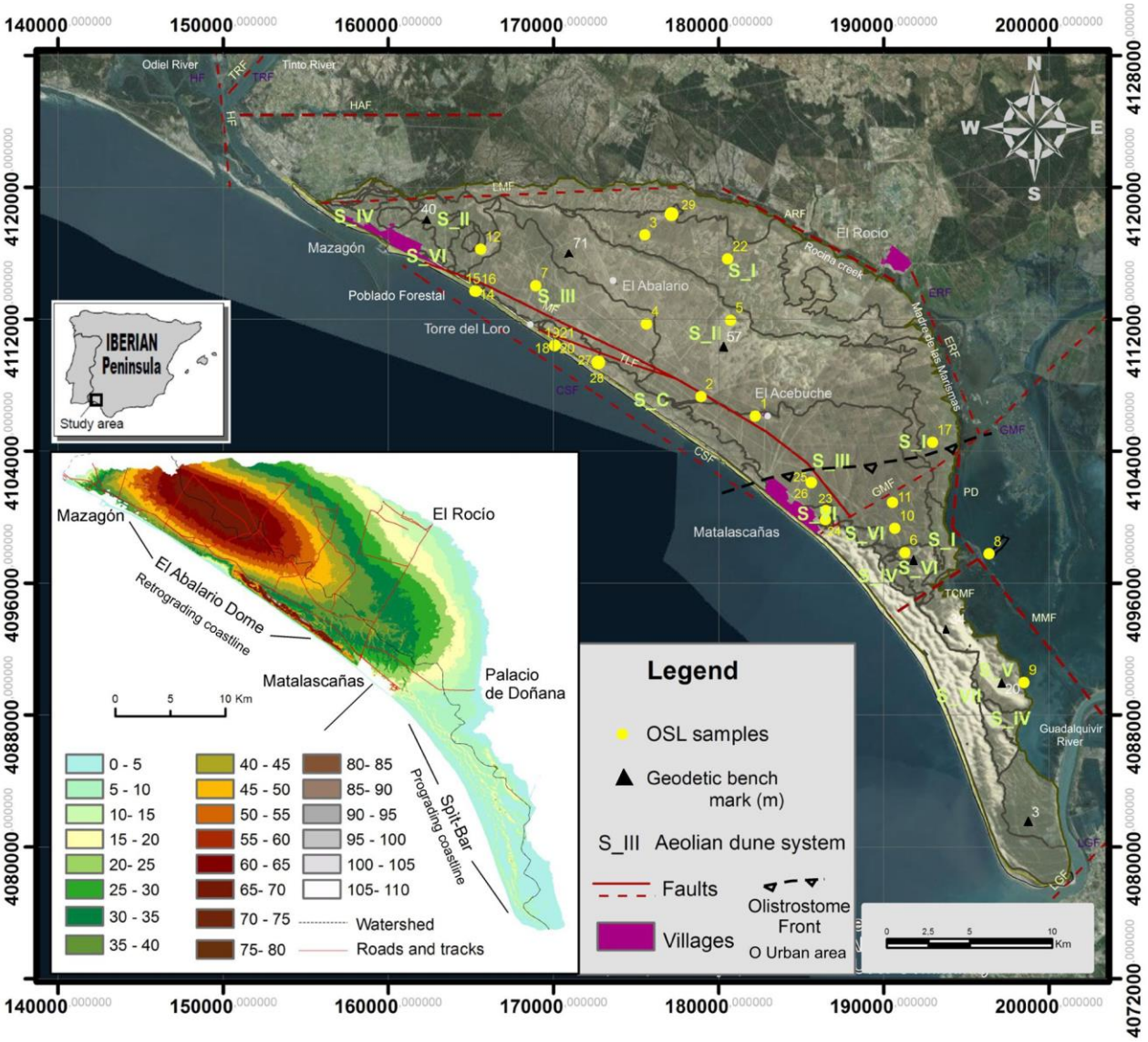

80

81 Fig. 1. Location sketch of the dune systems (grey lines) with main active faults (in red) affecting the area.
82 Location of samples for OSL (yellow dots and numbers). Fault and/or alignments represented are (from north
83 to south): Huelva Fault (HF), Tinto River Fault (TRF), Huelva-Ayamonte Fault (HAF), Las Madres Fault (LMF),
84 Arroyo Rocina Fault (ARF), Mazagón-Acebuche Fault (MAF). Torre del Loro Fault (TLF), El Rocio Fault (ERF),
85 Continental Shelf Fault (CSF), Guardamar-Matalascañas Fault (GMF), Palacio de Doñana Fault (PDF), Torre
86 Carbonero-Mari López Fault (TCMLF), Madre de las Marismas Fault (MMF), Bajo Guadalquivir Fault (LGF).

87

88 **2. Geological and geomorphological setting**

89 The study area is placed in SW Iberian Peninsula at the mouth of the Guadalquivir River, in the Cenozoic Basin
90 of Guadalquivir, the northern foreland basin of the Betic Cordillera, the passive margin of which is the Iberian
91 Massif located to the north. The Guadalquivir basin was progressively filled with marine sediments of

Miocene and Pliocene ages and, towards the Pleistocene, it was reduced to an estuary where the Guadalquivir River debouched. An aeolian dune complex accumulated at the distal seaward part of the estuary, resting upon the Holocene estuarine and Doñana spit bar to shallow-marine deposits

The mapped area includes two realms: the Abalario dome and the Doñana spit bar being limited by the Rocina creek (East), the present coastline (West), Mazagón (North) and the Guadalquivir River (South-east), (Fig. 1). Here, dune systems reach variable elevations, with a maximum at 106 m near the Asperillo coast. The drainage pattern is asymmetrical, with plenty, relatively long, creeks in the eastern side and few, short, creeks in the western side. For this reason, the dune systems in the eastern flank are more degraded. Between the localities of Mazagón and Matalascañas, the coastal side of the dome is a 28 km-long marine cliff, 16 to 20 m high (Fig. 2).

Numerous gravitational faults affect the estuary, largely controlling the accumulation of dune systems, allowing Zazo et al. (2005) to separate the coastal cliff in two paleogeographical realms: an uplifted one to the NW (from Mazagón to Torre del Loro) and a subsiding one to the SE (between Torre del Loro and Matalascañas).

Further neotectonic activity controls not only the general morphology but also the repartition of dune systems: the area is limited by extensional Quaternary faults running NE-SW, NW-SE and E-W, which delineate the El Abalario Dome (EAD) and the Doñana spit bar (DS). Some of these faults generated gravitational sliding (e.g. TLF: Torre del Loro Fault (Fig. 1). (Flores, 1993; Goy et al, 1994, 1996; Rodríguez-Ramírez et al., 2012, 2014)

In previous papers dealing with the aeolian deposits, most of the research was focused on the Pleistocene deposits exposed along the sea cliff wall. In contrast, the top-cliff dunes received only a marginal attention (Dabrio et al., 1996; Zazo et al., 1999, Zazo et al., 2005, and Zazo et al., 2008).

As one of the main aims of this paper is to study the Holocene aeolian systems and their space-temporal distribution, we refer below only to papers related to cartographic representations.

Geology: Geological Maps of Spain (MAGNA) scaled 1:50,000 Sheets of Moguer (Pastor and Zazo, 1976), El Abalario (Pastor, Leyva and Zazo, 1976), El Rocío (Leyva, Pastor and Goy, 1976) and Palacio de Doñana (Leyva, Pastor, Zazo and Goy, 1975). The dune systems are represented in a general way, with the main interest in sedimentology.

Physiography: "Mapa Fisiográfico del litoral atlántico de Andalucía (1:50,000): Punta Umbría-Matalascañas and Matalascañas-Chipiona" (Vanney and Menanteau, 1985, with geology by Zazo and Goy). Here landforms are mapped according to the various systems that generated them: submarine and coastal, aeolian, humid and terrestrial systems.

Ecology: "Mapa Ecológico de Doñana" scaled 1:40,000 (Montes et al., 1998) focused on ecotopes with a geomorphological base, including the dune systems. "Map of the marsh complex of Doñana" (Ruiz-Labourdette et al., 2004), with representation of aeolian, coastal and marsh ecosystems.

Borja (1992) and Borja and Díaz del Olmo (1996) presented a cartographic scheme including superposition of dunes, wind directions, sand sedimentology and approximate ages. They named the accumulations of sand as Aeolian Sheets (Mantos Eólicos), distinguishing five of such sand sheets. The oldest accumulation is the Lower Aeolian Sheet (LAS), a bimodal grainsized unit, with approximate age 15-14 Ka BP, and paleo-winds from WNW. The overlying Humid High Aeolian Sand sheet (HASS) consists of parabolic and transverse dunes of well sorted unimodal sand deposited around 11 ka BP under winds from the SW. The overlying Dry High Aeolian Sand Sheet (DHASS) include dunes of the same type deposited under winds from the W between 11 and 5.4 ka BP. Resting on these sediments there are Neolithic-Chalcolithic remains/artifacts. Above these, the Semi-stable Dunes Aeolian Sand Sheet of (SSD) with parabolic dunes accumulated by winds from the WSW in an estimated time span from late Middle Age to late 18th Century. The younger aeolian unit includes the active transverse dunes (AD) accumulated by SW winds in the two last centuries. These dunes are semi-

138 active in El Asperillo, because they are disconnected from the beach and have been reforested in recent
139 times.

140 Geomorphology: Zazo (1980) and Zazo et al., (1981), based on the cartography made (1:50,000) on the
141 southern part of the study zone, differentiate five large dune systems: 1st: Aeolian sheet with degraded
142 parabolic dunes; 2nd Barchans, at the beginning of the spit bar; 3rd: Parabolic dunes at the base of El
143 Asperillo system and W of Palacio de Doñana; 4th: Transverse dunes, closing the barrier of the paleocoast
144 between Torre del Loro and Matalascañas; and 5th: Transverse and longitudinal mobile dunes, over the
145 littoral spit bar.

146 A 1:50.000 map accompanied the monography "Geomorfología del Parque Nacional de Doñana y su entorno"
147 (Rodríguez Ramírez, 1998). This is the most significant analysis of the dune systems in Doñana, including the
148 dunes of the Médano Littoral. Besides the structural, slope, fluvial and fluvio-littoral morphologies, the
149 author distinguished five dune systems, called I, II, III, IV, and V, in stratigraphically ascending order.

150 Rodríguez-Vidal et al. (2014) used the cartography by Rodríguez Ramírez (1998) and correlated the deposits
151 described by him with the seven dune units (U1 to U7) distinguished and dated by Zazo et al. (2005) in the
152 downthrown block of the TLF. These authors distinguished five aeolian Dune Systems (I to V):

153 System I: parabolic dunes, winds from WSW, aged 31 to 18 ka BP, correlated with U-2.

154 System II: elongated parabolic dunes; winds from the W, age 14-11 ka, correlated with U-3.

155 System III, parabolic dunes, winds from WSW, age 11-5.4 ka, correlated with U-4.

156 System IV: active parabolic dunes, winds from the SW. Chronology based on archaeological remains: late
157 Neolithic-Chalcolithic-Roman (age 2.7 ka cal BP) and correlated this system with U-6. These authors include
158 in this same system, younger parabolic dunes coeval of the watch towers built in late 16th to early 17th
159 centuries.

System V: migrating transverse dunes, winds from the SW. Early 17th Century to present.

3. Materials and methods

The elaboration of geomorphological and geological maps of the Holocene dune systems required working at a variety of scales. (Fig. 2 and 3)

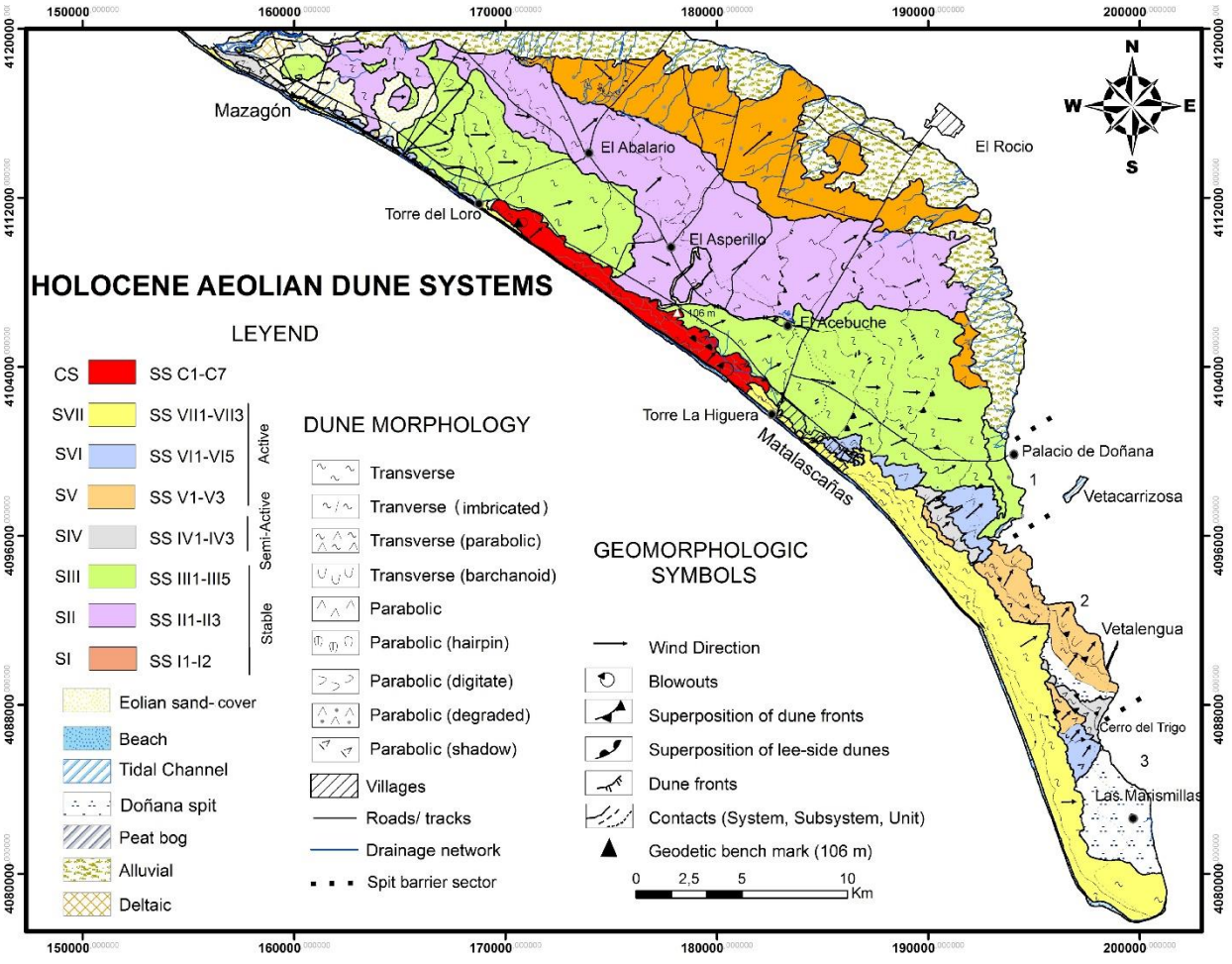

Fig. 2. Map of dune systems (colour) including morphological types of dunes, main wind directions, degree of aeolian activity (stable, semi-active and active dunes) and areal distribution of systems and subsystems (symbols). 1, 2 and 3 are sectors of Doñana Spit.

Photointerpretation of the whole study area used the aerial photographs scaled ~1:33,000 (Flight 1956, Ministry of the Army) with the help of the national survey scaled 1:18.000 (1980-1986) for specific areas. Orthophotographs of the National Plan for Aerial Orthophotography (PNOA) of the National Geographic Institute (IGN), shot in 2002, 2007 and 2009 (resolution 25 cm/pixel), scaled 1:10.000 were used for

172 comparison with the older 1956 aerial photographs. Comparison of the orthophotographs of 2009 and the
173 1956 flight with geo-positioning of the various advance fronts revealed changes of the dunes in the last 53
174 years, and the activity degree of the dune systems was evaluated (Fig. 4). These interpretations were checked
175 along several fieldwork surveys both for mapping and sampling for dating. This generated a vector layer of
176 points based on GPS data.

177 Topographic maps in raster format scaled 1:50.000 (MTN50) and 1:25.000 (MTN25), the last one
178 georeferenced. The geological base was the Plan Magna geological map, scaled 1:50.000, sheets: Moguer
179 (1000). El Abalario (1017). El Rocío (1018), Palacio de Doñana (1033) and Sanlúcar de Barrameda (1047). In
180 addition the geological map of the GEODE Project of the Geological and Mining Institute of Spain (IGME). The
181 resulting map was reduced to a 1:100,000 scale for a working document and, later, it was reduced to
182 publication format (approx. 1:250.000).

183

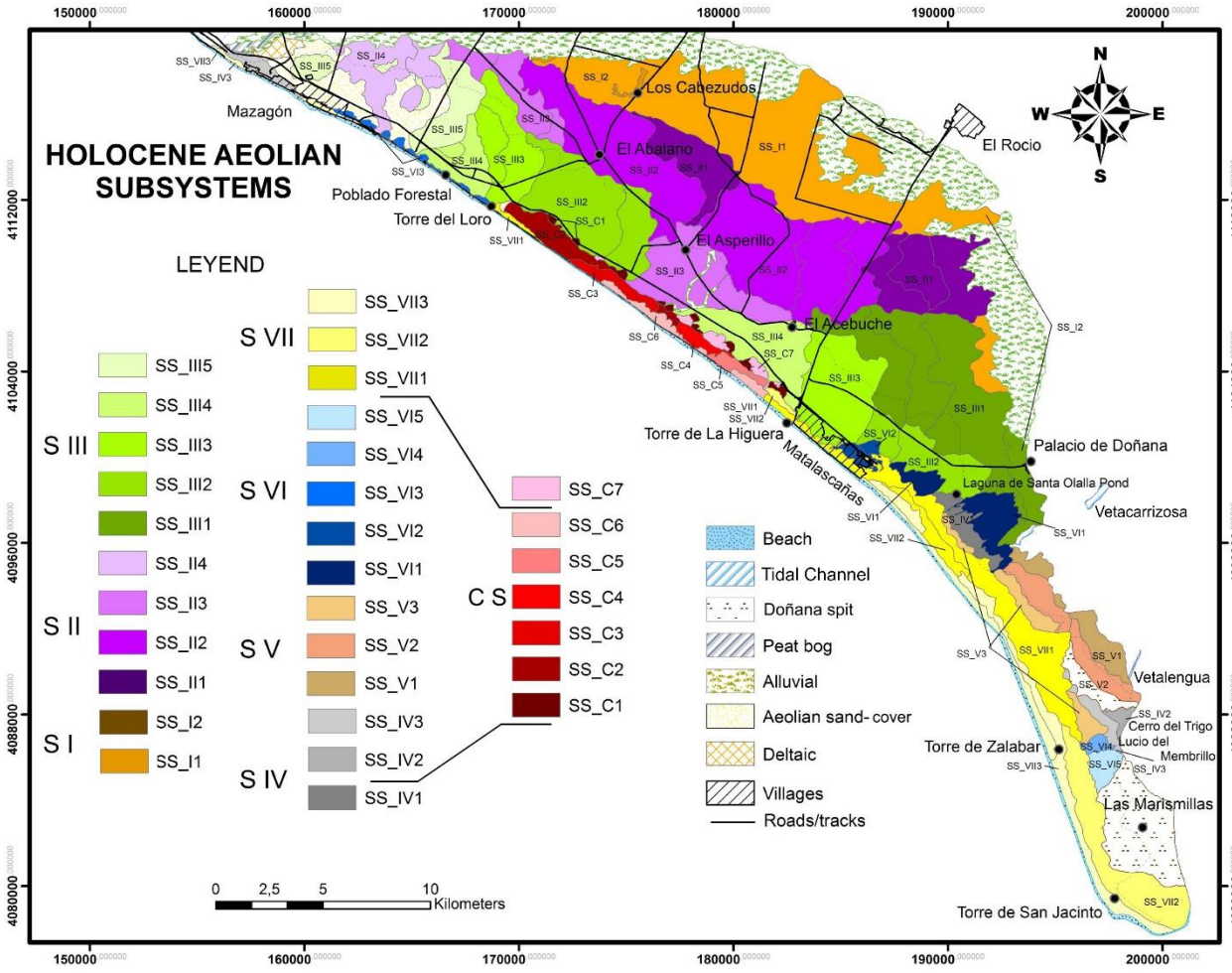

184

185 Fig. 3. Map of dune systems and subsystems from the Doñana National Park. Each system is represented by
186 a colour and subsystems by a different tone of each colour. The sequence of systems and subsystems
187 sequence goes from older (S-I, SS-I1) to younger (S-VII, SS-VII3). CS and SSC correspond to Complex System
188 and subsystems.

189 The virtual 3D analysis was processed using the ArcScene and ArcGlobe of the GIS (ArcGis v10.8), to obtain

190 views of the terrain or the virtual scenes from several orientations, such as in Figures 4 and 5.

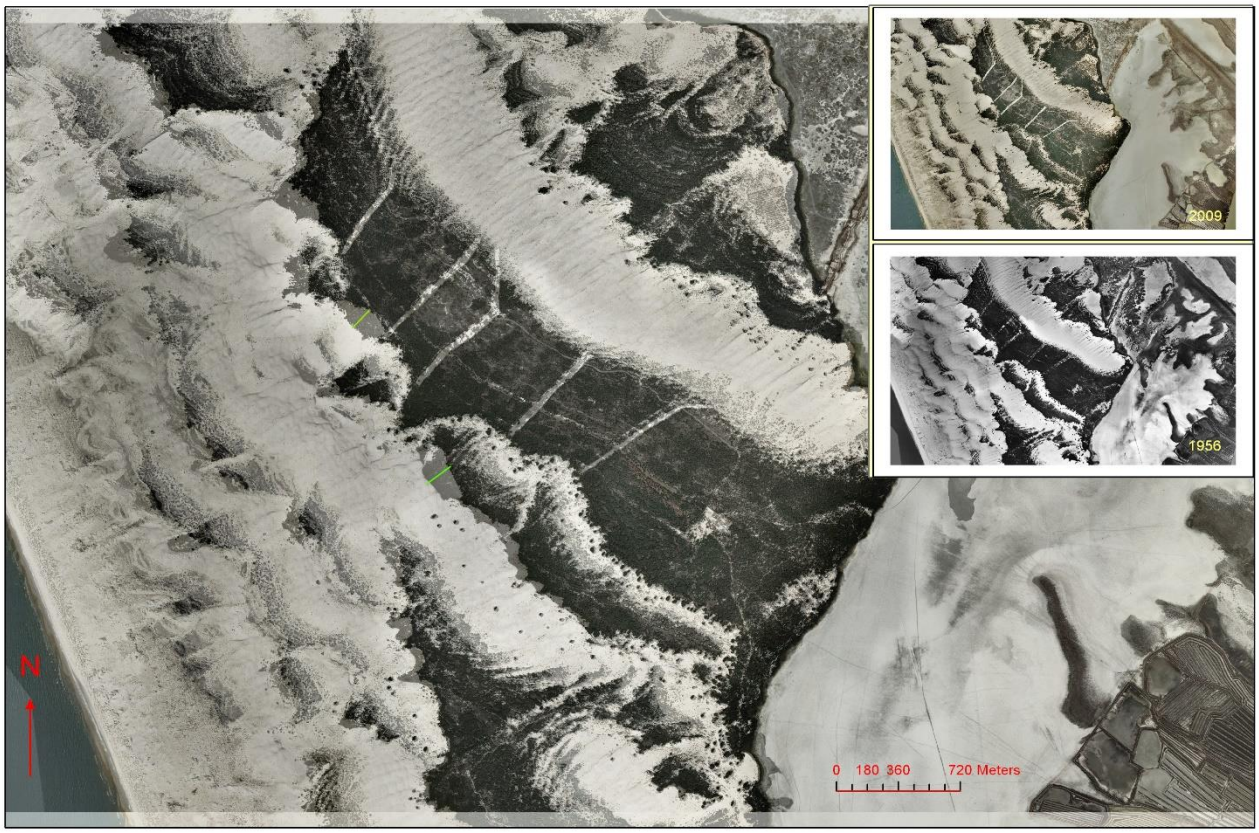

191

192 Fig. 4. Overlap of vertical photographic images (orthophotos) from 1956 and 2009 showing changes in dune
193 arrangements indicative of dune activity (greenish lines) during the 53 years period.

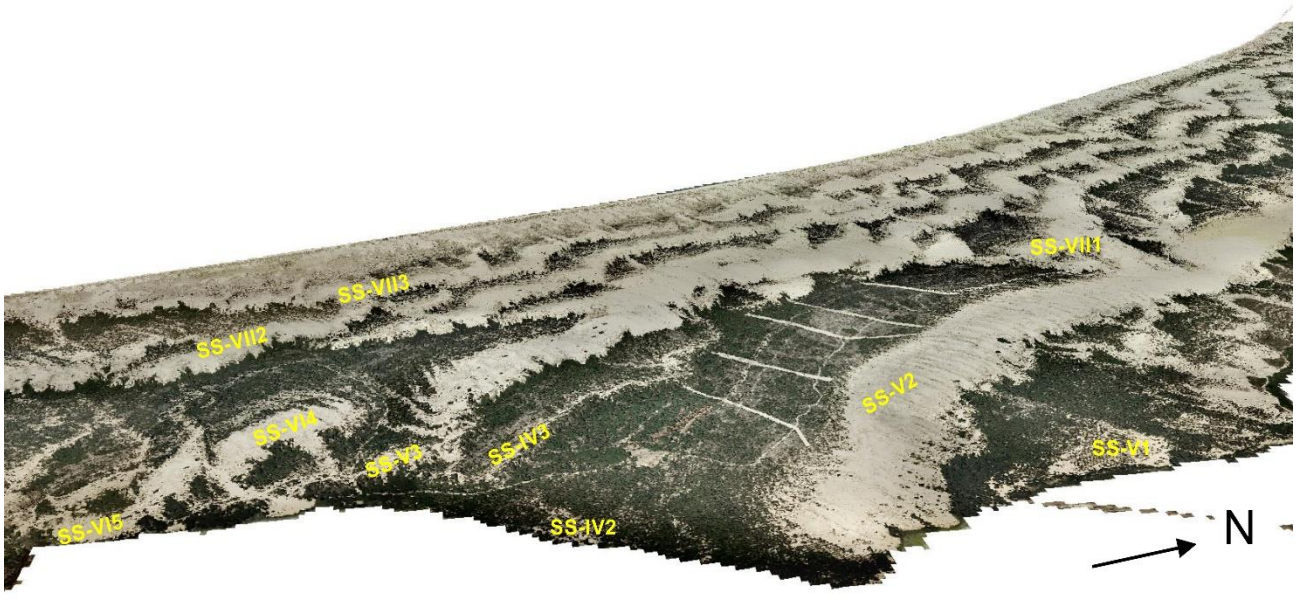

194

195 Fig. 5. Spatial relationship (overlapping) of various types of dunes from 3D images. Oblique photograph.

196

197 The digital elevation model (DEM) based on the Digital Terrain Model (DTM) with 5m resolution or pixel size
198 obtained with LIDAR data, improving the triangle irregular networks (TIN), allowed to draw contour curves
199 at an appropriate scale (1.5 and 10 m intervals). Using scrips of flow accumulation with GIS techniques, the
200 network of drainage pattern was reconstructed.

201 GIS techniques allowed calculations of the areas occupied by every dune system and subsystem, distances,
202 profiles, volumes, advances of dunes, and generation of models of evolution of Holocene dunes.

203 In this study eight aeolian systems (SI to SVII, plus a Complex System, CS) have been recognized (Fig. 2) on
204 the basis of prevailing wind directions at the time of accumulation, morphological type, degree of stability
205 and relative stratigraphic age, taking into account the inter-relation between systems, their relationships
206 with the Pleistocene paleo-dunes exposed in the cliff, and, in some cases, the position of the dune systems
207 and beach ridges in the Doñana spit, at the right, western, margin of the Guadalquivir river mouth.

208 The chronology of the system CS, placed along the littoral from Torre del Loro to Torre de la Higuera, is more
209 difficult to stablish because it is not connected to the other systems.

210 Dune systems (recognized by different colours), were subdivided in subsystems (SS) (different shades of
211 colours). Subsystems are composed of dune units, and have been conveniently separated with dotted lines
212 in the map (Figs. 2 and 3).

213 All these divisions and subdivisions are based upon the following criteria (Fig. 6): 1. Morphological type of
214 dunes (transverse, parallel, etc.); 2. Position and geometry of dune systems and subsystems (basal parabolic,
215 transverse, imbricate, etc.); 3. Paleo wind directions (measured in degrees); 4. Aeolian activity; 5. Size of dune
216 units and their progression (migration) fronts; 6. Degree of conservation; 7. Relations between systems,
217 subsystems and dune units (deduced from air photographs, and 2D and 3D images, (Figs. 4 and 5).

SYSTEM	SUB-YSTEM	NUMBER OF UNITS	PREVAILING WIND	DUNE MORPHOLOGY	DUNE ACTIVITY	ELEVATION (AREA km 2)	PRESERVATION	DATING	AGE ESTIMATE (Ka)	EVENTS BOND (BE)	EVENTS SEISMIC (*)	
COMPLEX SYSTEM	C_7	3	N40-50° E	Parabolic (shadow)	active	low (2)	good		0.15			
	C_6	1	~N 40° E	Recent transv.	active	high (2)	very good					
	C_5	4	~N 40° E ~N 70° E	Transv. imbr. Ph-4	semi-stable	very high (1)			0.7			
	C_4	4	N35-45° E	Transv. imbr. Ph-3	semi-stable	very high (1)						
	C_3	4	N35-45° E	Transv. imbr. Ph-2	semi-stable	very high (2)						
	C_2	4	~N 30° E ~N 60° E	Transv. imbr. Ph-1	semi-stable	very high (4)		1207 ± 106 1368 ± 108				
	C_1	3	N70-80° E	Basal parabolic	semi-stable	low (2)	good				*2.2	
VII	VII_3	4	~N 45° E	Transverse typical	active	low (14)	good		0.15			upper Holocene (Greenlandian)
	VII_2	4	~N 65° E	Transverse typical	active	high (14)				0.5 BE-0		
	VII_1	6	~N 55° E	Transverse typical	active	high (21.5)		661 ± 73	0.7			
VI	VI_5	6	~N 40° E	Parabolic	active	very high (2)	good					
	VI_4	1	~N 40° E	Transverse (barchanoid)	active	high (1)						
	VI_3	2	N50-70° E	Parabolic on cliff	active	middle (5)						
	VI_2	3	~N 65° E	Parabolic, hackle	active	low (2.5)						
	VI_1	3	~N 60° E	Parabolic	active	middle (8)		1200 ± 71 1118 ± 150	1.3			
V	V_3	3	~N 45° E	Transv. parabolic	active	high (2)	good			1.4 BE-1		
	V_2	2	~N 50° E	Transverse (large)	active	very high (13)						
	V_1	3	~N35° E	Transv. irregular (barchanoid)	active	low (5)			1.6			
IV	IV_3	3	~N 45° E	Transverse parabolic	semi-stable	high (5)	good					
	IV_2	4	~N35° E	Parabolic planar	semi-stable	low (1)	inter-medi-ate				*2.2	
	IV_1	3	~N 45° E	Transverse (barchanoid)	semi-stable	very low (3.5)	good		2.6			
III	III_5	3	~N 45° E ~N 135° E	Transverse (extense)	stable	middle ~3-6m (10)	inter-medi-ate			2.8 BE-2		middle Holocene (Northgryppian)
	III_4	2	~N 75° E	Transverse typical	stable	middle (18)	very good	2852 ± 164				
	III_3	2	~N 95-100° E	Transverse typical	stable	middle (27)		3660 ± 266 3773 ± 240 3835 ± 204				
	III_2	3	N60-70° E	Transverse parabolic	stable	middle (31)	good	4582 ± 249 4842 ± 575		4.3 BE-3		
	III_1	4	~N 90° E	Transverse typical	stable	middle ~10 m (42)	middle	5442 ± 768 5848 ± 595	5.9	5.9 BE-4		
II	II_4	2	~N 90° E	Transverse typical	stable	middle (11)	quite good					
	II_3	3	~N 100° E	Transverse typical	stable	middle (22)	quite good	7115 ± 421				
	II_2	3	~N 50° E	Transverse typical	stable	middle (59)	middle	8024 ± 457				
	II_1	3	N 70° E	Transverse typical	stable	middle (26)	bad sheet-flood		8.2	8.2 BE-5		lower Holocene (Megalayan)
I	I_2	2	~N 130° E	Parabolic	stable	middle (1.5)	good	8525 ± 715 9463 ± 678 9889 ± 668		9.5 BE-6		
	I_1	not visible	~N 45° E	Degraded (sheet flood)	stable	low (60)	poor	10101 ± 554 10761 ± 817	11.1	10.3 BE-7 11.1 BE-8		

Fig. 6. Summary of dune Systems and Subsystems with prevailing winds and directions of dune advance, morphological types, activity, preservation degree and chronology. Transv: transverse. Areas are indicated in square kilometers.

Lab. samples	Field samples	Grain size (μm)	Radionuclide concentrations				Cosmic dose rate (Gy Ka^{-1})	Equivalent dose (Gy)	Annual dose (μGy y^{-1})	**Age (yrBP)**
			U (ppm)	Th (ppm)	K_2O (%)	H_2O (%)				
1 -MAD-5445SDA	D08-1	2-10	0.01	8.06	0.65	0.50	0.91	6.19±0.25	2.17	2852±164
2 - MAD-5437SDA	D08-2	2-10	0.01	8.02	0.01	0.28	0.88	9.82±0.07	1.38	7115±421
3 - MAD-5446SDA	D08-3	2-10	1.22	1.28	0.18	0.51	0.86	14.95±0.21	1.48	10101±564
4 - MAD-5477SDA	D08-4	2-10	0.88	1.42	0.60	0.27	0.86	7.24±0.17	1.58	4582±249
5 - MAD-5447SDA	D08-5	2-10	0.15	3.18	0.01	0.46	0.86	9.71±0.05	1.21	8024±457
6 - MAD-5441SDA	D08-6	2-10	0.01	9.17	0.76	0.62	0.86	3.26±0.17	2.71	1202±71
7 - MAD-5464BIN	D08-7	2-10	0.01	9.26	0.31	0.74	0.77	6.52±0.18	1.70	3835±204
8 - MAD-5442BIN	D08-8	2-10	0.01	6.66	0.01	1.70	0.80	5.70±0.02	1.35	4222±285
9 - MAD-5478SDA	D08-9	2-10	0.01	1.66	0.10	0.69	0.68	1.44±0.01	0.92	1565±127
10 - MAD-5655SDA	D09-10	2-10	0.01	7.75	0.01	0.51	0.77	5.23±0.56	1.08	4842±575
11 - MAD-5656SDA	D09-11	2-10	0.47	3.06	0.01	0.15	0.77	5.79±0.47	0.99	5848±595
12 - MAD-5657SDA	D09-12	2-10	0.01	9.99	0.01	2.74	0.8	8.36±0.39	1.20	6966±559
14 - MAD-5658SDA	D09-14	2-10	1.25	2.69	0.01	3.85	0.85	71.03±2.72	1.59	44672±2813
15 - MAD-5660SDA	D09-15	2-10	1.68	0.01	0.37	3.01	0.9	16.75±1.07	1.77	9463±678
16 - MAD-5659SDA	D09-16	2-10	0.01	8.19	0.01	2.48	0.86	7.13±1.04	1.31	5442±768
17 - MAD-5661SDA	D09-17	2-10	0.77	0.01	0.01	6.45	0.78	6.11±0.57	0.92	6641±804
18 - MAD-5663SDA	D09-18	2-10	0.58	3.20	0.18	4.43	0.04	34.38±1.69	0.42	81857±6086
19 - MAD-5664SDA	D09-19	2-10	0.01	9.78	0.04	2.3	0.49	27.80±2.35	0.91	30549±3023
20 - MAD-5665SDA	D09-20	2-10	0.87	4.30	0.09	2.3	0.68	14.74±1.08	1.12	13160±1128
21 - MAD-5666SDA	D09-21	2-10	0.01	16.54	0.09	1.55	0.9	16.12±0.60	1.63	9889±688
22 - MAD-5662SDA	D09-22	2-10	0.17	4.66	0.01	1.99	0.77	8.44±0.48	0.99	8525±715
23 – MAD-5447SDA	DCHT 1.1	-	1.88	1.34	0.95	2.04	-	1.35	2.04	661±73
24 – MAD-5790SDA	DCHT 1.2	-	4.70	5.21	0.01	0.51	-	5.00	4.47	1118±150
25 - MAD-6342BIN	SQM 4	-	0.59	1.02	0.08	4.91	-	4.21	1.15	3660±266
26 - MAD-6343BIN	SQM 5	-	0.71	1.21	0.48	2.99	-	5.51	1.46	3773±240
27 - MAD-6384BIN	ATA 1	-	1.03	1.60	0.02	1.62	-	2.23	1.63	1368±108
28 - MAD-6387BIN	ATA 3	-	0.60	1.01	0.10	1.54	-	1.57	1.30	1207±106
29 - MAD-6146SDA	BME 4	-	1.33	1.18	1.33	2.95	-	13.99	1.30	10761±817

222 Table 1. OSL ages from samples of dunes.

Using these criteria we deduced a first relative chronology that narrowed the areas to be sampled for laboratory techniques such as optically stimulated luminescence (OSL), aimed at obtaining a more precise chronology (Table I, Figs. 1 and 6). Aeolian activity was deduced from comparison of air photographs taken in 1956 and 2009, and additional criteria, viz. antiquity, position of water table, dune morphology, and so on. Three main groups of dunes were separated: stable (no changes observed), semi-active (small, metric-sized displacements) and active (decametric migrations).

The first resulting map (Fig. 2) presents the Holocene aeolian dune systems with a geomorphological emphasis, indicated by different colours (I to VII, plus the CS, Complex System) and superimposed geomorphological symbols. The second resulting map (Fig. 3) includes the Holocene subsystems that are represented with a more chronological emphasis, as indicated by shades in the colours (increasing darkness with older relative age). A total of 25 subsystems have been described for the general sequence, plus 7 for the CS. This implies, obviously, a proposal of correlation between the CS and the other aeolian units.

4. Results

4.1. Pleistocene dune systems of Doñana

They crop out in the sea cliff between the localities of Mazagón and Matalascañas, forming the substratum of the Holocene dunes. They have been repeatedly studied but, here, we refer only to the paper by Zazo et al. (2005) because new radiogenic dating (OSL) and archaeological findings (lithic workshops) allow to refine the limits separating the Pleistocene and Holocene dune sequences and also the activity of the gravitational Torre del Loro Fault (TLF), both of which are closely related to the cartography of aeolian systems and their distribution, and the succession of depositional events after the late Pleistocene. The upthrown (Poblado Forestal) and downthrown (south of Torre del Loro) blocks of the TLF (Fig 7) were resampled and dated.

Downthrown block: In ascending order, the lower part of the cliff (0.5 m above the high tide mark) has been dated as ~82 ky BP. Previous data from the top part of this unit (~50 ky BP and 32 ky BP) point to a U-2 age for this unit. Just below a super-surface marked by a relatively-thick layer rich in organic matter aged 21 ky

247 BP (Fig. 7), a splinter with pseudolevallois shapes was found, the morphotechnological characteristics of
248 which are compatible with the typical middle Pleistocene cultures. The organic-rich layer marks the limit
249 between U-2 and U-3.

250 Unit 3 includes two erosional surfaces enriched in iron, including the occurrence of goethite, the oldest of
251 which (SsFe 1 in Fig. 7) is dated between 16 and 13 ky BP.

252 The last, uppermost, paleodune in the section (~9.9 ky BP in age) corresponds to the System I in this paper,
253 and it is topped by an mud-cracked, organic matter-rich layer. The sequence in the cliff ends with a degraded
254 layer rich in fragments of ferralithic crust, which corresponds to the erosional super-surface (SsFe2) at the
255 top of Unit 3 of Zazo et al. (2005).

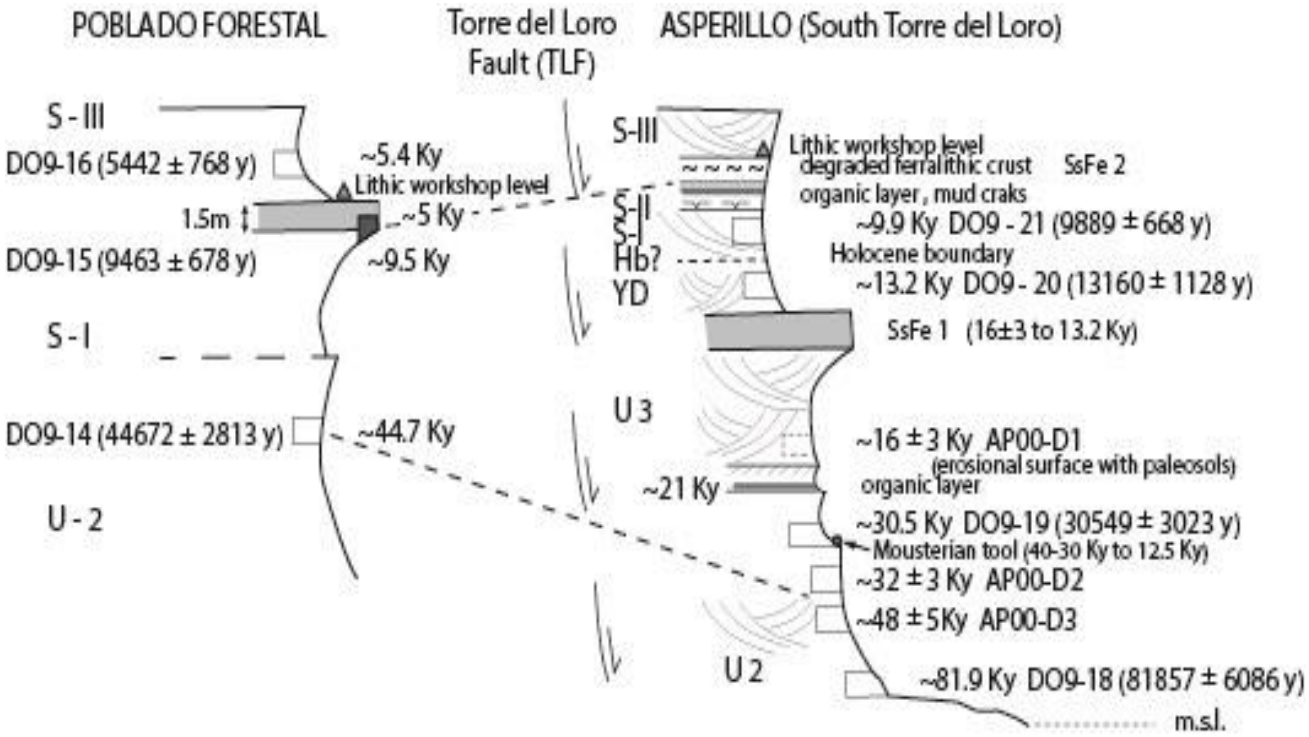

256

257 Fig. 7. Sketchy cross sections of the Asperillo Cliff between Poblado Forestal and SE Torre del Loro (TLF-Torre
258 del Loro F; Hb-Holocene boundary). U.2, U.3 (Pleistocene aeolian units defined by Zazo et al., 2005); S. I, S.II,
259 S.III (Holocene dune systems described in this work); DO09-19… and AP00-D1…: OSL samples.

260

Upthrown block: New sampling near the Poblado Forestal of Mazagón (Fig. 7) was aimed to refine the age of the top-cliff supersurface SsFe2, on top of which layers with lithic workshops of a post-Paleolithic context, mode 4, are found. The thickness of the ferralithic crust associated to this SsFe is 1.5 m, and the sample was taken 0.30 m below the top. The supersurface is covered by non-cemented aeolian dunes with OSL age 5.5 ky BP. In conclusion, and given de age of underlying S.I Unit, the age of the top-cliff supersurface SsFe2 is bracketed between 9.5 and 5.5 ky BP.

4.2. Holocene dune systems

The Holocene systems are mainly made up of transverse and parabolic dunes (Fig.2) accumulated in the last 11.7 ky. Eight of them have been defined: Systems I to VII, plus the CS, which is a lateral equivalent of part of SIV, V and VI. The big accumulation of sand in CS reaches locally 106 m in elevation. The restricted, narrow area that occupies this Complex System results from large scale gravitational sliding related to the uplift of El Abalario Dome; in fact, the conspicuous tectonic lineaments visible near the coast are slide scars. Sliding produced a void which was filled by the successive dune units forming the CS (Fig.1)

To interpret morphologically the parabolic dunes, we consider that they need an certain supply of sand, moderate to strong unidirectional winds and moderate vegetal cover. With increased sand supply, or reduced vegetal cover, parabolic dunes tend to evolve into the more mobile, transverse dunes. On the other hand, parabolic dunes can derive from transverse (stabilized or not), coastal foredunes, blowouts, transgressive dunes, etc. (Yan and Bear, 2015).

In some cases (Ardon et al., 2009) transverse dunes can evolve into parabolic, with not well-defined drag arms; this is rather usual in the study area. The occurrence of blowouts in the highest parts of transverse dunes is thought to indicate a deficit of sand (Pusty, 1988). This happens in the CS because the sea cliff separates the dunes from the active beaches nearby which supply sand. For this reason, parabolic dunes occur in the lee of system SS-C7 (Fig. 3). This is also the cause of the relatively high variability of dune morphologies (Fig. 6).

285 *4.2.1. Stable dune systems*

286 System I. It crops out in the north and northeast part of the study area. The main feature is the absence of
287 dune morphologies; for which reason it was named “aeolian sheet” by Leyva et al. (1975). Sand was supplied
288 by the Early Pleistocene Bonares Sands, a fluvial-deltaic deposit at the mouth of the Odiel and Tinto rivers,
289 that crop-out not far to the north, and transported by NW winds and former longshore drift. Two dune
290 subsystems (SS-I1, the older, and SS-I2, the younger) have been differentiated within this system. The first
291 one (SS-I1) occupies the largest area and it does not show any clear dune morphology because it is
292 crisscrossed by many creeks generated by the uplift of the Abalario Dome, and floods in these creeks
293 destroyed the dune fronts (Fig. 1 and 2). However, the distribution of some outcrops suggest that this
294 subsystem accumulated under winds blowing from the SW (Sheet 1 b).

295 The Subsystem I2 (SS-I2) is present only in the northern sector. It includes relatively well-preserved parabolic
296 dunes accumulated under NW winds and climbing over the degraded dunes of SS-I1 (Figs. 2 and 3, Sheet 1a
297 and b).

298 System II. This system partly covers S-I from the south, with a well-preserved dune front (Fig. 2, Sheet 1 a and
299 b). According with the prevailing winds that generated them (ranging from SW to NW), up to 11 dune units
300 have been distinguished and grouped into four subsystems (Fig. 3 and 6), very easy to separate thanks to
301 obvious superposition and neat, well exposed advance fronts.

302 SS-II1 and SS-II2 directly overlap SS-I1 and SS-I2 (Sheet 1a and b) while the younger subsystems (SS-II3 and
303 SS-II4) cover the older ones, with neat advance fronts and significant changes in wind directions (Figs. 2, 3
304 and 6).

305 System III. It is the most significant of the stable systems owing to its location and state of preservation. It
306 crops out in the central and north-western parts of the study area (Figs. 1, 2 and 3). In the central part it steps
307 on System II with two well marked, well preserved dune fronts (Fig. 2).

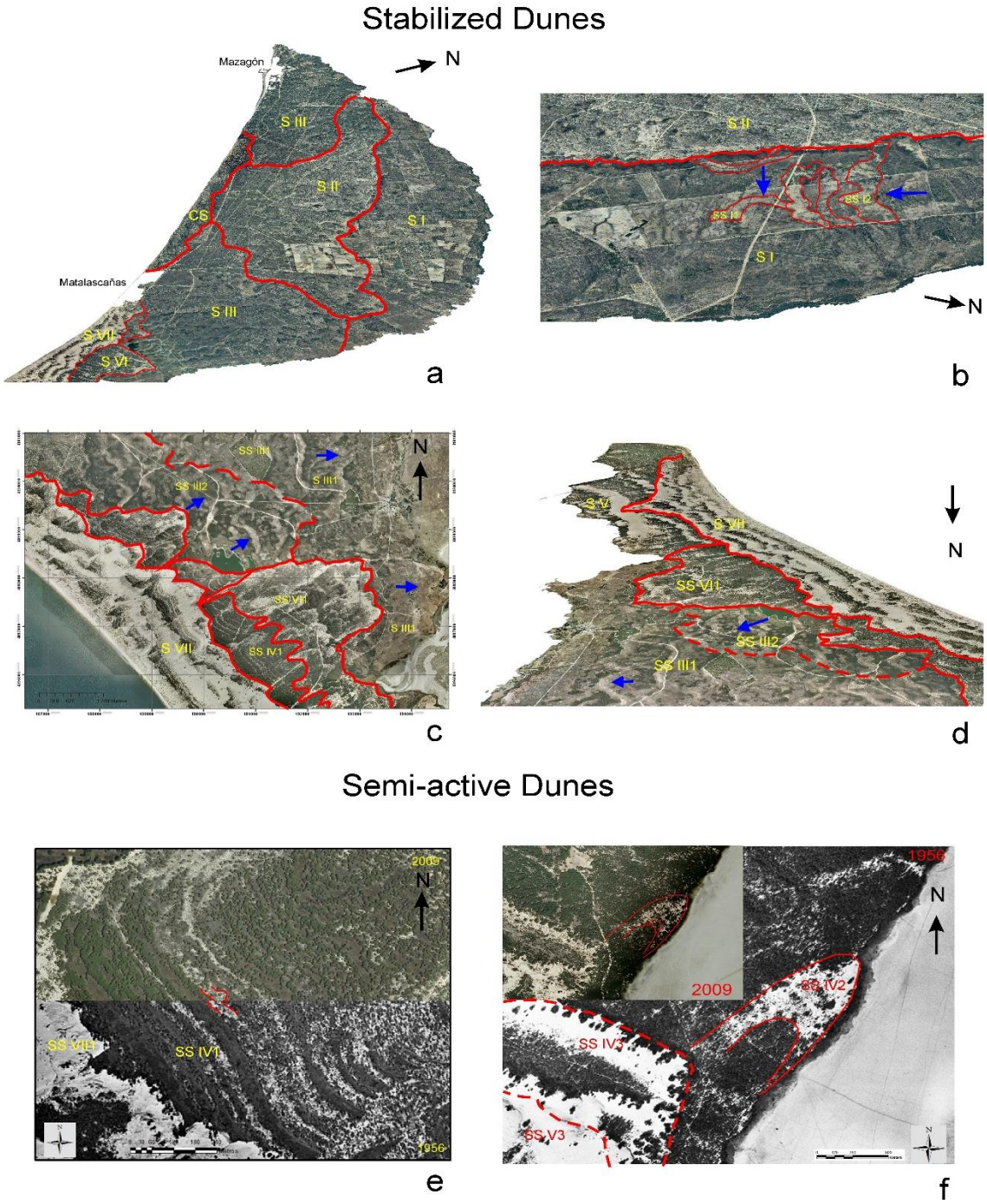

308

309 Sheet 1.: a) Ground plan distribution of dune systems I, II and III; b) Detail of the dune front of S-II over S-I;
310 SS-I1 and SS-I2 dune units and its wind directions (blue arrows); c) Relationship between dune systems S-III,
311 S-IV, S-VI and S-VII around Santa Olalla laguna (plan view, p.v.). Subsystems III1 and III" show different wind
312 directions (from N90E to N60-70E). d) oblique view (o.v.) of same area facing south; overlapping of SS-VI1
313 over SS-III2, SS-III2 over SS-III1 and S-VII over all of them. e) Detail of SS-IV1 (remains of barjanoids dunes).
314 Scarce movement between 1956 and 2009. f) SS-IV2 and SS-IV3 around Cerro del Trigo and marshland (Lucio
315 del Membillo). Scarce movement during the 53 years lapse. Sources: a and b: orthophoto PNOA 2007; c and
316 d: orthophoto PNOA 2009; e and f: 2009 orthophoto PNOA and 1956 aerial photo overlapping. Spatial
317 resolution MDT 5x5 m.

318 Five subsystems have been differentiated according to directions of prevailing winds and the superposition
319 of the transverse (with a slight parabolic component) dune fronts (Figs. 2, 3 and 6; Sheet 1c and 1d).

320 In the central zone (El Acebuche area, Figs. 2 and 3), dunes of SS-III1, migrating under winds from the W, step
321 on SS-II1 and SS-II2, that accumulated under winds from the SW. No direct relations between SS-III1 and SS-
322 II4 were observed in any of the two sectors, but there is a significant difference of ages measured in both
323 subsystems: SS-II4, sample 12, age 6966 y BP, SS-III1, sample 11, age 5848 y BP (Table I).

324 SS-III2, with winds from the SW (dune migration towards N60-70˚E), overlies SS-III1 in the north and NW of
325 Laguna de Santa Olalla (Fig.2 and Fig. 3), while SS-III3 steps on SS-III2 east of Matalascañas, under winds from
326 the west (dune migration towards N95-100˚E). SS-III4 is distinguished by a new change in wind direction,
327 from the SW (dune migration towards N75˚E), and SS-III5 outcrops only in the northern zone resting on SS-
328 III4 and SS-III3, with variable wind directions from SW (migration towards N45˚E) to the NW (migration to
329 N135˚E), what points to rapid changes in wind directions or seasonal winds (Fig. 8).

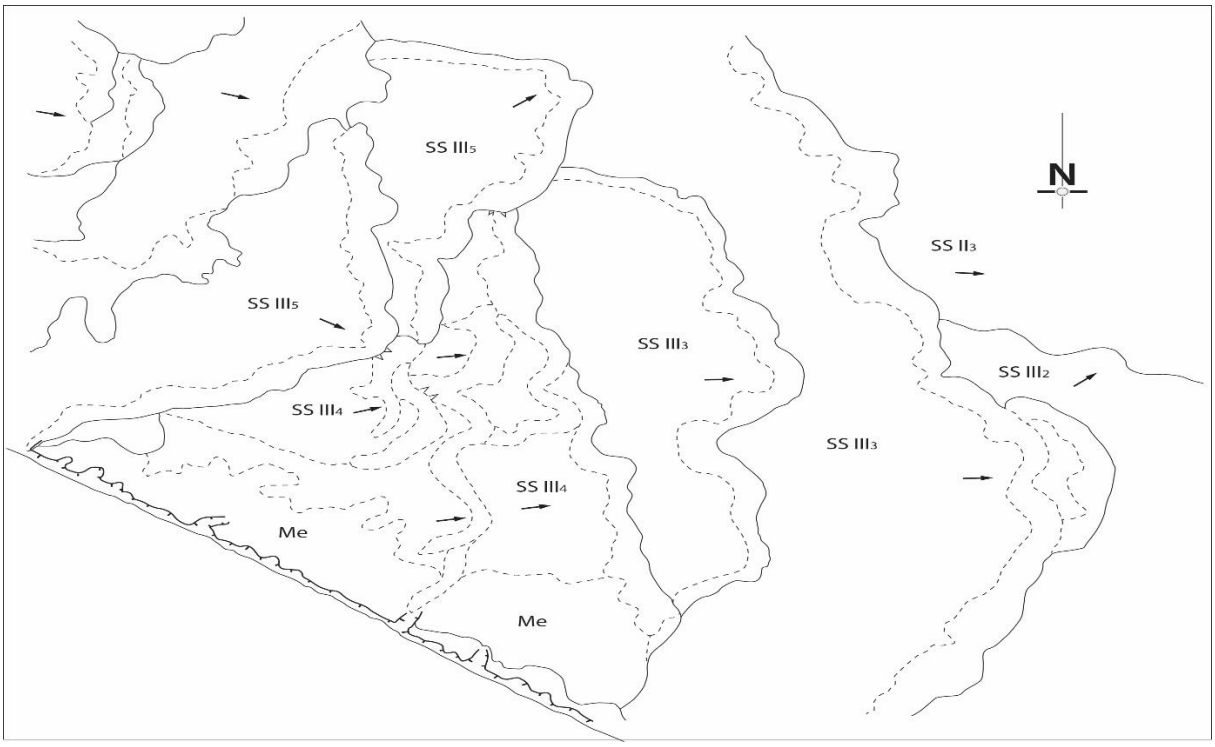

330

331 Fig. 8. Photogeological interpretation of System III between Mazagón and Poblado Forestal. Note the high
332 variability of prevailing wind directions deduced for SSIII-5.

333 *4.2.2. Semistable dune systems*

334 System IV. It crops only in the area occupied by the Doñana Spit (DS), from the south of Palacio de Doñana
335 to Lucio del Membrillo where it covers partially the sectors 1 and 2 of the spit, which are separated by the
336 tidal channel of Vetacarrizosa and limited to the south by the tidal channel of Vetalengua (Figs. 2 and 3).

337 A most relevant feature of System IV is that it is partly stabilized. It consists of three subsystems characterized
338 by their different dune morphology (Fig. 6) and their position on top of the Doñana spit, as long as wind
339 directions are quite constant in the three subsystems.

340 SS-IV1 rests on the older visible part of the Doñana spit (sector 1), south of Laguna de Santa Olalla (Fig. 3). Its
341 morphology is a rather flat sedimentary body made up of alternating clear and darker sandy strips which
342 curve convexly towards the direction of the prevailing winds. García Novo et al. (1975) referred to these strips
343 as “worms” and related their origin to fixation of the rear part of dune fronts by vegetation (Sheet 1c, 1e and
344 Sheet 2b), what evidences a very limited migration during the studied period. The resemblance of this system
345 of stripes with those of SS-V1 (irregular transverse to barchanoid) allows interpreting them as similar systems
346 that do no preserve the dune bodies (Sheet 3 a1 and a2).

347 SS-IV2 crops out to the NW of Lucio del Membrillo, on top of sector 2 of the Doñana spit (Fig.3), resting upon
348 an interdune depression (Corral de la Punta del Caño). It consists of rather low parabolic dunes with little
349 migration (Sheet 1f).

350 SS-IV3 is made up of transverse-parabolic dunes and covers the former SS-IV2 (Sheet 1f, Sheet 2a).

351 *4.2.3. Active dune systems*

352 System V. It is the first, older active dune system. It lays on top of sector 2 of the DS marked by large, extensive
353 transverse dune units, with various morphologies (Figs. 2 and 6). This system overlies System IV to the south
354 of Laguna de Santa Olalla and near Cerro del Trigo; it is overlain by the younger System VI north and south of

355 the DS, (Fig. 3). It is differentiated from the older System IV because an increased mobility and larger size of
356 dune units. Three subsystems (SS) have been distinguished: SS-V1 with transverse, barchanoid dunes having
357 lobate fronts that overly the oldest zone of the sector 2 of the dune sheet (DS) (Sheets 2a and 3a2). SS-V2
358 consists of large transverse dunes that reach up to 35m in elevation and 3x5 km in plant (Cerro de los
359 Ánsares). It is followed in the southern part by a large interdune through, up to 1.5 km wide (Fig. 3, Sheet 2a)
360 separating it from SS-V3.

361 In general, the mobility of these large dunes is smaller in the central parts as compared with the margins.
362 Vallejo and García (2013) estimated a displacement of 2 m/a in the last half century.

363 SS-V3 includes three parabolic, transverse dune units separated in a north-south direction. The oldest one
364 develops in the central sector, hence located more to the inner part of sector 2 of the Doñana spit, with a
365 well-developed advance front covering the previous SS (Fig. 3, Sheet 2a).

366 System VI. Includes the most characteristic parabolic dunes in the studied area, with various morphologies
367 (typical parabolic, hackle, cliff, and asymmetrical, (Figs. 2, 3 and 6). These are active dunes that have migrated
368 in the studied timespan. Rates of movement and dune sizes depend on the type of dunes. Six subsystems
369 and fifteen dune units have been identified within this System.

370 SS-VI1: well preserved, symmetrical parabolic dunes, with arms 1.5 to 2.5 km long. They show a low relief
371 ranging from 5 m (the oldest) to 15 m (the younger ones), and migration rates between 0.7 and 1.5 m/a
372 respectively. They step upon the SS-V3 and SS-IV1 to the south of Laguna de Santa Olalla (Sheet 1c and 1d,
373 Sheet 2b, Sheet 3a1).

374 SS-VI2: hackle parabolic dunes found west of Matalascañas. Dune bodies and arms are narrow, likely owing
375 to a deficit of sediment supply, as far as they accumulated in the transition zone from the retrograding to the
376 prograding areas of the coastline (Fig. 1). The aeolian activity is therefore smaller (migration rates between
377 0.2 and 0.5m/a) than in the former subsystem (Sheet 2c).

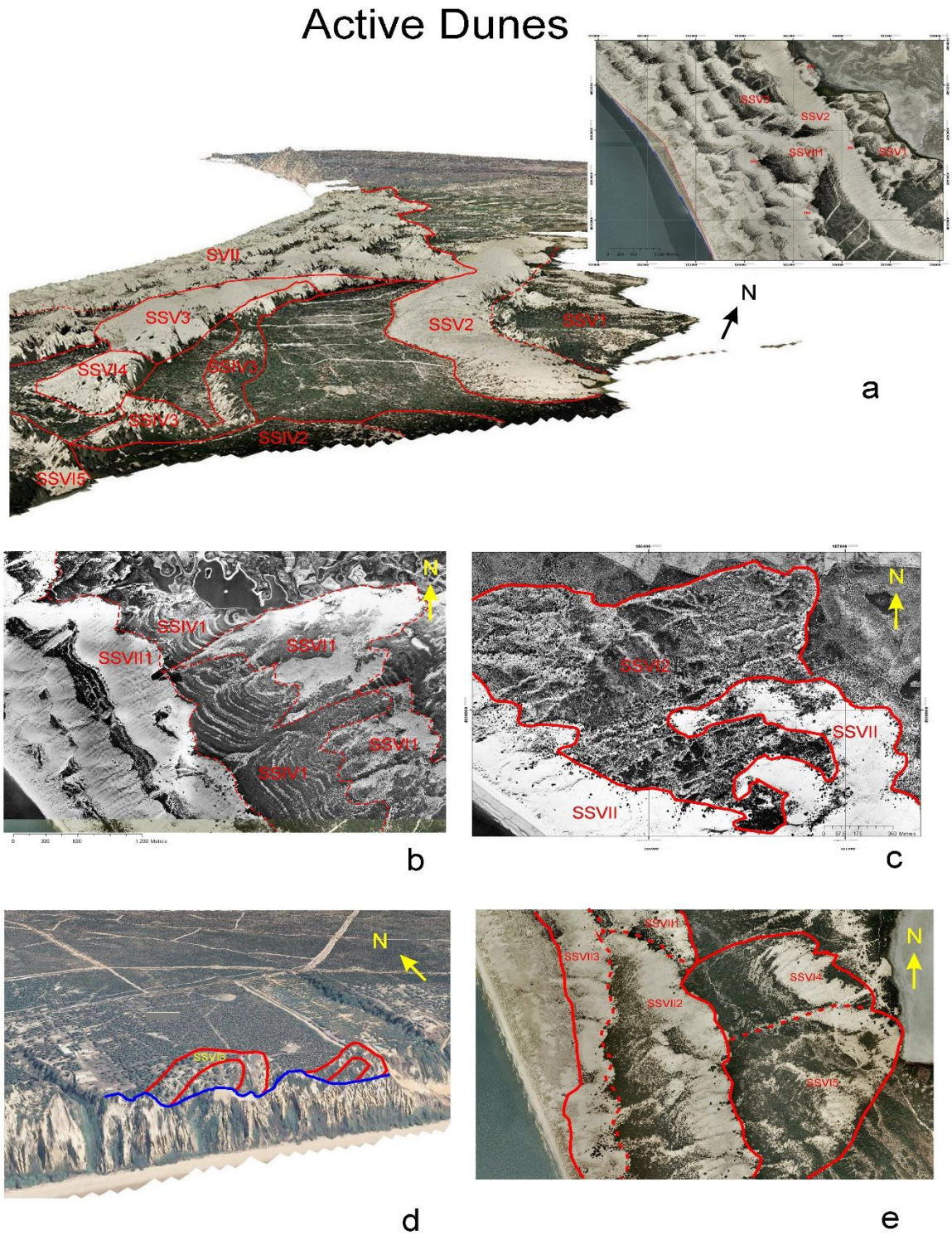

Sheet 2. a) Relationship between SIV, V, VI and VII. The first one (SIV) consists of semistable dunes, the other three (SV, VI, AND VII) are made of mobile dunes. Overlapping of SS-IV3 and SS-IV2; SS-V2 and SS-V1; SS-Vi and SS-IV3, SS-VII and SS-V2, and SS-VII1 and SS-V3. b) SS-VII1 parabolic dunes over SS-IV1 transverse dunes (barjanoids), SS-VII1 over two of them. c) SS-VI2 parabolic dunes under SVII transverse dunes. d) SS-VI3 parabolic dunes on cliff between Torre del Loro and Mazagon. e) SS-VI4 and SSVI-5 dunes over the spit bar and under SS-VII2 and SS-VII1. Origin of images: a: 2009 PNOA orthophoto, oblique view, and 1956 aerial photo, in plan; b and c: 1956 aerial photo; d: 2009 PNOA orthophoto; e) Plan views of 2009 orthophoto PNOA. Spatial resolution MDT 5x5 m.

SS-VI3: located at the northern part of the study area, it is found on top of the present sea-cliff between Torre del Loro and Mazagón; the rest on the stable dunes of Systems II and III, and aeolian sand cover (Fig. 3). This subsystem consists of parabolic dunes that, at present, migrate landwards very slowly, and have their arms cut off by the sea cliff as a consequence of the coastal retreat since the time of accumulation (Sheet 2d). Rates of cliff retreat to the south of Torre de la Higuera have been estimated as 0.7-0.8 m/a, which means a cliff retreat of 700-800 m in the last thousand years (Rodriguez Ramirez et al., 2014, 2019).

SS-VI4: it crops out in a small area to the west of Lucio del Membrillo. These are well-preserved barchanoid dunes, quite similar to those of SS-VI.1, that occur sandwiched between SS-VI.3 (below) and SS-VI.5 (above), (Figs. 3, 5, and Sheet 2e).

SS-VI5: parabolic dunes with better-developed arms and higher elevation and thickness towards the right-hand side (SE). It includes six dune units with decreasing dimensions in stratigraphically ascending order. The relatively larger size of the older dune systems seems to be related to an increased sediment supply in the northern area of the outcrop (Figs. 3, 5, and sheet 2e).

System VII. It consists of large, active transverse dunes with several advance fronts separated by interdune troughs (locally referred to as ‘corrales’), which accumulated under intense, maintained southwestern winds. Migration rates exceed 200 m for the considered half century time span. Some dunes exhibit a certain parabolic trend (Sheet 2 a, b, c, and e).

The dunes of System VII are best developed in the area between Torre de la Higuera and Torre del Zalabar (Figs. 2 and 3), with deflation surfaces and well-marked advance fronts separated by wide interdune troughs.

Up to fourteen superposed dune units can be distinguished, with a slight onlap towards the SW. These were grouped into three subsystems, according to variable wind directions, degree of activity, size and superpositions (Figs. 3 and 6, Sheet 2a and e, Sheet 3 a1 and a2).

409 Subsystem SS-VII1 is the most important according to its extension and number of units (6), but also for the
410 mobility (ca 200m in 53 years) and size of the dune units. The first four units are transverse, the fifth one is a
411 small-sized parabolic dune, and the sixth is a transverse dune. The size of the four transverse dune units
412 decrease towards the south. The first of them lays on top of the SS-VI.1 and 2 (Fig 3, Sheet 2b and c) and the
413 youngest upon the barchanoid dunes of SS-VI4 (Sheet 2e). The wide interdune troughs include counter-dunes
414 that look as elongate, narrow, flat-topped, sandy ridges related to the advance of the dune units (Sheet 2a
415 and 3 a.1) over areas of very shallow water table where vegetation partly traps the moving sand.

416 Dunes in this Subsystem migrate actively under strong south-westerly winds which moved the abundant
417 sediment constantly supplied by the Odiel and Tinto river mouths to the beach to be incorporated later to
418 the aeolian dunes, promoting advance rates in the central sector ranging from 2.4 to 3.8 m/y.

419 Subsystem SS-VII2 is similar to the previous one but with less extensive and lower dune units. It consists of
420 four dune units migrating towards N65˚E under winds from WSW (Fig. 6), clearly differentiating it from SS-
421 VII1. It consists of transverse dunes parallel to the dunes of SS-VII1 to which they overly (Sheet 3 a.2) both
422 north and south of Doñana spit (Fig.3). It is best represented to the south of the study area from Torre de
423 Zalabar to the extremity of the spit.

424 To the north of Torre de la Higuera this subsystem bypasses the former and advances downwind of it (Sheet
425 3 e).

426 Subsystem SS-VII3 consists of four dune units that overly the former subsystems. They are smaller than the
427 dune units of SS-VII2 and extend parallel to them all along the prograding sector of the DS, but with migrating
428 direction towards N45˚E (southwestern winds).

429 To the south of DS, the limit with the former subsystem is the dune where the Torre de San Jacinto was built,
430 which means an age around late 16th to early 17th century (De Mora Figueroa, 1981).

431

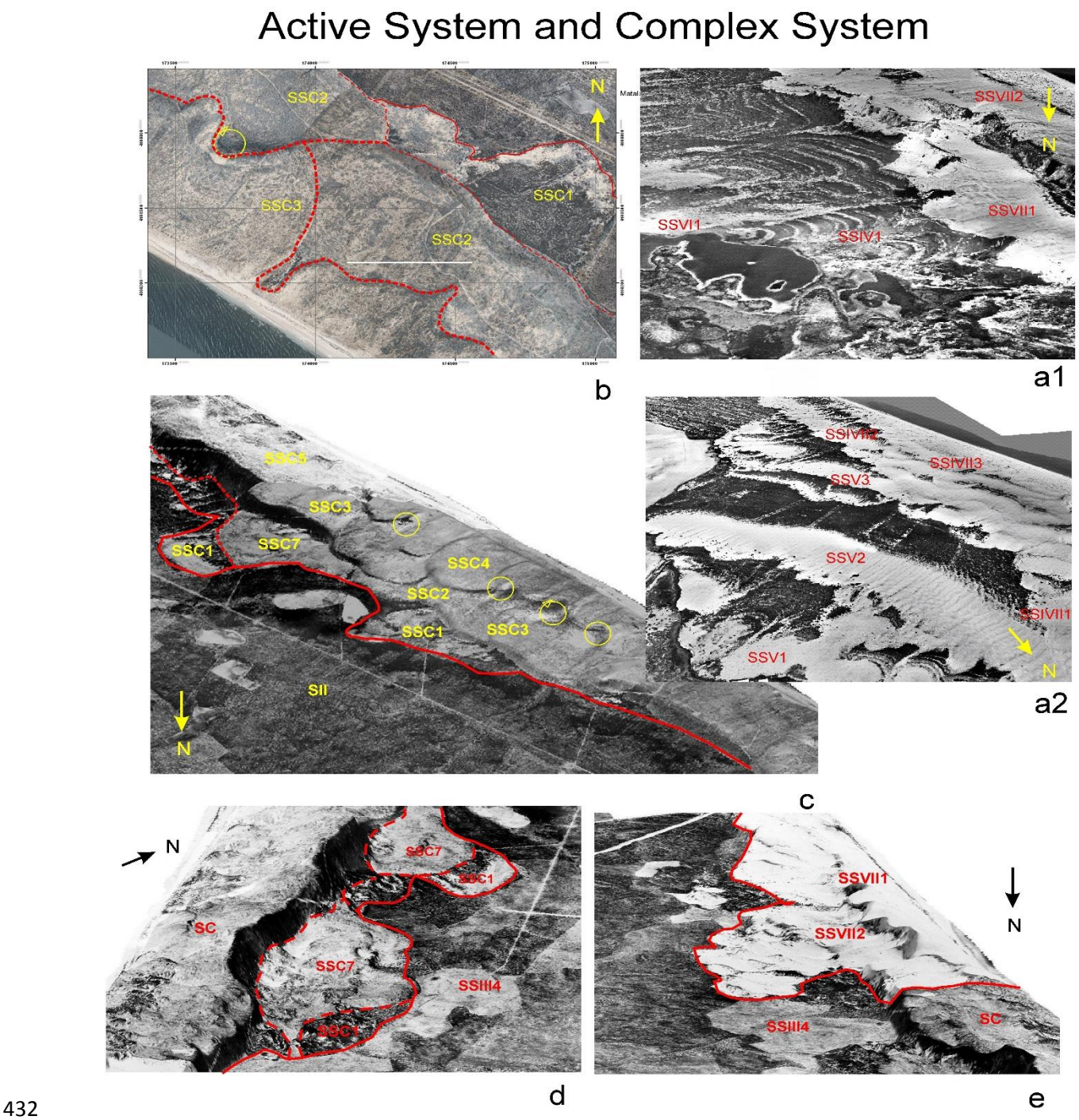

Sheet 3. Overlapping of dune subsystems. a1. Oblique view of the overlapping of SS-VI1, SS-Vi1, SS-VII1 and SSVII-2. a2) Overlapping between subsystems of SV, similarity of SS-V1 forms (worms), with SS-IV1 (see a1); b) Complex system; overlapping of dunes from SS-C3, SS-C2 and SS-C1. Dunes in the oldest SS are parabolic but are imbricated transverse in the others two; c) Complex system, overlapping of dunes, SC-1 is under Asperillo Dunes system SC-2, SC-3, SC-5 and SC-5 and over stable dunes from SS-IV4 and SS-II3. Blowout (yellow circles) indicate erosion, d) Shadow dunes from Complex System over SC-1 parabolic dunes and SS-III4; e) S-VII dunes over Complex System. In this case S-VII cover the internal zone and deposited over stable systems. Origin of images: a: oblique view 1956 aerial photo; b: overlapping of 2009 PNOA orthophoto and 1956 aerial photo; c, d and e: oblique view of 1956 aerial photo from MDT. Spatial resolution MDT 5x5 m.

442 Complex System (CS) is the most important dune complex of the study area and, consequently, of the Iberian
443 Peninsula littoral. The CS crops out between Torre del Loro (SE from Mazagón) and Torre de la Higuera (NW
444 of Matalascañas) along the erosional sea cliff cut in sediments from the Last Interglacial to the recent
445 Holocene (Zazo et al., 1999, 2005,2011).

446 The CS was first referred to as "coarse sands" (arenas gordas) by Pastor et al. (1976), Vanney and Menanteau
447 (1979),and Vanney et al. (1979). It was also named "stable dunes of the External System", (Rodríguez Vidal
448 et al. (1993), which Borja and Díaz del Olmo (1987, 1994) included in the Aeolian Mantle of Active Dunes
449 (AMAC). Rodríguez Ramírez (1998), on his turn, considered the CS as an active system in the recessing
450 (erosional) sector and included it in his systems IV and V.

451 We consider the CS as a part of the semi-stable (semi-mobile) aeolian dunes owing to their modest migration
452 rates in recent times. It is formed by a vertical stack of partly vegetated dune units (SS-C1 to C7) that, locally
453 (to the SE of El Asperillo), reaches elevations in excess of 100 m (Fig. 2). The system is being reworked at
454 present, as evidenced by numerous blowouts, because it is disconnected from the source area, the beach,
455 fed by the longshore drift. In some localities, to the lee of the complex, the blown sand feeds new dune units
456 (SS-C7) (Sheet 3, b and c). The transverse dunes of subsystems SS-C2 to SS-C6 moved under SW winds with
457 variable directions, and imbricate or step differently in each sector (Fig. 3)

458 The CS steps on fixed sands of Systems II and III (Fig. 2), but it is covered by System VII in both NW and SE
459 extremities of the outcrop (Torre del Loro and Matalascañas respectively, (Figs. 2 and 3).

460 *4.2.4. Chronology*

461 The chronological model is based on 29 OSL samples (Table 1), four of which corresponds to Late
462 Pleistocene dune units outcropping in the Asperillo cliff (Fig. 7), supporting previous chronologies assigned
463 to these aeolian dunes (Zazo et al., 2005), refining their ages and narrowing the age-intervals calculated for
464 the Super-surfaces. One of the samples (sample 20 in Table 1 and Fig. 10A, D09-20 in Fig. 7) gave an age

compatible with the Younger Dryas allowing us to mark more precisely the Late Pleistocene – Holocene Boundary (Hb in Fig. 7).

The other 25 samples have been plotted (Fig. 9) giving key clues for the Holocene climatic evolution of the area. Most Bond Events coincide with changes in prevailing winds and/or changes in the type of dunes (Fig. 6) remarked by changes in successive Systems/Subsystems. The chronology of the dune systems and subsystems accumulated during the Greenlandian, Northgrippian and early Meghalayan (Systems I to III) reveals a millennial cyclicity. In contrast, the more recent dune systems and subsystems (S.IV, V, VI and VII) exhibit a centennial cyclicity. Bond Events BE-5 (8.2ky BP), BE-4 (5.9 ky BP) and BE-1 (1.4 ky BP) have been reported to be the most prominent in the Iberian Peninsula (Cacho et al., 2010). In our case the change between System I and II (coincident with BE-5) is accompanied by a marked change in the direction of prevailing winds (Fig. 6). BE-4 marks the change between System II and III which is the most significant of the stable dune systems. Within system III, BE-3 and BE-2 are represented by changes in wind direction (Fig. 6). Finally, BE-1 marks the limit between System V and System VI, with a marked change in type of dune and sand supply.

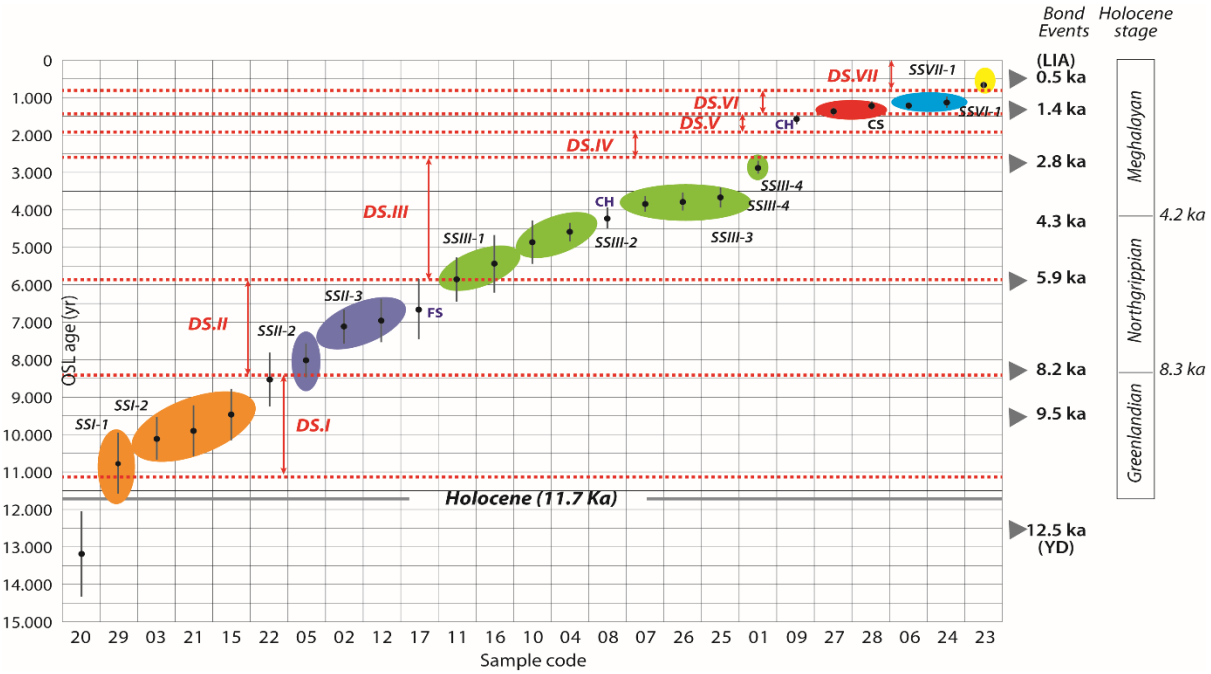

Fig. 9. Chronology of dune systems and subsystems based on the ages obtained from OSL dating (DS-Dune System, SS-Dune subsystem, CS-Complex system, FS-Fluvial System, CH-Tidal channel).

5. Discussion

A general chart has been prepared to present the results of this study and to extend the findings to other parts of Western Europe (Fig.10). The chart compares the aeolian dune sequence of Doñana (Fig.10 A) with aeolian deposits in the Iberian Peninsula and southern France (Fig.10 B) studied by a panoply of authors: Garcia-Hidalgo et al. (2007) in the Duero basin; Bernat and Pérez-González (2005 and 2008), Bernat et al. (2011) in Duero basin and La Mancha; Costas et al. (2012) in south Portugal; Clarke and Rendell (2006) in central and northern Portugal and, finally, Clarke et al. (2002) yielded numerical data about dunes in Aquitaine (southern France). Figure 10 C includes general papers dealing with Holocene climate changes deduced from lacustrine, estuarine, aeolian, marine and terrestrial (pollen) sedimentary records aimed to separate arid and humid periods, more or less prone to dune accumulation respectively, and to further refine the age of some of the recent subsystems. Remarkable selected papers are: Cacho et al. (2010) for the Iberian Peninsula; Schneider et al. (2016) for the coast of Algarve in southern Portugal; Martín-Puertas et al. (2008) in lake Zoñar (Córdoba, Southern Spain) who proposed a complete climatic sequence, particularly for the last 2000 years; Fletcher et al. (2007) and Fletcher and Zielhofer (2013), in southern Portugal; and, Jalut et al. (2000) for SE Spain and France. Figure 10 D presents the data from the two most significant areas with interconnected spit bar and dune deposits in Spain. In the study area, Zazo et al. (1994) and Borja et al. (1999) cited several aeolian systems (Systems IV, V, VI, and VII) related to the spit bar of Doñana. In the coast of Almería (SE Spain), the most complete and well dated coastal plain of the Iberian Peninsula has been described (12 in Fig. 10 D). The depositional history of these coastal deposits offers valuable information concerning the coastal dynamics, viz. phases of progradation and gaps in the systems related to climatic parameters and aridity vs. humidity.

The Bond Events (BE 1 to 9) (Bond et al., 1997, 2001) included in Fig. 10 A represent rapid (lasting from some decades to a couple of hundred years) oscillations which altered the climatic conditions during the Holocene (last 11.7 ky) with the exception of BE-9 which is older. Important regional differences have been described

506 for most Bond Events (Mayewsky et al., 2004) and, according to Cacho et al. (2010), the most significant ones
507 are BE-5 (8.2 ky BP), BE-4 (5.9 ky BP) and BE-1 (1.4 ky BP).

508 The sequence studied (Fig. 10 A) starts with the paleodunes outcropping below the SSFe1 in the downthrown
509 block of TLF along the coastal cliff (Fig. 7). The age of the dune immediately overlying this supersurface, is
510 13.2 ky BP (sample 20 in Table I; Figs. 7, and 10A), thus probably representing the aridity and cooling of the
511 Younger Dryas (YD) caused by a reorganization of the circulation pattern of the North Atlantic (Hughen et al.,
512 2000).

513 After the YD, the seven Holocene dune systems (SI to SVII, Fig. 10A) have been included in strips with the
514 same colours than in the general map (Fig. 2), separated by void spaces that represent moments of reduced
515 or null aeolian sedimentation. The age of dune systems and subsystems is stablished by our own
516 chronological data (Table I). A good correspondence comes out when comparing our results from Doñana
517 (Fig. 10A) with other dune systems of the Iberian Peninsula and southern France (Fig. 10B), the Holocene
518 climate data of Iberia and southern France (Fig. 10C), and the genetic relationships between spit bars and
519 associated dune systems, both in Atlantic and Mediterranean coasts of Spain (Fig. 10D).

520 Pre-Holocene dunes. There is good correspondence between our ages (13.2 ky BP, Fig.10A, OL and Sample
521 20 Table I) and those given for the Duero Basin and La Mancha (13.8 and 12.5 ky BP; see 1 and 2 in Fig. 10B)
522 and South Portugal (12.6 ky BP; see 3 in Fig. 10B) where they attribute them to the Younger Dryas. The same
523 occurs when comparing with the paleoclimate given by Cacho et al. (2010) between 13 and 11,5 ky BP
524 (reference 6 in Fig. 10 C) and by Fletcher et al. (2007) between 12,9 and 11,7 ky BP (reference 7 in Fig. 10C).
525 The cold and arid climate proposed by all these authors for this period fits well with the environmental
526 requirements for the accumulation of these dune systems.

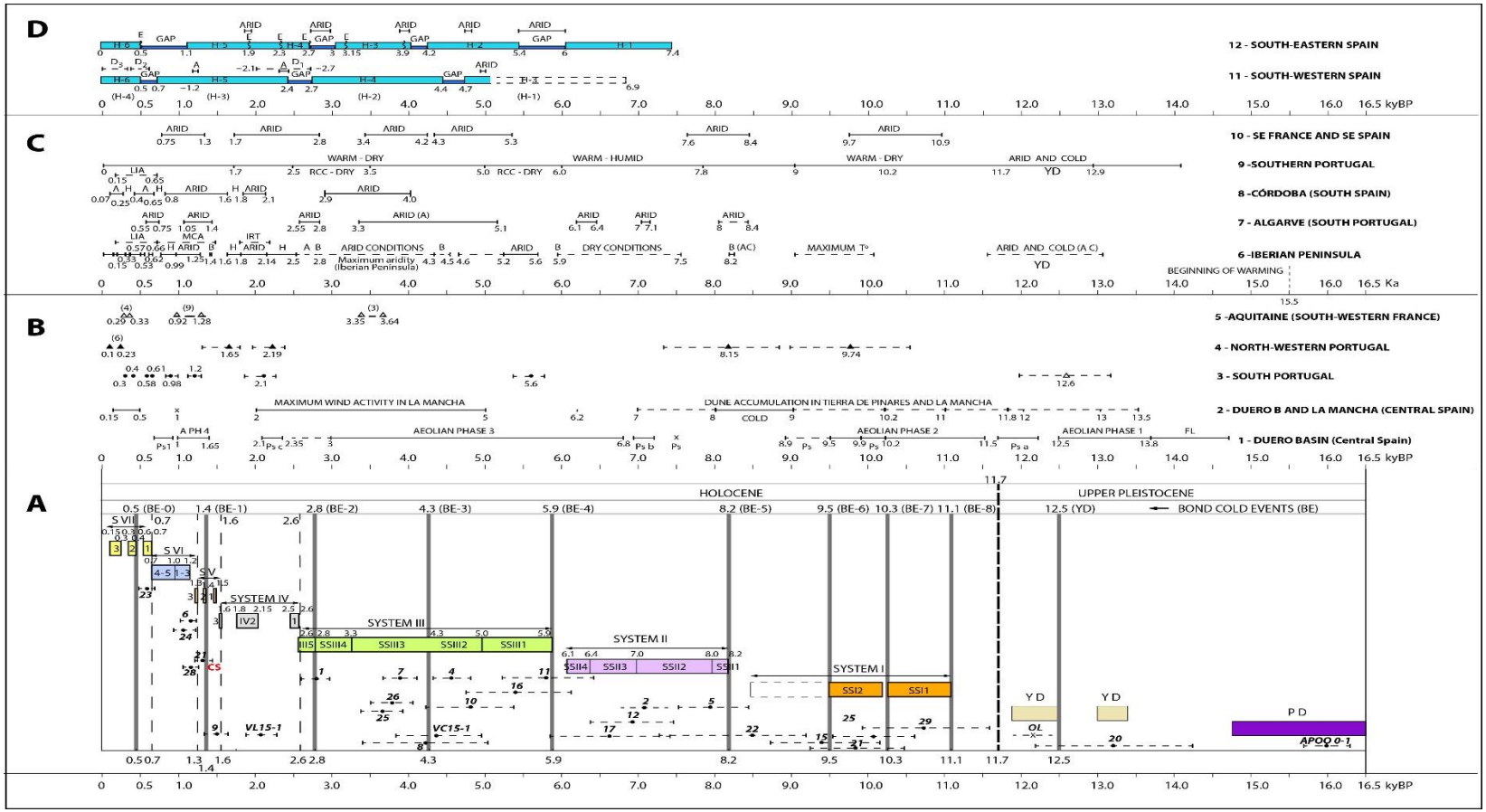

527

528 Fig. 10. A) Chronological synthesis of dune systems and subsystems (SS) included in this work. Same colors for dune Systems than in Fig. 3. PD-Paleodune, OL-Organic layer (age in
529 Zazo et al., 1999), YD-Younger Dryas, VL-Vetalengua, VC-Vetacarrizosa, 1,2,3…sample number, CS-Complex System. B) Iberian dune sequences studied by authors: 1. García-Hidalgo
530 et al. 2007; 2. Bernat and Pérez-González, 2008; Bernat et al., 2011; 3. Costas et al., 2012; 4. Clarke and Rendell, 2006; 5. Clarke et al., 2008. Ps: Paleosols; (4) number of dating
531 samples; FL-Fluvial. C) Climatic records from different locations in the Iberian Peninsula and France; 6. Cacho et al., 2010; 7. Schneider et al., 2016; 8. Martin-Puertas et al., 2008; 9.
532 Fletcher et al., 2007, Fletcher and Zielhofer, 2013; 10. Jalut et al., 2007. A: Arid, C: Cold, B: Bond, H: Humid, IRT-Imperial Roman Time, MCA-Medieval Climate Anomaly, LIA-Little Ice
533 Age. D) Spit bar systems from the Atlantic and Mediterranean coasts of Iberian Peninsula; 11. Zazo et al., 1994, Borja et al., 1999; 12. Goy et al., 2003, Zazo et al., 2008; H1,
534 H2…prograding units, GAP-Large swale, E-Erosion, D1, D2, D3-Dunes.

System I. Composed of two subsystems. The older SS-I1 appears very degraded and its dune units not preserving their morphology due to stream erosion (Fig. 2). An age between 11.1 ky BP (Bond Event BE-8) and 10.3 ky BP (BE-7) has been attributed to this system, based both on the age of sample 29 (10.8 ky BP), which is the oldest Holocene dating, and on the age of the next subsystem (SS-I2) (10.1 ky BP; sample 3, Table I). Subsystem SS-I2 crops out near Los Cabezudos, to the north of the surveyed area (Fig. 3). It is formed by well-preserved parabolic dunes, clearly superimposed to the previous SS (Sheet 1b). Similar chronologies have been obtained in dunes at El Asperillo cliff, on both sides of the Torre del Loro fault (Fig.7), with ages of 9.9 ky BP (sample 21), in the downthrown block and 9.5 ky BP (sample 15), in the upthrown one (Poblado Forestal = Forest Village). This latter sample has been collected at the base of the degraded iron supersurface SsFe2, represented as a ferralithic crust marking a period of non-deposition. These chronologies allow us to bracket the age of SS-I2 between 10.3 ky BP (BE-7) and 9.5 ky BP (BE-6), since at this age no dunes but only soil formation took place.

A maximum age range between 11.1 ky BP (BE-8) and 8.2 ky BP (BE-5) has been assigned to this System I. Nevertheless (Fig. 10A) we have considered as probable the age of 8.5 ky BP, which is the age of the youngest sample from this system, and 9.5 ky BP (BE-6) as a fixed limit (upper limit of the SS-I2), obtained from the sample of the cliff of El Asperillo (Forest Village) at the base of the degraded iron crust. The age of sample 22 (8.5 ky BP), could correspond to a new System I subsystem or to the beginning of the SS-II1.

These values correlate well with the Aeolian Phase 2, age 11.5 - 9.5 ky BP in the Duero basin (1 in Fig. 10B), and the long-lasting period of dune accumulation (13.5 to 7 ky BP) in Duero basin and La Mancha (2 in Fig. 10B), however punctuated by two periods of dune stabilization and soil formation at 11.8 and 10.2 ky BP. These authors correlate the first one with a climatic warming by the end of YD and the second may be equivalent to the limit between subsystems SS-I1 and SS-I2. Some dune units in the western Portuguese coast aged 9.7 ky BP (4 in Fig. 10B) are coeval to those of SS-I2.

558 The time span assigned to System I coincides with arid conditions in SE France and Spain (10 in Fig. 10C). In
559 Southern Portugal the warm and rather dry climate period between 11.7 and 9.0 ky BP was interrupted by a
560 rapid/short episode of extreme aridity around ca. 10.2 ky BP (9 in Fig. 10B).

561 System II. This system is clearly on top of S-I in El Asperillo cliff (Fig. 7) and covered by S-III in El Acebuche and
562 El Abalario areas (Fig. 3). OSL ages obtained for this unit (samples 2, 5, 12 and 17 in Table I and Fig. 10A) are
563 compatible with the interval between Bond Events BE5 and BE4 (Fig. 10A).

564 its age must be younger than 9.5 ky BP. It was assigned the interval between Bond Events 5 and 4, with
565 approximate age between 8.2 and 5.9 ky BP.

566 Chronologically, this system correlates well with the final part of the dune sequence of Tierra de Pinares in
567 Duero basin and La Mancha described by Bernat and Pérez-González (2008) and Bernat et al. (2011), (13.5 –
568 7 kyBP; 2 in Fig. 10 B) and the beginning (at 6.8 a 3 ky BP) of the Aeolian Phase 3 of García-Hidalgo et al.
569 (2007), (in Fig. 10B). In addition, the beginning of this system coincides approximately with the dunes
570 accumulated on the northwestern Portuguese coast dated at ca. 8.15 ky BP (4 in Fig. 10B).

571 Some periods of arid climate have been identified in SE France and Iberia between 8.4-7.6 ky (10 in Fig. 10C)
572 and also in the coast of Algarve (7 in Fig. 10C) at 8.2-7.7 kyBP, 7-7.1 kyBP and 6.4-6.15 kyBP. The changes in
573 wind directions that characterize the four subsystems differentiated within this System (Fig. 6) can be
574 correlated to these arid periods.

575 These can be used to date the subsystems distinguished inside System II by changes in wind directions and
576 superposition criteria (Fig. 6).

577 SS-II1 can be attributed to Bond Event BE-5 (ca. 8.2 ky BP) and correlated with dunes in northwestern Portugal
578 (4 in Fig. 10B) and Duero basin and La Mancha (2 in Fig. 10B). The overlying SS-II2 was dated at 8.0 ky BP
579 (sample 5 in Table 1 and Fig. 10A). Two samples collected from SS-II3 (samples 2 and 12 in Table I and Fig.
580 10A) were dated at ca. 7 ka, coeval with the final episodes of dune development in Duero basin and La

581 Mancha (2 in Fig. 10B), and the beginning of the Aeolian Phase 3 of Duero basin (1 in Fig. 10B). Cacho et al.
582 (2010) (6 in Fig. 10C) and Schneider et al. (2016) (7 in Fig. 10C) recognized an arid phase at ca.7 ky BP. The
583 scarcely-represented SS-II4 couldn't be sampled, but its geomorphological and stratigraphic position, allowed
584 us to we consider that it may be coeval to the arid period recorded in the Algarve coast (S Portugal) between
585 6.4 and 6.1 ky BP (7 in Fig. 10C).

586 System III. We estimate its age between 5.9 and 2.6 ky, so including Bond Events BE-4, BE-3 and BE-2 (Fig.
587 10A). Luminescence dating and morpho-stratigraphy suggest a correlation with the most recent part of the
588 aeolian phase PH3 of García-Hidalgo et al. (2007), between 6.8 and 3 ky BP, and probably including paleosol-
589 c dated at ca. 2.5 ky BP (1 in Fig. 10B). It correlates well also with the period of maximum aeolian activity
590 recorded in La Mancha between 5 and 2 ky BP (2 in Fig. 10B). Likewise, coeval dunes have been described in
591 southern Portugal at 5.6 ka BP (3 in Fig. 10B) and in Aquitaine between 3.64 and 3.55 ky BP (5 in Fig. 10B).

592 From the climate point of view, several arid episodes prone to dune generation have been recognized
593 between 5.6 and 5.2 ky BP (6 in Fig. 10C), 5.1 and 3.3 ky BP (7 in Fig. 10C), 5-1.7 ky BP (9 in Fig. 10C), and 5.3-
594 3.4 and 2.8-1.7 ky BP (10 in Fig. 10C). The beach ridges of Doñana spit also record two phases of reduced
595 coastal accretion (gaps) at 4.7-4.4 ky and 2.7-2.4 ky BP, interpreted as caused by reduced rainfall (Zazo et al.,
596 1994, Borja et al., 1999; 11 in Fig. 10C).

597 Five subsystems have been identified within this system:

598 Subsystem SS-III1, accumulated under westerly winds, was dated with two luminescence samples (samples
599 11: 5.8 kyBP and 16: 5.4 ky BP; Table I; Figs. 6 and 10A). It is correlated with the phase PH-3 of Duero basin-
600 Tierra de Pinares, 6.8 to 3 ky BP in age (García-Hidalgo et al., 2007), and southern Portugal with age 5.6 ky
601 according to Costas et al., 2012. This is a time of regional arid conditions, dated in the Iberian Peninsula
602 between 5.6 and 5.2 ky BP (Cacho et al., 2010); between 5.3 and 4.3 ky BP in SE France and SE Spain (Jalut et
603 al 2000); between 5.8 and 5.0 ky BP in western Portugal (Queiroz and Mathius, 2004 in Schneider et al. 2016);
604 between 5.9 and 4.8 ky BP in NE Iberia (Morellón et al., 2008), 5.2 and 5.0 ky BP in SW Iberia (Santos et al.,

605 2003), and between 5.5 and 5.0 ky BP in SE Iberia (Carrión et al., 2002). According to all these data, a
606 chronology for this subsystem between 5.9 and 5.2/5.0 ky BP is proposed here.

607 Subsystem SS-III2 overlies the former one, e.g. in Laguna de Santa Olalla, and accumulated under winds from
608 the SW (Fig. 2 and 6). OSL ages (samples 10: 4.8 ky BP, and 4: 4.6 ky BP; Fig. 10A, Table 1) make this subsystem
609 coeval with the middle part of aeolian phase PH-3 of Duero basin (1 in Fig. 10B) and the beginning of the
610 maximum aeolian activity in La Mancha (2 in Fig. 10B).

611 From a climate point of view, it coincides chronologically with the beginning of an arid phase that lasted from
612 5.1 to 3 ky BP in Algarve (7 in Fig. 10C), a period of aridity (4 to 2.8 cal kyr BP) in south Spain (lake Zóñar,
613 Córdoba, 8 in Fig. 10C), a dry-warm phase in southern Portugal that lasted from 4.8 to 1.7 ky BP (9 in. Fig
614 10C), the arid phase lasting from 5.3 to 4.3 ky BP in SE France and Spain (Jalut et al., 2000) and, finally, with
615 the oldest exposed sedimentary gap recorded in Doñana spit between 4.7 and 4.4 ky BP (11 in Fig. 10D).

616 According to all these criteria, and considering also the age of the overlying subsystem, we place
617 chronologically subsystem SS-III2 between ca. 5.0 and 4.3 ky BP.

618 Subsystem SS-III3 overlies the precedent, as observed NE from Matalascañas (Fig.2). OSL ages suggest a
619 duration between ca. 4.3 ky (more or less coincident with BE-4) and ca. 3.3 ky BP (samples 7, age 3.8 ky BP;
620 25, age 3.7 ky BP, and 26, age 3.8 ky BP; Table I and Fig. 10A). This time span coincides with moments of dune
621 accumulation in southern Duero basin, Aquitaine and maximum wind activity in La Mancha (1, 2 and 5 in Fig.
622 10B). We consider likely that the younger limit of this system coincides with an arid event at 3.3 ka BP (6 in
623 Fig. 10C) and with the final stages of the arid episode that lasted from 5.1 to 3.3 ky BP in El Algarve (7 in Fig.
624 10C). It is chronologically included in the period of aridity that extended from 4 to 2.9 cal kyr BP recorded in
625 lake Zóñar, Córdoba (8 in Fig. 10C); in the warm-dry period (3.5 to 2,5 ky BP) recorded in south Portugal (9 in
626 Fig. 10C), and in the final part of the arid period recorded in SE France and SE Spain (10 in Fig. 10C). The
627 system of beach ridges in Almería (SE Spain) also records a gap in sedimentation between 4.2 and 3.9 ky BP

628 (12 in Fig. 10D). At a supra-regional scale, a big drought affected the low latitudes between 4.2 and 3.8 ka BP,
629 when the Acadian Empire in Mesopotamia collapsed (Mayewski et al., 2004).

630 Subsystem SS-III4. This subsystem accumulated under southwestern winds and OSL age date it at ca. 2.85 ky
631 BP (Fig. 6; sample 1 in Table 1 and Fig.10A). This age makes it almost coeval to the end of PH-3 in Duero basin
632 (1 in Fig. 10B), coinciding partially with the phase of maximum wind activity recorded in La Mancha. SS-III4
633 can be climatically correlated also with an arid period recorded in the Algarve at 2.8-2.55 ky BP (7 in Fig. 10C);
634 a warm-dry phase recorded in the Western Mediterranean between 3.5 and 2.5 ky BP, peaked at 3.1 ky BP
635 (9 in Fig. 10C), and a large sedimentary gap in the coastal plain of Roquetas, Almería (12 in Fig. 10D). According
636 to all these data, we assign SS-III4 to an age between 3.3 and 2.8 ky BP, coincident with BE-2.

637 Subsystem SS-III5 includes dunes with not well-defined wind directions (from SW to NW, Fig. 6) which overly
638 the previous unit, as observed near the Poblado Forestal (Figs. 2, 3 and 8). No OSL data are available, but this
639 system is younger than 2.8 ky BP (SS-III4, sample 1 in Fig. 10A), well inside the period of maximum aeolian
640 activity in La Mancha (2 in Fig. 10B). Regarding climate, Schneider et al. (2016) record an arid climate, prone
641 to aeolian dune accumulation, between 2.8 and 2.55 ky BP in Southern Portugal (7 in Fig. 10C). Also, a humid
642 phase is recorded in Iberia between 2.5 and 2.1 ky BP, after a long-lasting period of aridity (6 in Fig. 10C);
643 and an arid phase between 2.8 and 1.7 ky has been recognized in SE Spain and France (10 in Fig. 10C).
644 Concerning the coastal environment, a sedimentary gap in the system of beach ridges in Doñana separates
645 the prograding spit units H3 and H4 between 2.7 and 2.4 ky BP (11 in Fig. 10D) with dune accumulation
646 between ca. 2.8 and 2.6 ky BP (Borja et al., 1999).

647 System IV. It is made up of almost-immobile, semi-stable dunes. Three subsystems have been distinguished
648 according to dune morphology (Fig. 6, Sheet 1e and 1f, Sheet 2a). Age assignations between 2.6 and 1.6 ky
649 BP are estimative, since it is younger than the youngest System III unit and covers the archaeological site of
650 Cerro del Trigo, ca. 1.8 ky, in the Imperial Roman Period (ca. 2.4 to ca. 1.8 ky BP).

651 Subsystem SSIV-1 consists of barchanoid dunes resting on top of the H1 (6.9-4.4 ky BP) prograding unit (not
652 exposed) of the Doñana spit, covering partially the younger part of prograding unit H2 (4.4-2.4 ky BP). For
653 this reason, it is assigned an age 2.6-2.5 ky BP, lying within the period of maximum aeolian activity in La
654 Mancha (5.0 to 2.0 ky BP; 2 in Fig. 10B). It is also coeval with a period of regional aridity recorded in the
655 Iberian Peninsula (2.6-2.45 ky BP; 6 in Fig. 10C) and in South Portugal (2.8-2.55kyBP; 7 in Fig. 10C) as well as
656 with a phase of rapid change to dry conditions recorded in El Algarve between 3.5 and 2.5 ky BP (Fletcher
657 and Zielhofer, 2013). In the beach ridge system of Doñana spit the period between 2.7 and 2.4 ky shows a
658 gap due to reduced sediment supply and no progradation (11 in Fig. 10C).

659 Subsystem SSIV-2 consists of parabolic dunes resting on the prograding unit H2 of Doñana spit, i.e., it is
660 younger than 2.4 ky BP, and they fossilize the Roman site of Cerro del Trigo with age 4th Century (ca. 1700
661 to 1600 y BP; Menanteau, 1979). Two tombs separated by interstratified dune deposits fix the age of the
662 lower dune as older than 1700 y BP, whereas the overlying dune must be younger than 1600 y BP. Similar
663 ages have been attributed to dunes in South and North of Portugal (2.1 and 2.2ky BP; 3 and 4 in in Fig. 10B),
664 and they can be correlated to the climatic maximum of the Imperial Roman Time, between 2.14 and 1.8 ky
665 BP (IRT in Fig. 10C). This subsystem is assimilated chronologically to the lower dune recorded in lake Zóñar (8
666 in Fig. 10C) most likely accumulated during the arid period between 2.1 and 1.8 ky BP. All these data lead us
667 to suggest and estimated age between 2.15 and 1.8 ky BP for this subsystem.

668 Subsystem SSIV-3 covers the former (Fig. 2, Sheet 1f) including dunes that fossilize the Cerro del Trigo
669 archaeological site (estimated age ca.1.7-1.6 ky BP), so we assume an age of 1.6 ky BP for this subsystem
670 following the humid period between 1.8-1.6 ky BP) recorded in the Iberian Peninsula (6 in in Fig. 10C) and
671 lake Zóñar, Córdoba (8 in Fig. 10C).

672 System V. It is made up mostly of transverse dunes that rest on the H2 prograding unit of Doñana spit (4.4-
673 2.4 ky BP; 11 in Fig. 10D). In the absence of any isotopic or luminescence dating, its stratigraphic position

674 sandwiched between Subsystems IV-3 and VI-1 (Fig. 2, Sheet 2a), points to an age between 1.6 and 1.3 ka
675 BP.

676 Subsystem SSV-1 rests upon the tidal channel of Vetalengua dated as 2.1 ka (sample VL-15.01) and 1.6 ka
677 (sample 9; Table 1, Fig. 10 A), the latter collected some 500 m away from the spit, may be the age of these
678 dunes. Similar ages have been recognized in dunes from the western coast of Portugal (1.485 ky BP; 5 in Fig.
679 10B), so we propose an age between 1.6 and 1.5 ky BP for this subsystem.

680 Subsystem SSV-2 includes two very large, active, transverse dune units (Cerro de los Ánsares) younger than
681 the previously described subsystem. Considering these data and the record of an arid episode between 1.4
682 and 1.05 ky BP in the coast of Algarve (7 in Fig. 10C) and between 1.6 and 0.8 ky BP in lake Zóñar (8 in Fig.
683 10C, we propose an age of ca. 1.4 ky BP for this subsystem, coincident with BE-1.

684 Subsystem SSV-3 includes three dune units, smaller than the former ones, and locally resting on top of them
685 (Fig. 2, Sheet 2a, Sheet 3a2). Its age is bracketed between the previous subsystem (SSV-2, 1.4 ky BP) and the
686 following one (SSVI-1, 1.2 Ky BP), so we estimate an age of ca 1.3 Ky BP for this subsystem. Dunes of similar
687 ages have been described in the Duero basin (PH4, 1.4-1.0 ky BP; 1 in Fig. 10B), and Aquitaine (1.28-0.92 ky;
688 5 in Fig. 10B). Likewise, there is a record of arid periods prone to dune accumulation between 1.4 and 1.05
689 ky BP in the Algarve (7 in Fig. 10C), between 1.6 and 0.8 ky BP in lake Zóñar (8 in Fig. 10C) and between 1.8
690 and 0.7 ky BP in SE France and Spain (10 in Fig. 10C).

691 The ages estimated for these three subsystems of System V point to the occurrence of a centennial cyclicity
692 of dune development along this time span.

693 System VI. It includes several subsystems which extend N-S along the littoral, with assigned ages between
694 1.3 and 0.7 ky. Two OSL samples were dated as 1.2 and 1.1 ka (samples 6 and 24 respectively; Table I, Fig.
695 10A).

696 Subsystems SSVI-1 and VI-2 occupy the central littoral area. They are well preserved, active, parabolic (SSVI-
697 1) and parabolic-hackle (SSVI-2) dunes, the latter related to reduced sediment supply owing to its location
698 close to a retrograding sea cliff (Sheet 2 b and c). Migration rates have been calculated in 2m/yr and 0.5 m/yr
699 respectively.

700 Correlation with dune development and aeolian activity in Duero Basin (PH4, 1.65-1 ky BP; 1 in Fig. 10B),
701 southern Portugal (1.2 to 0.98 ky BP; 3 in Fig. 10B) and Aquitaine-France (1.28-0.92 ky BP; 5 in Fig. 10B), lead
702 us to estimate an age between ca. 1.2 and 1.0 ky BP or this subsystem.

703 Increased temperatures and aridity reigned in the Iberian Peninsula during the Medieval Climatic Anomaly
704 (MCA in Fig. 10C) between 1.4 to 0.7 ky BP. This was also recorded in Algarve (1.4 -1.05 ky BP; 7 in Fig. 10C),
705 in southern Spain (1.8-1.05 ky BP; 8 in Fig. 10C), in the Iberian Peninsula (1.25-0.99 ky BP; 6 in Fig. 10C) and
706 in SE France and SE Spain (1.3 – 0.75 ky BP; 10 in Fig. 10C).

707 Subsystem SSVI-3 consists of parabolic dunes along the upper line of the sea cliff which cover stable dunes
708 from System III (SSIII-5) between Mazagón and Torre del Loro, (Fig.3, Sheet 2d). The suggested age, ca. 1.2
709 ka, is the same as other parabolic dunes elsewhere in the Iberian Peninsula (1 and 3 in Fig. 10B).

710 Subsystems SSVI-4 and VI-5 cover the sector 3 of Doñana spit and we consider them younger than the
711 subsystems just described above, i.e. younger than 1.2 ky BP. SSVI-4 includes only a single transverse to
712 barchanoid dune unit whereas SSVI-5 consists of six asymmetric, parabolic dune units, (Fig. 3, Sheet 2e).
713 Assuming that they are younger than 1.2 ky BP, they must be coeval with the arid period and dune
714 stabilization recorded in Duero basin and La Mancha at ca. 1.0 ky BP (2 in Fig. 10B) as well as with the dune
715 development occurred in south Portugal and Aquitaine (0.98 ky BP and 0,92 ky BP; 3 and 5 in Fig. 10B).
716 Additionally, an arid episode has been recognized in SE France and SE Spain between 1.3 and 0.7 ky BP (10 in
717 Fig. 10C) and in south Spain between and 1.6 and 0.8 ky BP (8 in Fig. 10C). Having all these data into
718 consideration, and also taking into account that these units rest on top of the oldest part of the prograding

719 unit H6 of Doñana spit (11 in Fig. 10D), the time span for accumulation of these subsystems can be narrowed
720 to 1.0 to 0.7 ky BP.

721 System VII. It includes large transverse dunes with several advance fronts that moved up to 200 m in the
722 surveyed period of 53 yr. They are separated by interdune depressions, locally called “corrales”. Some units
723 show certain parabolic trend (Figs. 2 and 3, Sheet 2a, b and e, Sheet 3 a1 and a2). There are at least fourteen
724 superimposed dune units that tend to onlap south-westwards. They can be grouped into three subsystems
725 according to wind directions, activity and dune size (Figs. 3 and 6). System VII rests on System VI (SS VI-5 and
726 6, attributed age between 1 and 0.7 ky BP) and is genetically related to the prograding units H5 and H6 of
727 Doñana spit (Table 1).

728 Subsystem SSVII-1. One OSL sample yielded an age of 0.66±0.73 ky BP (sample 23, Table 1, Fig. 10A). Dunes
729 of similar age (0.61 and 0.58 ky BP; 3 in Fig. 10B) occur in southern Portugal, while arid periods have been
730 also recorded in the Iberian Peninsula between 0.68 and 0.62 ky BP (6 in Fig. 10C), 0.75 and 0.55 ky (7 in Fig.
731 10C) and 0.65 and 0.40 ky BP (8 in Fig. 10C). Additionally, three erosional episodes at 675-600 yr BP, 500-450
732 yr BP and 400 yr BP (Zazo et al. 2008) have been recognized in de Doñana spit bar. With all these data, it is
733 proposed here that the age of this subsystem ranges between 700 and 600 yr BP.

734 Subsystem SSVII-2. It presents similar characteristics to the previous, underlying SSVII-1 and extends parallel
735 to it (Fig. 3, Sheet 2e and 3a1). Thus, it is younger than 700-600 ky BP but older than Torre de San Jacinto
736 (late 16th – early 17th century; de Mora Figueroa, 1989). Dunes of similar ages have been described in the
737 Duero Basin and La Mancha (500-150 y BP, 2 in Fig. 10B), and Southern Portugal (580-400 y BP; 3 in Fig. 10B).
738 This episode of dune development coincides roughly with an arid phase recorded in the Iberian Peninsula
739 between 570-530 y BP (6 in Fig. 10C), in South Portugal between 750 and 550 y BP(7 in Fig. 10C) and in South
740 Spain between 650 and 400 y BP (8 in Fig. 10C). An erosional phase is also recorded at 500-450 y BP in the
741 spit bar of Doñana Spit (11 in Fig. 10D). Consequently, and according to all these data we propose an age of
742 ca. 500-400 y BP for tis subsystem.

743 Subsystem SSVII-3. Smaller in extension and dune height than the previous subsystems, this one accumulated
744 closer to the coast along the Doñana Spit (Figs. 3 and 6; Sheet 2e and 3a3). In Duero Basin and La Mancha (2
745 in Fig. 10B) a phase of dune formation occurred between 500 and 150 y BP, as well as in South Portugal (400-
746 300 y BP; 3 in Fig. 10B), North Portugal (230-100 y BP; 4 in Fig. 10B) and Aquitaine (330-290 y BP; 5 in Fig.
747 10B). Climatically arid episodes of similar ages have been reported in the Iberian Peninsula between 330 and
748 150 y BP (6 in Fig. 10C), or between 250 and 75 y BP (8 in Fig. 10C). Thus, the age proposed for this subsystem
749 ranges from 350 to 150 y BP.

750 During the last 150 y, active foredunes accumulated to the south of Mazagón and along the present-day
751 beaches.

752 Complex System (CS). The chronology of this system is based on its morphological position with respect to
753 Systems III and VII: it overlies SS-III.4 (age ca 3.3- 2.8 ka BP) but is covered by SS-VII.1 (age ca 0.7-0.6 ka BP),
754 both in the northern (Torre del Loro) and southern (NW Matalascañas) sectors. We relate the origin of this
755 system to the occurrence of two fractures (Mazagón Fault and Torre del Loro Fault; MF and TLF respectively
756 in Fig. 1) generated as a result of a gravitational, rotational slide which supplied a large amount of sediment
757 to the shore that was redistributed by the dominant SE longshore drift to the beaches in this sector. Much
758 sand was later taken by the prevailing southwesterly winds and accumulated as an extraordinary dune that
759 reached some 100 m in elevation south of El Asperillo (Fig 2 and 3).

760 The active phase of these faults can be placed between SSIV-1 (2.6-2.5 ky BP) and SS IV-2 (2.15-1.8 ky BP),
761 coincident with the 8.0 magnitude seismic event located SW of Cabo San Vicente in 218 BC (2218 y BP),
762 (Campos, 1991; Lario et al.,2011) which affected the whole coast of the Gulf of Cadiz, including the present
763 study zone, and the human settlements prior to the 3rd Century BC. Some of these settlements were
764 abandoned (according to Rodríguez-Vidal et al., 2011; Rodríguez Ramírez et al, 2014) e.g. La Algaida spit in
765 the old Roman Lake Ligustinus, the present Marismas (marshlands) de Doñana. This earthquake provoked

766 large submarine slides in the vicinity of the Gorringe Bank (Atlantic Ocean), the probable epicenter of the
767 event, according to the Catalogue of the Geological Effects of Earthquakes in Spain (Silva et al., 2014).

768 The age of the first six SS of the Complex System can be encompassed between SSIV-2 and SSVI-5 (ca 2.2 ka
769 BP and 0.7 ka BP). The lower limit is assigned to the age of the seismic event whereas the upper limit coincides
770 with the oldest age of SVII which, as said before, fossilizes it towards the north and south.

771 SS-C.7 accumulated following the partial erosion of the oldest dunes of the Complex System, which implies
772 an age coeval, at least in part, to SVII.

773 **6. Conclusions**

774 This paper presents a geomorphological map of the Holocene dune systems that gathers information about
775 aeolian activity, morphology of the various dune types, directions of prevailing winds during the
776 accumulation of each system, and spatial arrangement and relative ages of these systems.

777 The map of the Holocene dune subsystems, actually a map of the Quaternary, represents chronologically the
778 main aeolian subsystems (25), and the correlation with the Complex System.

779 Regarding the Pleistocene dunes in the Asperillo sea cliff, the ages of the iron-enriched paleosurfaces (SsFe1
780 and SsFe2) have been adjusted according to the available data. The older one has been assigned an age
781 between 16 and 13 ky BP, whereas the younger one is ca. 9.5 ky BP in age.

782 A detailed chronology of the dune subsystems is also offered, based on an initial chrono-stratigraphy, OSL
783 age measurements, correlation with other dune systems in the Iberian Peninsula, Holocene climate events
784 and stratigraphic relations with the growing Doñana spit.

785 The age of Systems and Subsystems is presented graphically (Figs. 9 and 10 A). System I is Early Holocene
786 (Greenlandian) in age, System II and half of System III (SSIII-1 and SSIII-2) accumulated during the Middle

Holocene (Northgrippian), and the remaining SSIII-3, SS-III.4, SSIII-5 and Systems IV to VII are of Late Holocene (Meghalayan) age.

The chronological sequence of the dune subsystems reveals a double cyclicity: a millennial one for the subsystems of Early, Middle and early Late Holocene (S-I to S-III) and a centennial cyclicity for the younger ones (S-IV to S-VII).

The origin of the Complex System is related to neotectonics. The activity of Mazagón (MF) and Torre del Loro (TLF) gravitational faults generated a rotational slide which supplied large amounts of sediment to the coast, that were subsequently removed by longshore currents towards the E-SE.

The movement of Mazagón and Torre del Loro faults has been dated as 2.2 ky BP, the age of a magnitude 8.0 earthquake with epicenter SW off Cape San Vicente, which shook the whole Gulf of Cádiz including the area of Doñana. The Complex System has been assigned an age between 2.2 ky, coeval to S-VII, and 0.7 ky, equivalent to SSIV-2 to SS-VII-1, as the latter covers partially SS-C.6 near Matalascañas. SS-C.7 is equivalent to System VII.

Acknowledgements. Supported by Spanish FEDER-MINECO projects CGL15-69919-R and CGL2015-67169-P.

References

Ardon, K., Tsoar, H., Blumberg, D.G. 2009. Dynamics of nebkhas superimposed on a parabolic dune and their effect on the dune dynamics. Journal of Arid Environments, 73: 1014-1022.

Bernat Rebollal, M., Pérez-González, A. 2005. Campos de dunas y mantos eólicos de Tierra de Pinares (sureste de la Cuenca del Duero, España). Boletín Geológico y Minero, 116,23-38

808 Bernat Rebollal, M., Pérez-González A. 2008. Inland aeolian deposits of the Iberian Peninsula: Sand dunes
809 and clay dunes of the Duero Basin and the Manchega Plain. Palaeoclimatic considerations. Geomorphology,
810 102, 207–220.

811 Bernat Rebollar, M., Peréz_González, A., Rodríguez García, J., Bateman, M. D. 2011. Los sistemas eólicos del
812 interior de España: geomorfología eólica del Pleistoceno superior y del Holoceno de Tierra de Pinares y de la
813 Llanura Manchega (Capitulo 20). In: Las Dunas en España. Sanjaume, E., Gracia, F. J (Eds. Sociedad Española
814 de Geomorfología. 747 p

815 Bond, G., Shower, W., Cheseby, M., Lotti, R., Almasi, P., de Menocal, P., Priore, P., Cullen, H., Hajdas, I.,
816 Bonani, G. 1997. A pervasive millennial-scale cycle in North Atlantic Holocene and Glacial climates. Science
817 258, 1257–1266.

818 Bond, G., Kromer, B., Beer, J., Muscheler, R., Evans, M.N., Showers, W., Hoffmann, S., Lotti-Bond, R., Hajdas,
819 I., Bonani, G. 2001. Persistent solar influence on North Atlantic climate during the Holocene. Science 294,
820 2130–2136.

821 Borja, F. 1992. Cuaternario reciente, Holoceno y periodos históricos del SW de Andalucía. Paleogeografía de
822 medios litorales y fluvio-litorales de los últimos 30.000 años. Tesis Doctoral. Universidad de Sevilla, 520 pp.,
823 inédita

824 Borja, F., Díaz del Olmo, F. 1987. Complejos húmedos del Abalario (entorno de Doñana, Huelva). Oxyura 4
825 (1), 27-44

826 Borja, F., Díaz del Olmo, F. 1994. El acantilado del Asperillo: Cuaternario reciente y fases históricas en el litoral
827 de Huelva. Geogaceta, 15, 94-97

828 Borja, F., Díaz del Olmo, F. 1996. Manto eólico litoral (MEL) del Abalario (Huelva, España): Episodios
829 morfogenéticos posteriores al 22.000 BP. En: Dinámica y Evolución de Medios Cuaternarios (Pérez Alberdi,

A., Martini, A.P., Chessworth, W., Martínez Cortizas, A. (Eds.) Xunta de Galicia, Santiago de Compostela, Spain, 375 – 390.,

Borja, F., Zazo, C., Dabrio, C.J., Diaz del Olmo, F., Goy, J.L., Lario, J. 1999. Holocene aeolian phases and human settlements along the Atlantic coast of southern Spain. The Holocene, 9, 333 – 339.

Cacho I., Valero Garcés B., González Sampériz, P. 2010 . Revisión de las reconstrucciones paleoclimáticas en la Península Ibérica desde el último periodo glacial, In Clima en España: pasado presente y futuro. Pérez F. Fiz, Boscolo R. (Edit) 9-24 pp.

Campos, M.L. 1991. Tsunami hazard on the Spanish coasts of the Iberian Peninsula. Science of Tsunami Hazards 9, 83-90

Carrión, J. S. 2002. Patterns and processes of Late Quaternary environmental change in a montane region of southwestern Europe, Quaternary Science Reviews, 21, 2047-2066

Clarke, M. L., Rendell, H. M. 2006. Effects of storminess, sand supply and the North Atlantic Oscillation on sand invasion and coastal dune accretion in western Portugal, The Holocene 16,3, 341-355

Clarke, M. L., Rendell, H. M., Tastet, J.P., Clave, B., Masse L. 2002. Late-Holocene sand invasion and North Atlantic storminess along the Aquitaine Coast, southwest France (2002). The Holocene, 12,2, 231-238

Costas, S., Jerez, S., Trigo, R. M., Goble, R. Rebelo, L. 2012. Sand invasion along the Portuguese coast forced by westerly shifts during cold-climate events. Quaternary Science Reviews, 42, 15-28

Dabrio, C.J., Borja, F., Zazo, C., Boersma, R.J., Lario, J., Goy, J.L., Polo, M.D. 1996. Dunas eólicas y facies asociadas pleistocenas y holocenas en el acantilado de El Asperillo (Huelva). Geogaceta, 20, 1089 – 1092.

De Mora Figueroa, L. 1981. Torres de Almenara de la costa de Huelva. Excma. Diputación Provincial de Huelva. Instituto Padre Marchena, 19 pp.

851 Fletcher, W.J., Boski, T., Moura, D. 2007. Palynological evidence for environmental and climatic change in the
852 lower Guadiana valley, Portugal, during the last 13000 years. The Holocene, 17 (4): 481-494.

853 Fletcher, W.J., Zielhofer, C. 2013. Fragility of Western Mediterranean landscapes during Holocene rapid
854 climate changes. Catena, 103: 16-29.

855 Flores, E. 1993. Tectónica reciente en el margen ibérico suroccidental. Tesis Doctoral. Universidad de Huelva,
856 458 pp. Inédita.

857 García Novo, F, Ramírez, L. & Torres, A. 1975. El sistema de dunas de Doñana. Naturalia Hispánica, 5, 56 pp.

858 García-Hidalgo J. F., Temiño, J., Segura, M. 2007. Holocene aeolian development in Central Spain; chronology,
859 regional correlations and causal processes Quaternary Science Reviews 26, 2661–2673

860 Goy, J.L., Zazo, C., Dabrio, C.J., Lario, J. 1994. Fault-controlled shifting shorelines in the Gulf of Cadiz since 20
861 Ky BP. Abstract Volume, 1st symposium Atlantic Iberian Continental Margin, Lisbon, p. 24.

862 Goy, J.L., Zazo, C., Dabrio, C.J., Lario, J., Borja, F., Sierro, F.J., Flores, J.A. 1996. Global and regional factors
863 controlling changes of coastlines in southern Iberia (Spain) during the Holocene. Quat. Sci. Rev. 15, 773–780.

864 Goy, J.L., Zazo, C., Dabrio, C.J., 2003. A beach-ridge progradation complex reflecting periodical sea-level and
865 climate variability during the Holocene (Gulf of Almeria, Western Mediterranean). Geomorphology 50, 251–
866 268

867 Hughen K. A., Southon, J., Lehman, S. J., Overpeck, J. T. 2000. Synchronous radiocarbon and climate shifts
868 during the last deglaciation, Science, 290, 1951-1954.

869 Jalut, G., Esteban, A., Bonnet, L., Gauquelin, T., Fontugne, M. 2000. Holocene climatic changes in the Western
870 Mediterranean, from south-east France to south-east Spain. Palaeogeography, Palaeoclimatology,
871 Palaeoecology, 160, 255-290

872 Lario, J., Zazo, C., Goy, J.L., Silva, P.G., Bardají, T., Cabero, A., Dabrio, C.J., 2011. Holocene palaeotsunami
873 catalogue of SW Iberia. Quat. Int. 242, 196–200.

874 Leyva, F., Pastor, F., Goy, J.L. 1976. Mapa Geológico de España 1:50.000 (2ª serie). El Rocio (1018). Cartografía
875 1974. Instituto Geológico y Minero de España.

876 Leyva, F., Pastor, F., Zazo, C.; Goy, J.L. 1975. Mapa Geológico de España 1:50.000 (2ª serie). Palacio de Doñana
877 (1033). Cartografía 1973. Instituto Geológico y Minero de España.

878 Martín-Puertas, C., Valero-Garces, B. L., Mata, M. Pilar, Gonzalez-Sampériz, P., Bao, R., A. Moreno, Stefanova,
879 V. 2008. Arid and humid phases in southern Spain during the last 4000 years: the Zonar Lake record, Cordoba,
880 The Holocene, 18, 907-921.

881 Mayewski, P. A., Rohling, E. E., Curt Stager, J., Karlen, W., Maasch, K. A., David Meeker, L., Meyerson, E. A.,
882 Gasse, F., Van Kreveld, S., Holmgren, K. 2004. Holocene climate variability, Quaternary Research, 62, 243.

883 Menanteau, L., 1979. Les Marismas du Guadalquivir: Exemple de transformation d'un paysage alluvial au
884 cours du Quaternaire récent. (Thèse 3e cycle) , Université de Paris-Sorbonne, 252 pp.

885 Montes, C., Borja, F., Bravo, M.A., Moreira, J.M. 1998. Reconocimiento Biofísico de Espacios Naturales
886 Protegidos. Doñana: una aproximación ecosistémica. Consejería de Medio Ambiente, Junta de Andalucía, 311
887 pp.

888 Morellón, M., B. Valero-Garcés, T. Vegas, P. González-Sampériz, A. Delgado-Huertas, P. Mata, A. Moreno, M.
889 Rico, Corella J. P. 2009. Late glacial and Holocene palaeohydrology in the western Mediterranean region: the
890 Lake Estanya record (NE Spain), Quaternary Science Reviews, 28, 2582–2599

891 Pastor, F., Leyva, F., Zazo, C. (1976). Mapa Geológico de España 1:50.000 (2ª serie). El Abalario (1017).
892 Cartografía 1973. Instituto Geológico y Minero de España.

893 Pastor, F., Zazo, C. 1976. Mapa Geológico de España 1:50.000 (2ª serie). Moguer (1001). Cartografía 1973.
894 Instituto Geológico y Minero de España.

895 Psuty, N.P. 1988. Dune/beach interaction. J Coastal Res Special Issue No 3

896 Rodríguez-Ramírez, A., 1998. Geomorfología del Parque Nacional de Doñana y su entorno. Organismo
897 Autónomo Parques Nacionales del Ministerio de Medio Ambiente, Madrid (146 pp.).

898 Rodríguez-Ramírez, A., Flores, E., Contreras, C., Villarías-Robles, J.J.R., Celestino-Pérez, S., León, A., 2012.
899 Indicadores de actividad neotectónica durante el Holoceno reciente en el P. N. de Doñana (SO, España). In:
900 González-Díez, A., González-Díez, A., et al. (Eds.), Avances de la geomorfología en España, 2010-2012: Actas
901 de la XII Reunión Nacional de Geomorfología, Santander, 17-20 septiembre 2012. Publican, Ediciones de la
902 Universidad de Cantabria, Santander, pp. 289–292.

903 Rodríguez-Ramírez, A., Flores-Hurtado, E., Contreras, C., Villarías-Robles, J.J.R., Jiménez-Moreno, G., Pérez-
904 Asensio, J.N., López-Sáez, J.A., Celestino-Pérez, S., Cerrillo-Cuenca, E., León, Á., 2014. The role of neotectonics
905 in the sedimentary infilling and geomorphological evolution of the Guadalquivir estuary (Gulf of Cadiz, SW
906 Spain) during the Holocene. Geomorphology 219, pp. 126–140.

907 Rodríguez-Ramírez A., Villarías-Robles J.J.R., Pérez-Asensio J.N., Celestino-Pérez S. 2019. The Guadalquivir
908 Estuary: Spits and Marshes. In: Morales J. (eds.) The Spanish Coastal Systems, Dynamic Processes, Sediments
909 and Management. Springer, 517-541

910 Rodríguez-Vidal J, Rodríguez-Ramírez A, Cáceres LM, Clemente L (1993) Coastal dunes and post-Flandrian
911 shoreline changes. Gulf of Cádiz (SW Spain). INQUA Mediterr Black Sea Shoreline Subcomm News 15:12–15

912 Rodríguez-Vidal, J.; Bardají, T.; Zazo, C.; Goy, J.L.; Borja, F.; Dabrio, C.J.; Cáceres, L.; Ruiz, F.; Abad, M. 2014.
913 Coastal dunes and marshes in Doñana National Park. In: Landscapes and Landforms of Spain (F. Gutiérrez and

914 M. Gutiérrez, Eds.), World Geomorphological Landscapes, Springer Science + Business Media Dordrecht, 229-
915 238.

916 Rodríguez-Vidal, J., Ruiz, F., Cáceres, L.M., Abad, M., González-Regalado, M.L., Pozo, M., Carretero, M.I.,
917 Monge, A.M., Gómez, F. 2011. Geomarkers of the 218–209 BC Atlantic tsunami in the Roman Lacus Ligustinus
918 (SW Spain): a palaeogeographical approach.Quat. Int. 242, 201–212.

919 Ruiz-Labourdette, D., Coleto, C., Bravo, M. A., Borja, F., Borja, C., Montes, C., 2004. Complejo Palustre de los
920 arenales litorales de Doñana (E. 1:60000). Consejería de Medio Ambiente. Junta de Andalucía.

921 Santos, L., Sanchez-Goñi, M.F., Freitas, M.C., Andrade, C., 2003. Climatic and environmental changes in the
922 Santo Andre´ coastal area (SW Portugal) during the last 15,000 years. Quaternary climatic changes and
923 environmental crises in the Mediterranean Region, pp. 175–179.

924 Schneider, H., Höfer, D.,Trog, C., Mäusbacher, R., 2016. Holocene landscape development along the
925 Portuguese Algarve coast- A high resolution palynological approach. Quaternary International, v 407, 47-63

926 Silva, P.G.; Rodríguez Pascua, M.A.; Giner, J.L.; Pérez López, R.; Lario, J.; Perucha, M.A.; Bardají, T.; Huerta, P.;
927 Roquero, E.; Bautista, M.B. 2014. Catálogo de Efectos Geológicos de los terremotos en España. (Silva P.G.,
928 Rodríguez-Pascua M.A. Eds.). Serie Riesgos Geológicos / Geotecnia IGME. Vol., 4. Instituto Geológico y Minero
929 de España, Madrid. 350 pp.

930 Vallejo, I., García, D. 2013. Descripción de megaformas dunares en el sistema de dunas activas del P.N. de
931 Doñana. Geotemas, 14: 103-106. VII Jornadas de Geomorfología Litoral, Oviedo.

932 Vanney, J.R., Menanteau, L. 1979. Tipes de reliefs littoraux et dunaires en Basse- Andalousie. (De Huelva à
933 l'embouchure du Guadalquivir). Mélanges de la Casa Velázquez, 15, 5 – 52.

934 Vanney, J.R., Menanteau, L. , Zazo, C. 1979. Physiographie et evolution des dunes de basse andalousie (Golfe
935 de Cádix, Espagne). Actes de Colloques, 9, 277 – 286.

936 Vanney, J.R., Menanteau, L., Zazo, C., Goy, J.L. 1985. MF02. Punta Umbría- Matalascañas. Mapa fisiográfico
937 del litoral atlántico de Andalucía, E:1/50.000. Junta de Andalucía, Consejería de Política Territorial, Agencia
938 del Medio Ambiente. Sevilla, 1 mapa, 29 pp.

939 Yan, N., Baas, A. 2015. Parabolic dunes and their transformations under environmental and climatic changes:
940 Toward a conceptual framework for understanding and prediction. Global and Planetary Change, 124: 123-
941 148.

942 Zazo, C., 1980. El Cuaternario marino-continental y el límite Plio- Pleistoceno en el litoral de Cádiz. Tesis
943 Doctoral, Universidad Complutense de Madrid. Inédita

944 Zazo, C., Dabrio, C.J., Goy, J.L., Menanteau, L. 1981. Torre del Oro. Actas V Reunión G.E.T.C., Guía de la
945 excursión: Litoral de Huelva. Sevilla, 356 – 361.

946 Zazo, C., Goy, J.L., Somoza, L., Dabrio, C.J., Belluomini, G., Improta, S., Lario, J., Bardaji, T., Silva, P.G., 1994.
947 Holocene sequence of sea-level fluctuations in relation to climatic trends in the Atlantic-Mediterranean
948 linkage coast. J. Coast. Res. 10, 933–945.

949 Zazo, C., Dabrio, C.J., Borja, J., Goy, J.L., Lézine, A.M., Lario, J., Polo,M.D., Hoyos, M., Boersma, J.R., 1999.
950 Pleistocene and Holocene aeolian facies along the Huelva coast (southern Spain): Climatic and neotectonic
951 implications. Geol. Mijnb. 77, 209–224.

952 Zazo, C., Mercier, N., Silva, P.G., Dabrio, C.J., Goy, J.L., Roquero, E., Soler, V., Borja, F., Lario, J., Polo, D., Luque,
953 L., 2005. Landscape evolution and geodynamic controls in the Gulf of Cadiz (Huelva coast, SW Spain) during
954 the Late Quaternary. Geomorphology 68, 269–290.

955 Zazo, C., Dabrio, C. J., Goy, J. L., Borja, F., Silva, P. G., Lario, J., Roquero, E., Bardají, T., Cabero, A., Polo, M. D.,
956 Borja, C. 2011. El complejo eólico de El Abalario (Huelva). (Capitulo 16). En: Las Dunas en España (Eds.
957 Sanjaume, E., Gracia, F. J.). Sociedad Española de Geomorfología. 747 p

958 Zazo, C., Dabrio, C.J., Goy, J.L., Lario, J., Cabero, A., Silva, P.G., Bardají, T., Mercier, N., Borja, F., Roquero, E.
959 2008. The coastal archives of the last 15 Ka in the Atlantic-Mediterranean Spanish linkage area: sea level and
960 climate changes. Quat. Int. 181 (1), 72–87.Bailey, G.N., Reynolds, S.C., King, C.P., 2011. Landscapes of human
961 evolution: models and methods of tectonic geomorphology and the reconstruction of hominid landscapes.
962 Journal of Human Evolution 60, 257-280. DOI: 10.1016/j.jhevol.2010.01.004.

963

964

965

966

967

968

969

970 FIGURE CAPTIONS

971 Fig. 1. Location sketch of the dune systems (grey lines) with main active faults (in red) affecting the
972 area. Location of samples for OSL (yellow dots and numbers). Fault and/or alignments represented
973 are (from north to south): Huelva Fault (HF), Tinto River Fault (TRF), Huelva-Ayamonte Fault (HAF),
974 Las Madres Fault (LMF), Arroyo Rocina Fault (ARF), Mazagón-Acebuche Fault (MAF). Torre del Loro
975 Fault (TLF), El Rocio Fault (ERF), Continental Shelf Fault (CSF), Guardamar-Matalascañas Fault (GMF),
976 Palacio de Doñana Fault (PDF), Torre Carbonero-Mari López Fault (TCMLF), Madre de las Marismas
977 Fault (MMF), Bajo Guadalquivir Fault (LGF).

978

979 Fig. 2. Map of dune systems (colour) including morphological types of dunes, main wind directions,
980 degree of aeolian activity (stable, semi-active and active dunes) and areal distribution of systems
981 and subsystems (symbols). 1, 2 and 3 are sectors of Doñana Spit.

982

983 Fig. 3. Map of dune systems and subsystems from the Doñana National Park. Each system is
984 represented by a colour and subsystems by a different tone of each colour. The sequence of systems
985 and subsystems sequence goes from older (S-I, SS-I1) to younger (S-VII, SS-VII3). CS and SSC
986 correspond to Complex System and subsystems.

987

988 Fig. 4. Overlap of vertical photographic images (orthophotos) from 1956 and 2009 showing changes
989 in dune arrangements indicative of dune activity (greenish lines) during the 53 years period.

990

991 Fig. 5. Spatial relationship (overlapping) of various types of dunes from 3D images. Oblique
992 photograph.

993

994 Fig. 6. Summary of dune Systems and Subsystems with prevailing winds and directions of dune
995 advance, morphological types, activity, preservation degree and chronology. Transv: transverse.
996 Areas are indicated in square kilometers.

997

998 Fig. 7. Sketchy cross sections of the Asperillo Cliff between Poblado Forestal and SE Torre del Loro
999 (TLF-Torre del Loro F; Hb-Holocene boundary). U.2, U.3 (Pleistocene aeolian units defined by Zazo
1000 et al., 2005); S. I, S.II, S.III (Holocene dune systems described in this work); DO09-19… and AP00-
1001 D1…: OSL samples

1002

1003 Fig. 8. Photogeological interpretation of System III between Mazagón and Poblado Forestal. Note
1004 the high variability of prevailing wind directions deduced for SSIII-5.

1005

1006 Fig. 9. Chronology of dune systems and subsystems based on the ages obtained from OSL dating
1007 (DS-Dune System, SS-Dune subsystem, CS-Complex system, FS-Fluvial System, CH-Tidal channel).

1008

1009 Fig. 10. A) Chronological synthesis of dune systems and subsystems (SS) included in this work. Same
1010 colors for dune Systems than in Fig. 3. PD-Paleodune, OL-Organic layer (age in Zazo et al., 1999), YD-
1011 Younger Dryas, VL-Vetalengua, VC-Vetacarrizosa, 1,2,3…sample number, CS-Complex System. B)
1012 Iberian dune sequences studied by authors: 1. García-Hidalgo et al. 2007; 2. Bernat and Pérez-
1013 González, 2008; Bernat et al., 2011; 3. Costas et al., 2012; 4. Clarke and Rendell, 2006; 5. Clarke et
1014 al., 2008. Ps: Paleosols; (4) number of dating samples; FL-Fluvial. C) Climatic records from different
1015 locations in the Iberian Peninsula and France; 6. Cacho et al., 2010; 7. Schneider et al., 2016; 8.
1016 Martin-Puertas et al., 2008; 9. Fletcher et al., 2007, Fletcher and Zielhofer, 2013; 10. Jalut et al.,
1017 2007. A: Arid, C: Cold, B: Bond, H: Humid, IRT-Imperial Roman Time, MCA-Medieval Climate
1018 Anomaly, LIA-Little Ice Age. D) Spit bar systems from the Atlantic and Mediterranean coasts of

1019 Iberian Peninsula; 11. Zazo et al., 1994, Borja et al., 1999; 12. Goy et al., 2003, Zazo et al., 2008; H1,
1020 H2…prograding units, GAP-Large swale, E-Erosion, D1, D2, D3-Dunes.

1021

1022

1023 Table I. OSL ages from samples of dunes.

1024

1025

1026 Sheet 1.: a) Ground plan distribution of dune systems I, II and III; b) Detail of the dune front of S-II
1027 over S-I; SS-I1 and SS-I2 dune units and its wind directions (blue arrows); c) Relationship between
1028 dune systems S-III, S-IV, S-VI and S-VII around Santa Olalla laguna (plan view, p.v.). Subsystems III1
1029 and III" show different wind directions (from N90E to N60-70E). d) oblique view (o.v.) of same area
1030 facing south; overlapping of SS-VI1 over SS-III2, SS-III2 over SS-III1 and S-VII over all of them. e) Detail
1031 of SS-IV1 (remains of barjanoids dunes). Scarce movement between 1956 and 2009. f) SS-IV2 and
1032 SS-IV3 around Cerro del Trigo and marshland (Lucio del Membillo). Scarce movement during the 53
1033 years lapse. Sources: a and b: orthophoto PNOA 2007; c and d: orthophoto PNOA 2009; e and f:
1034 2009 orthophoto PNOA and 1956 aerial photo overlapping. Spatial resolution MDT 5x5 m.

1035

1036 Sheet 2. a) Relationship between SIV, V, VI and VII. The first one (SIV) consists of semistable dunes,
1037 the other three (SV, VI, AND VII) are made of mobile dunes. Overlapping of SS-IV3 and SS-IV2; SS-V2
1038 and SS-V1; SS-Vi and SS-IV3, SS-VII and SS-V2, and SS-VII1 and SS-V3. b) SS-VII1 parabolic dunes over
1039 SS-IV1 transverse dunes (barjanoids), SS-VII1 over two of them. c) SS-VI2 parabolic dunes under SVII
1040 transverse dunes. d) SS-VI3 parabolic dunes on cliff between Torre del Loro and Mazagon. e) SS-VI4

and SSVI-5 dunes over the spit bar and under SS-VII2 and SS-VII1. Origin of images: a: 2009 PNOA orthophoto, oblique view, and 1956 aerial photo, in plan; b and c: 1956 aerial photo; d: 2009 PNOA orthophoto; e) Plan views of 2009 orthophoto PNOA. Spatial resolution MDT 5x5 m.

Sheet 3. Overlapping of dune subsystems. a1. Oblique view of the overlapping of SS-VI1, SS-Vi1, SS-VII1 and SSVII-2. a2) Overlapping between subsystems of SV, similarity of SS-V1 forms (worms), with SS-IV1 (see a1); b) Complex system; overlapping of dunes from SS-C3, SS-C2 and SS-C1. Dunes in the oldest SS are parabolic but are imbricated transverse in the others two; c) Complex system, overlapping of dunes, SC-1 is under Asperillo Dunes system SC-2, SC-3, SC-5 and SC-5 and over stable dunes from SS-IV4 and SS-II3. Blowout (yellow circles) indicate erosion, d) Shadow dunes from Complex System over SC-1 parabolic dunes and SS-III4; e) S-VII dunes over Complex System. In this case S-VII cover the internal zone and deposited over stable systems. Origin of images: a: oblique view 1956 aerial photo; b: overlapping of 2009 PNOA orthophoto and 1956 aerial photo; c, d and e: oblique view of 1956 aerial photo from MDT. Spatial resolution MDT 5x5 m.

Table 1

Click here to access/download;Table;Goy et al. Table 1.doc

Lab. samples	Field samples	Grain size (µm)	Radionuclide concentrations				Cosmic dose rate (Gy Ka^{-1})	Equivalent dose (Gy)	Annual dose (µGy y^{-1})	**Age (yrBP)**
			U (ppm)	Th (ppm)	K_2O (%)	H_2O (%)				
1 -MAD-5445SDA	D08-1	2-10	0.01	8.06	0.65	0.50	0.91	6.19±0.25	2.17	2852±164
2 - MAD-5437SDA	D08-2	2-10	0.01	8.02	0.01	0.28	0.88	9.82±0.07	1.38	7115±421
3 - MAD-5446SDA	D08-3	2-10	1.22	1.28	0.18	0.51	0.86	14.95±0.21	1.48	10101±564
4 - MAD-5477SDA	D08-4	2-10	0.88	1.42	0.60	0.27	0.86	7.24±0.17	1.58	4582±249
5 - MAD-5447SDA	D08-5	2-10	0.15	3.18	0.01	0.46	0.86	9.71±0.05	1.21	8024±457
6 - MAD-5441SDA	D08-6	2-10	0.01	9.17	0.76	0.62	0.86	3.26±0.17	2.71	1202±71
7 - MAD-5464BIN	D08-7	2-10	0.01	9.26	0.31	0.74	0.77	6.52±0.18	1.70	3835±204
8 - MAD-5442BIN	D08-8	2-10	0.01	6.66	0.01	1.70	0.80	5.70±0.02	1.35	4222±285
9 - MAD-5478SDA	D08-9	2-10	0.01	1.66	0.10	0.69	0.68	1.44±0.01	0.92	1565±127
10 - MAD-5655SDA	D09-10	2-10	0.01	7.75	0.01	0.51	0.77	5.23±0.56	1.08	4842±575
11 - MAD-5656SDA	D09-11	2-10	0.47	3.06	0.01	0.15	0.77	5.79±0.47	0.99	5848±595
12 - MAD-5657SDA	D09-12	2-10	0.01	9.99	0.01	2.74	0.8	8.36±0.39	1.20	6966±559
14 - MAD-5658SDA	D09-14	2-10	1.25	2.69	0.01	3.85	0.85	71.03±2.72	1.59	44672±2813
15 - MAD-5660SDA	D09-15	2-10	1.68	0.01	0.37	3.01	0.9	16.75±1.07	1.77	9463±678
16 - MAD-5659SDA	D09-16	2-10	0.01	8.19	0.01	2.48	0.86	7.13±1.04	1.31	5442±768
17 - MAD-5661SDA	D09-17	2-10	0.77	0.01	0.01	6.45	0.78	6.11±0.57	0.92	6641±804
18 - MAD-5663SDA	D09-18	2-10	0.58	3.20	0.18	4.43	0.04	34.38±1.69	0.42	81857±6086
19 - MAD-5664SDA	D09-19	2-10	0.01	9.78	0.04	2.3	0.49	27.80±2.35	0.91	30549±3023
20 - MAD-5665SDA	D09-20	2-10	0.87	4.30	0.09	2.3	0.68	14.74±1.08	1.12	13160±1128
21 - MAD-5666SDA	D09-21	2-10	0.01	16.54	0.09	1.55	0.9	16.12±0.60	1.63	9889±688
22 - MAD-5662SDA	D09-22	2-10	0.17	4.66	0.01	1.99	0.77	8.44±0.48	0.99	8525±715
23 – MAD-5447SDA	DCHT 1.1	-	1.88	1.34	0.95	2.04	-	1.35	2.04	661±73
24 – MAD-5790SDA	DCHT 1.2	-	4.70	5.21	0.01	0.51	-	5.00	4.47	1118±150
25 - MAD-6342BIN	SQM 4	-	0.59	1.02	0.08	4.91	-	4.21	1.15	3660±266
26 - MAD-6343BIN	SQM 5	-	0.71	1.21	0.48	2.99	-	5.51	1.46	3773±240
27 - MAD-6384BIN	ATA 1	-	1.03	1.60	0.02	1.62	-	2.23	1.63	1368±108
28 - MAD-6387BIN	ATA 3	-	0.60	1.01	0.10	1.54	-	1.57	1.30	1207±106
29 - MAD-6146SDA	BME 4	-	1.33	1.18	1.33	2.95	-	13.99	1.30	10761±817

Figure1

Click here to access/download;Figure (Color);Goy et al. Fig1.jpg

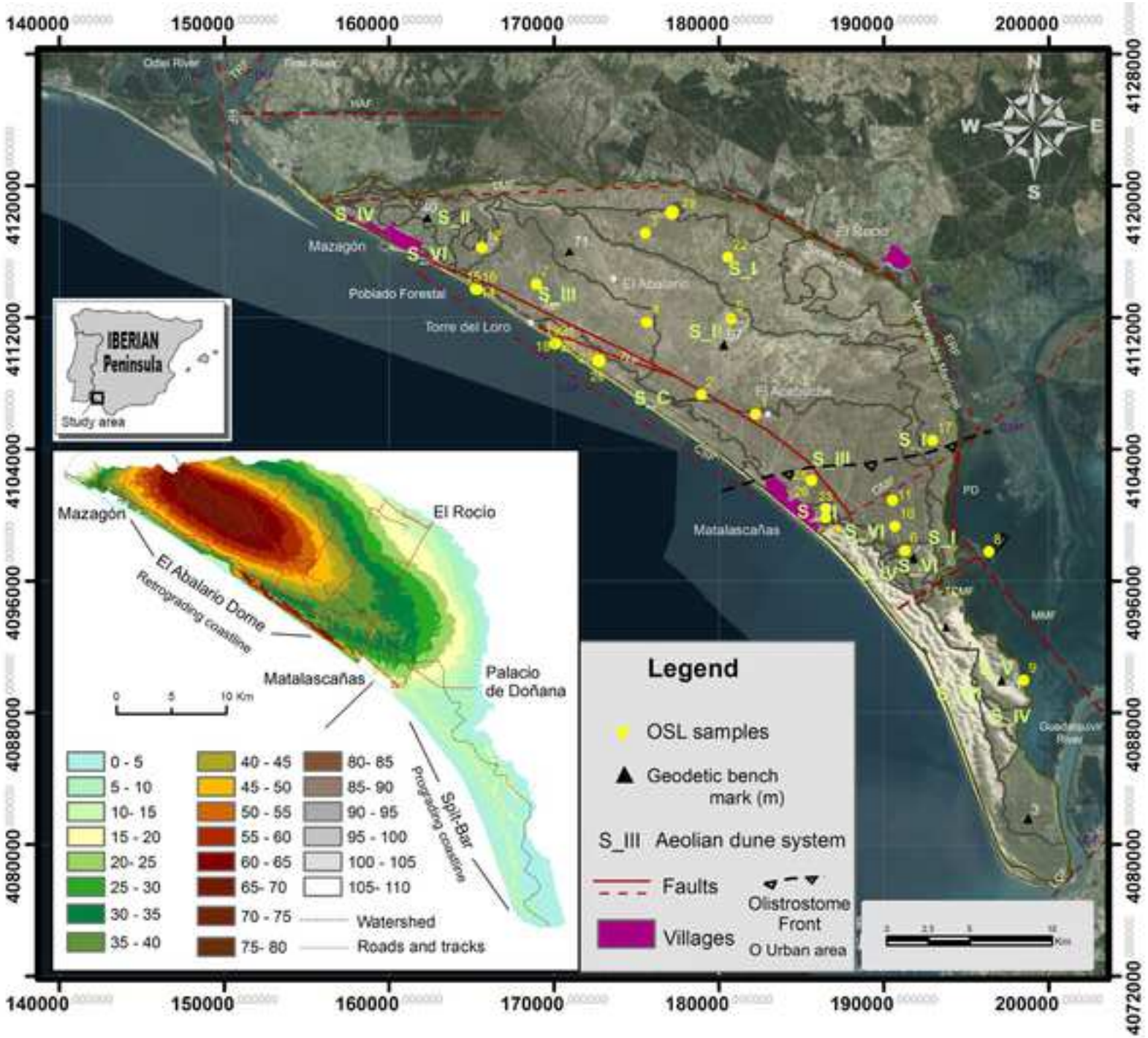

Figure 2

Click here to access/download;Figure (Color);Goy et al. Fig 2.jpg

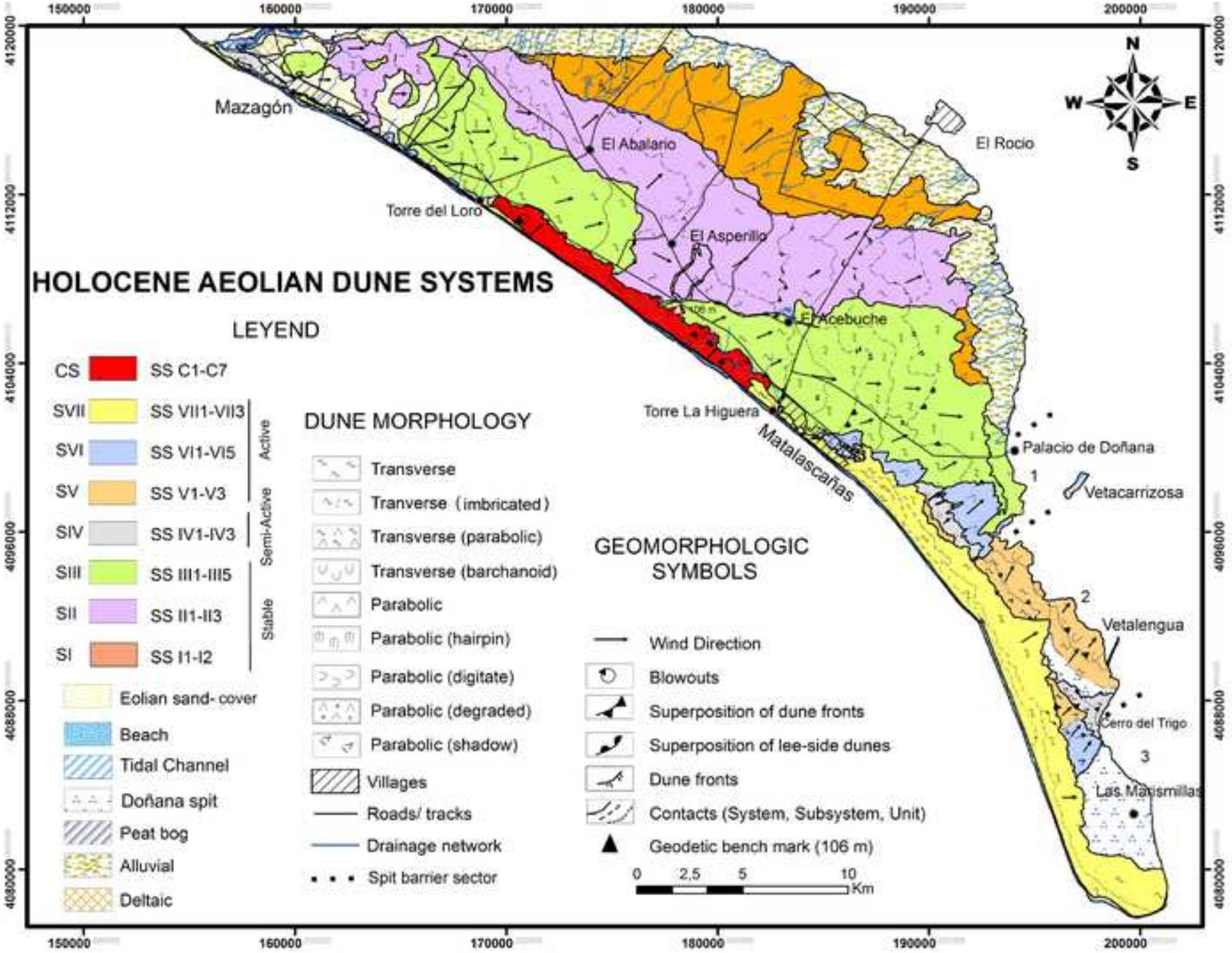

Figure 3

Click here to access/download;Figure (Color);Goy et al. Fig 3.jpg

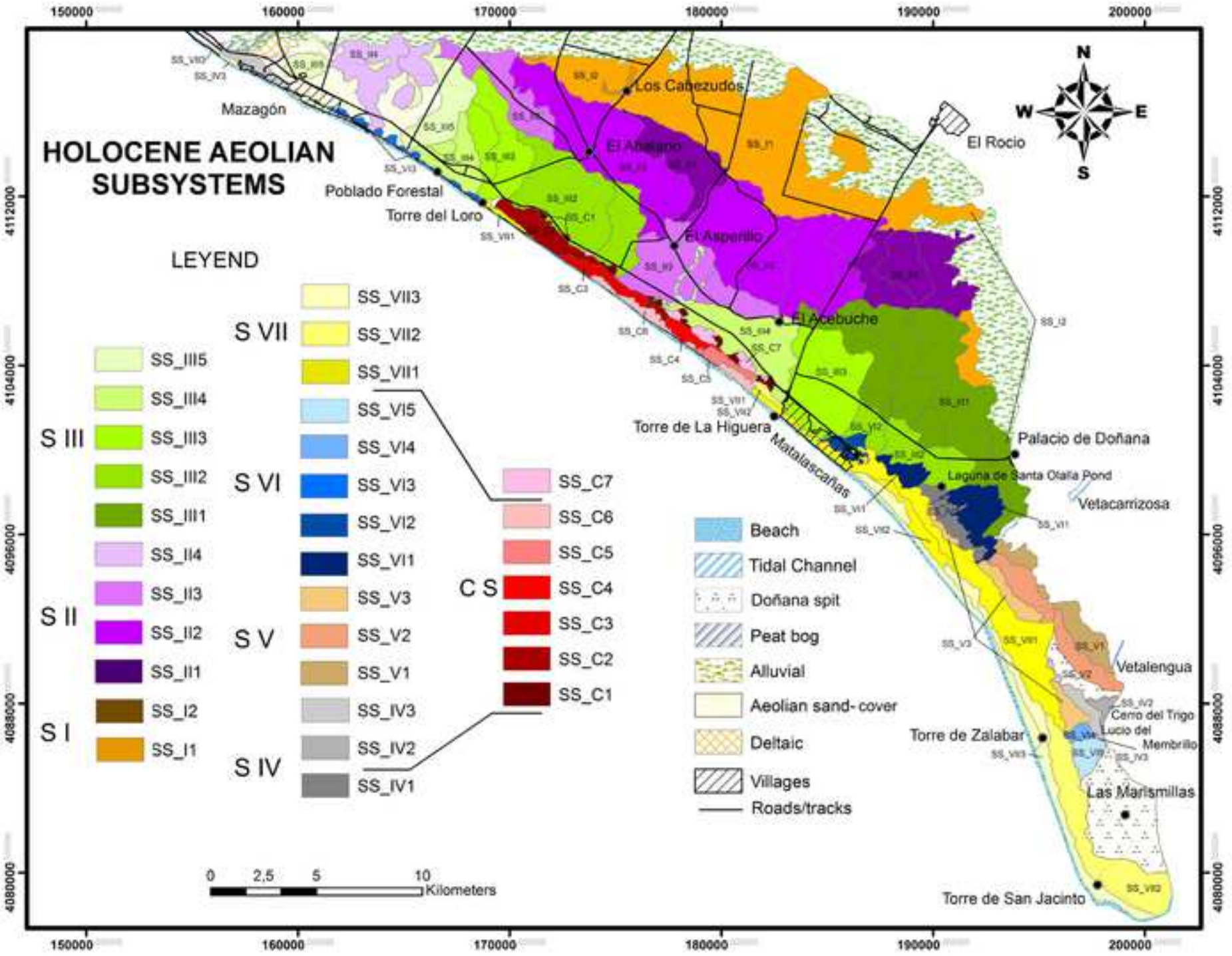

Figure 4

Click here to access/download;Figure (Color);Goy et al. Fig 4.jpg

Figure 5

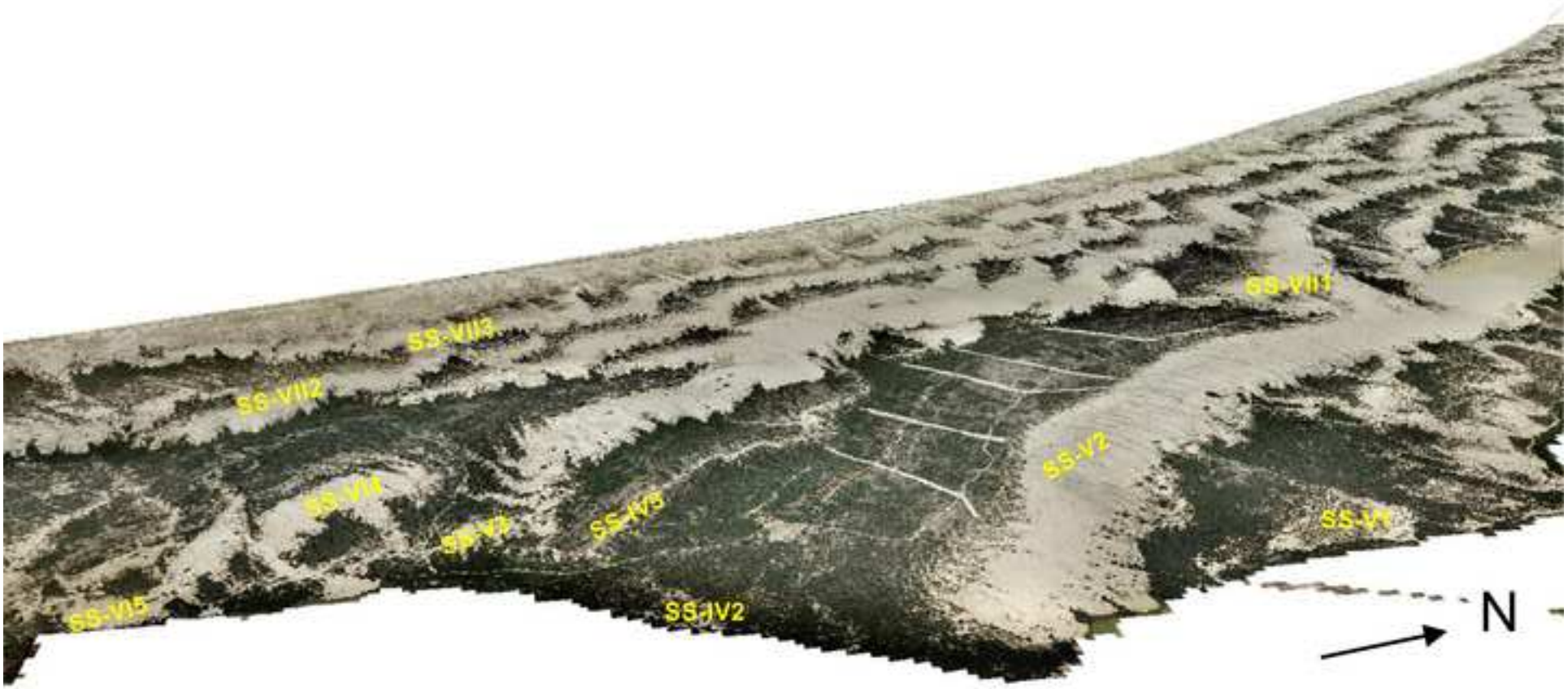

Figure 6

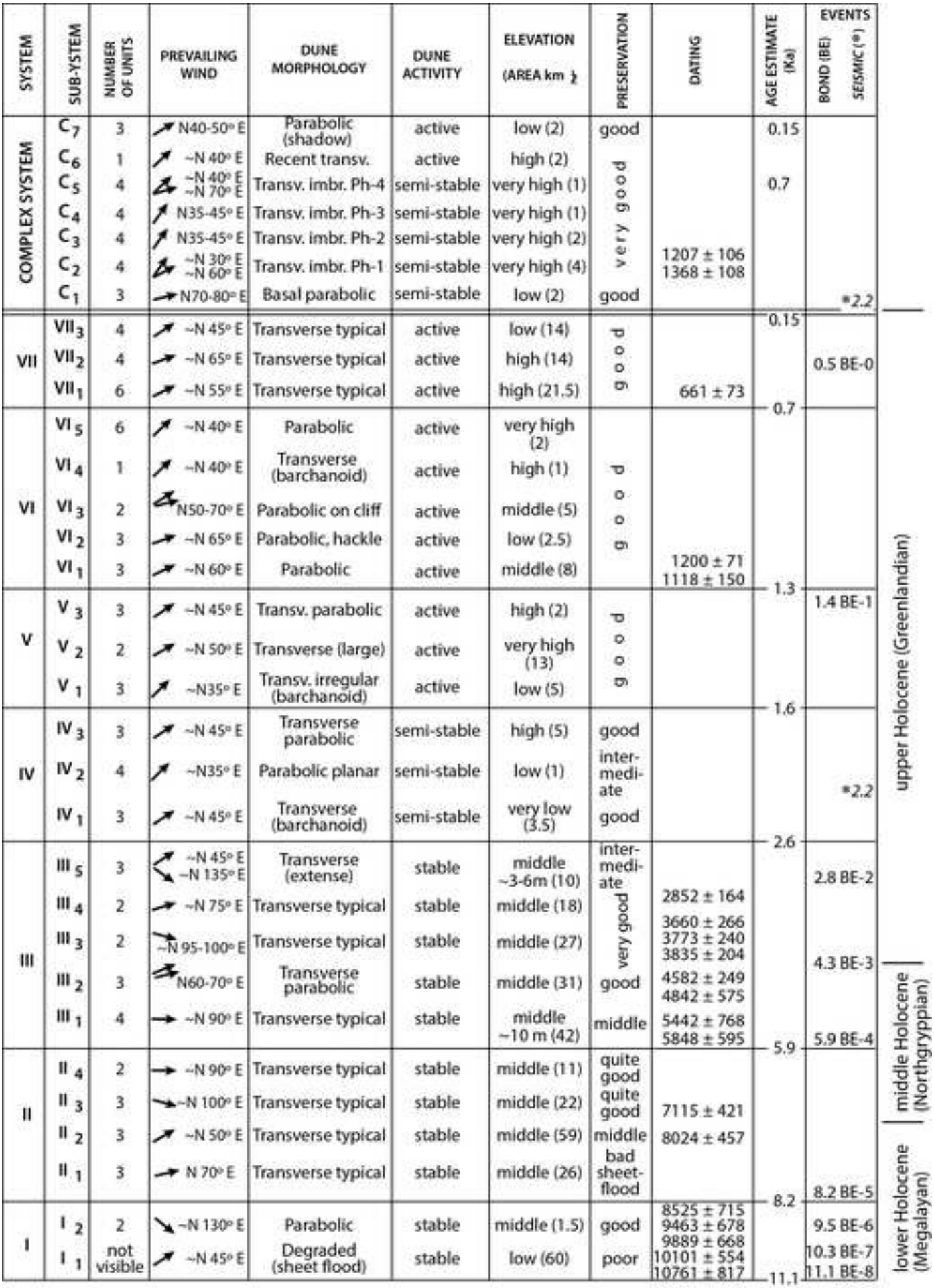

SYSTEM	SUB-YSTEM	NUMBER OF UNITS	PREVAILING WIND	DUNE MORPHOLOGY	DUNE ACTIVITY	ELEVATION (AREA km ²)	PRESERVATION	DATING	AGE ESTIMATE (Ka)	EVENTS BOND (BE)	EVENTS SEISMIC (*)	
COMPLEX SYSTEM	C_7	3	N40-50° E	Parabolic (shadow)	active	low (2)	good		0.15			
	C_6	1	~N 40° E	Recent transv.	active	high (2)	very good					
	C_5	4	~N 40° E ~N 70° E	Transv. imbr. Ph-4	semi-stable	very high (1)			0.7			
	C_4	4	N35-45° E	Transv. imbr. Ph-3	semi-stable	very high (1)						
	C_3	4	N35-45° E	Transv. imbr. Ph-2	semi-stable	very high (2)						
	C_2	4	~N 30° E ~N 60° E	Transv. imbr. Ph-1	semi-stable	very high (4)		1207 ± 106 1368 ± 108				
	C_1	3	N70-80° E	Basal parabolic	semi-stable	low (2)	good				*2.2	
VII	VII_3	4	~N 45° E	Transverse typical	active	low (14)	good		0.15			upper Holocene (Greenlandian)
	VII_2	4	~N 65° E	Transverse typical	active	high (14)				0.5 BE-0		
	VII_1	6	~N 55° E	Transverse typical	active	high (21.5)		661 ± 73	0.7			
VI	VI_5	6	~N 40° E	Parabolic	active	very high (2)	good					
	VI_4	1	~N 40° E	Transverse (barchanoid)	active	high (1)						
	VI_3	2	N50-70° E	Parabolic on cliff	active	middle (5)						
	VI_2	3	~N 65° E	Parabolic, hackle	active	low (2.5)						
	VI_1	3	~N 60° E	Parabolic	active	middle (8)		1200 ± 71 1118 ± 150	1.3			
V	V_3	3	~N 45° E	Transv. parabolic	active	high (2)	good			1.4 BE-1		
	V_2	2	~N 50° E	Transverse (large)	active	very high (13)						
	V_1	3	~N35° E	Transv. irregular (barchanoid)	active	low (5)			1.6			
IV	IV_3	3	~N 45° E	Transverse parabolic	semi-stable	high (5)	good					
	IV_2	4	~N35° E	Parabolic planar	semi-stable	low (1)	inter-medi-ate				*2.2	
	IV_1	3	~N 45° E	Transverse (barchanoid)	semi-stable	very low (3.5)	good		2.6			
III	III_5	3	~N 45° E ~N 135° E	Transverse (extense)	stable	middle ~3-6m (10)	inter-medi-ate			2.8 BE-2		middle Holocene (Northgryppian)
	III_4	2	~N 75° E	Transverse typical	stable	middle (18)	very good	2852 ± 164				
	III_3	2	~N 95-100° E	Transverse typical	stable	middle (27)		3660 ± 266 3773 ± 240 3835 ± 204				
	III_2	3	N60-70° E	Transverse parabolic	stable	middle (31)	good	4582 ± 249 4842 ± 575		4.3 BE-3		
	III_1	4	~N 90° E	Transverse typical	stable	middle ~10 m (42)	middle	5442 ± 768 5848 ± 595	5.9	5.9 BE-4		
II	II_4	2	~N 90° E	Transverse typical	stable	middle (11)	quite good					
	II_3	3	~N 100° E	Transverse typical	stable	middle (22)	quite good	7115 ± 421				
	II_2	3	~N 50° E	Transverse typical	stable	middle (59)	middle	8024 ± 457				
	II_1	3	N 70° E	Transverse typical	stable	middle (26)	bad sheet-flood		8.2	8.2 BE-5		lower Holocene (Megalayan)
I	I_2	2	~N 130° E	Parabolic	stable	middle (1.5)	good	8525 ± 715 9463 ± 678		9.5 BE-6		
	I_1	not visible	~N 45° E	Degraded (sheet flood)	stable	low (60)	poor	9889 ± 668 10101 ± 554 10761 ± 817	11.1	10.3 BE-7 11.1 BE-8		

Figure 7

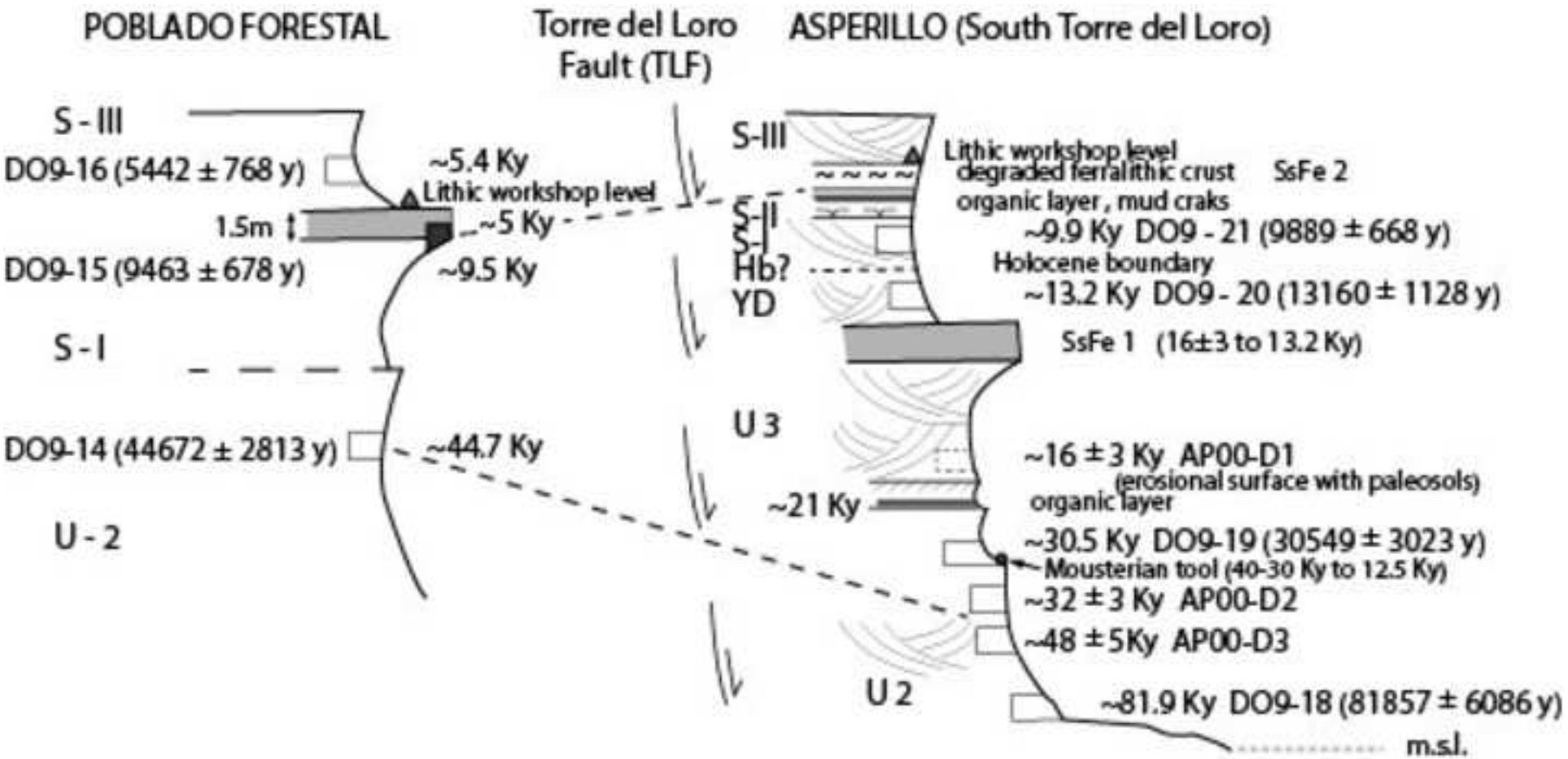

Figure 8

Click here to access/download;Figure (Color);Goy et al. Fig 8.jpg

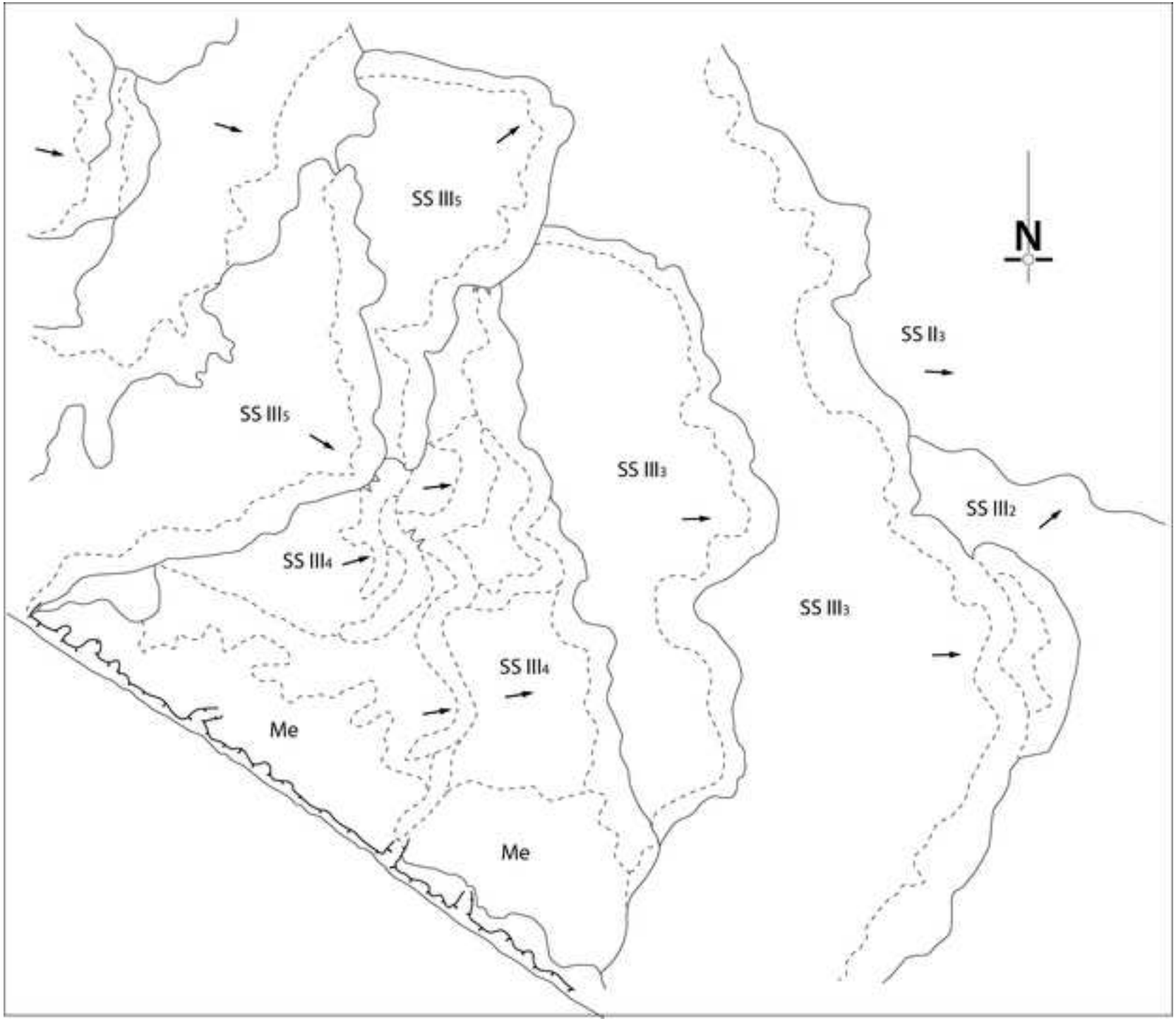

Figure 9

Click here to access/download;Figure (Color);Goy et al. Fig 9.tif

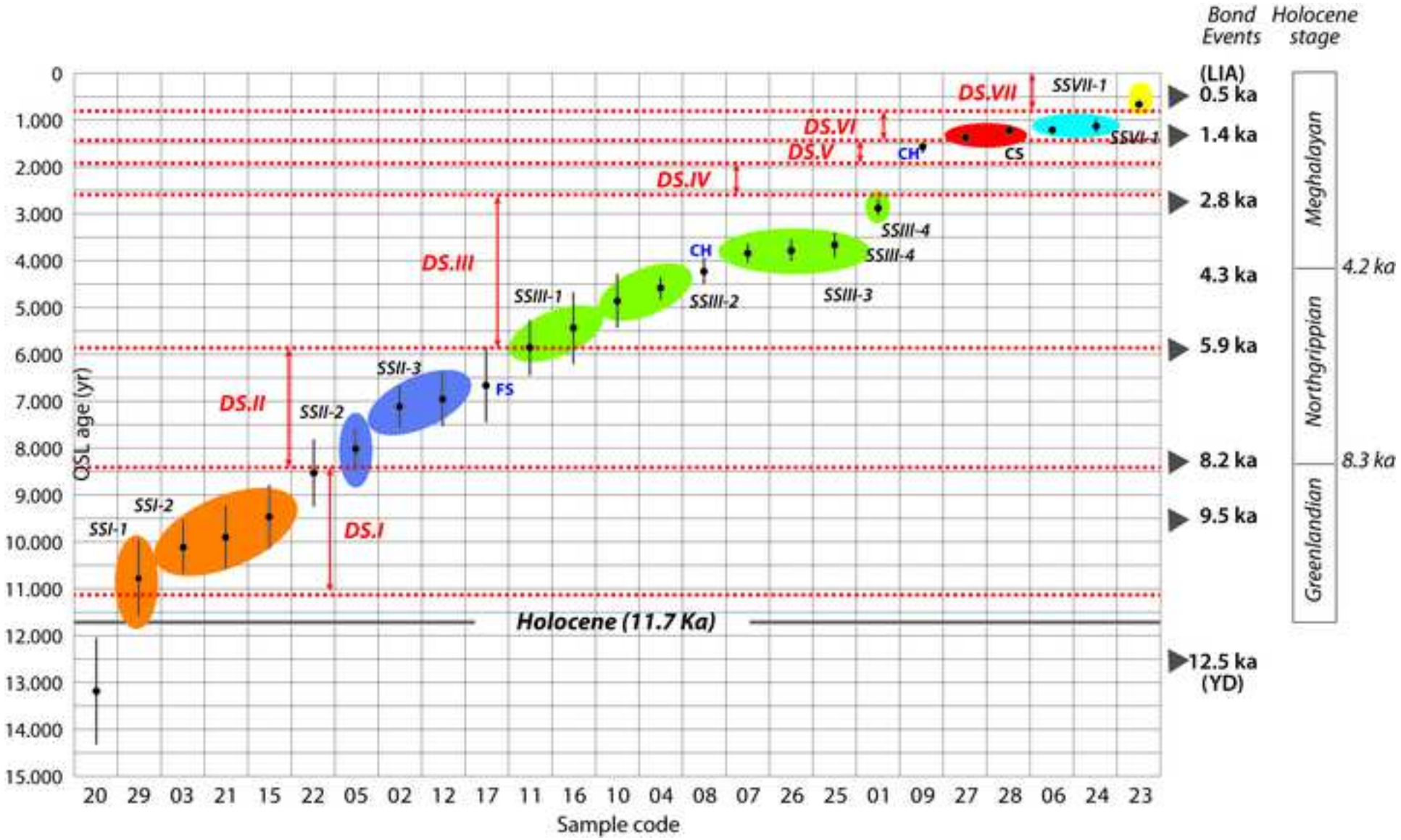

Figure 10

Click here to access/download;Figure (Color);Goy et al. Fig 10.jpg

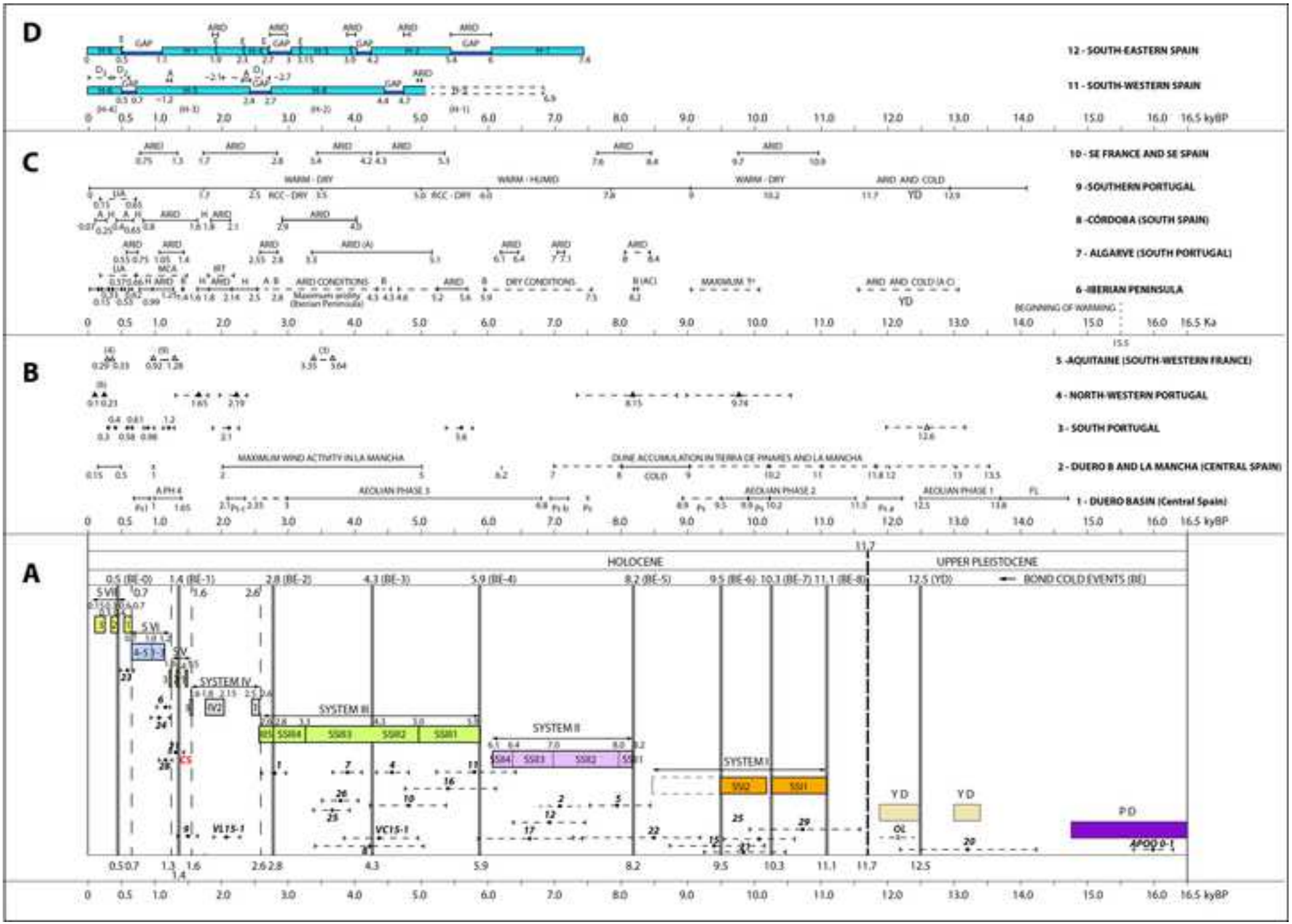

SHEET 1

Stabilized Dunes

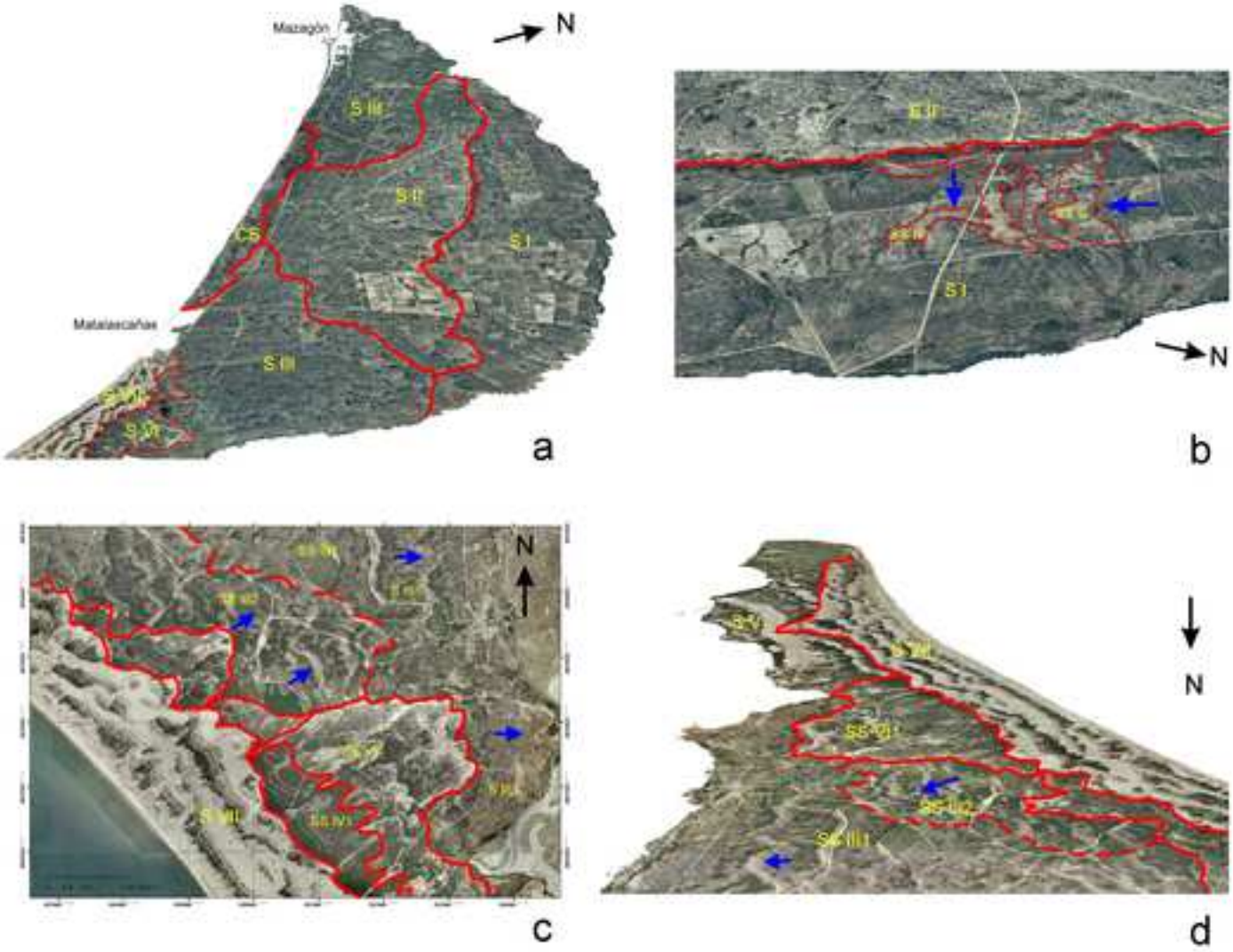

Semi-active Dunes

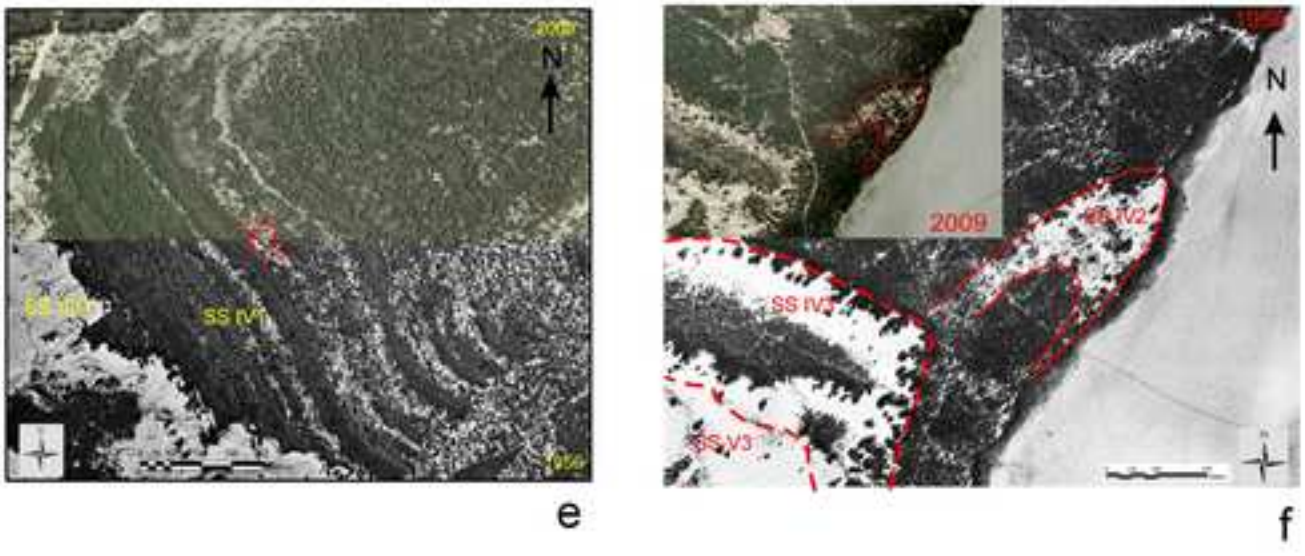

SHEET 2

Active Dunes

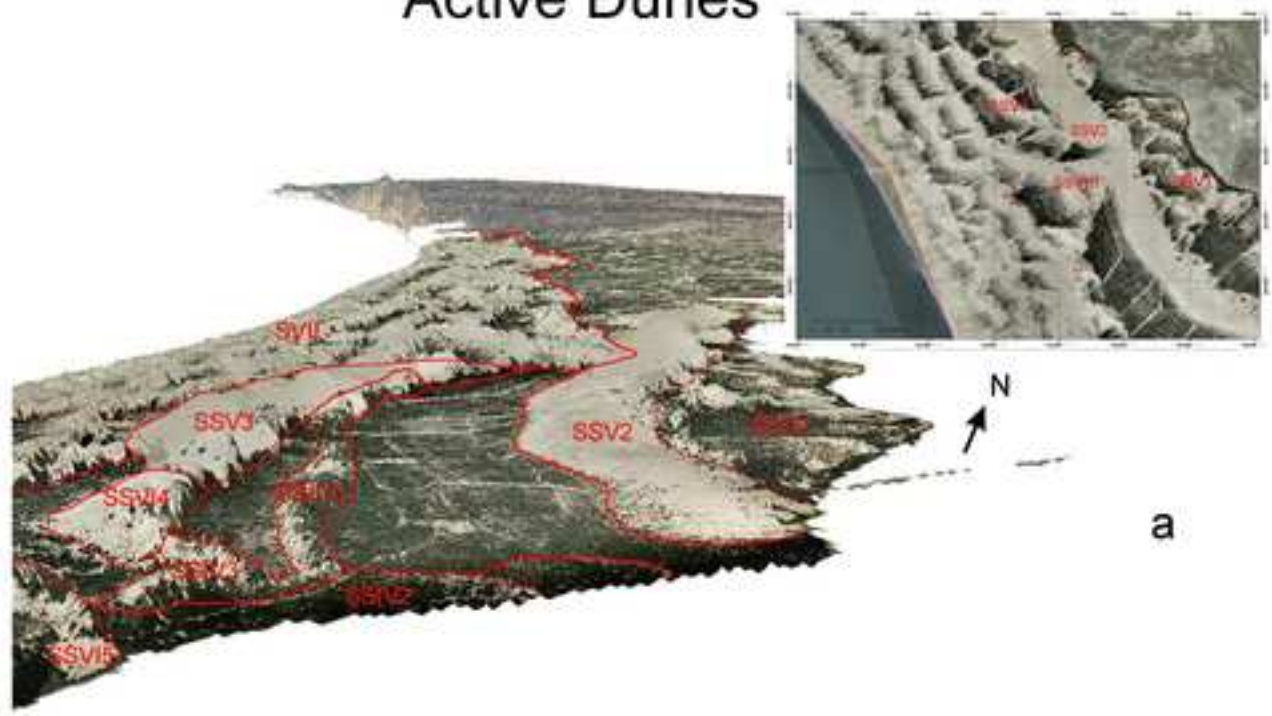

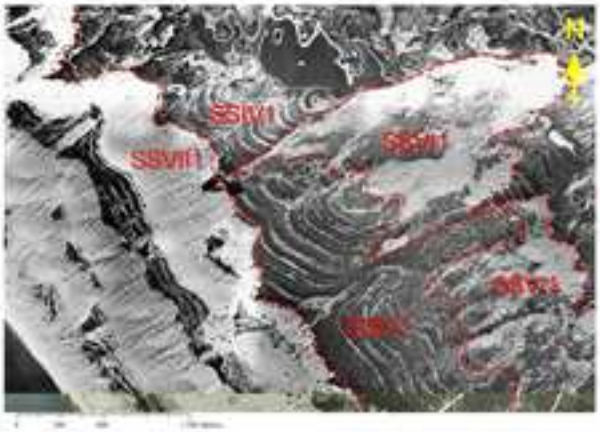

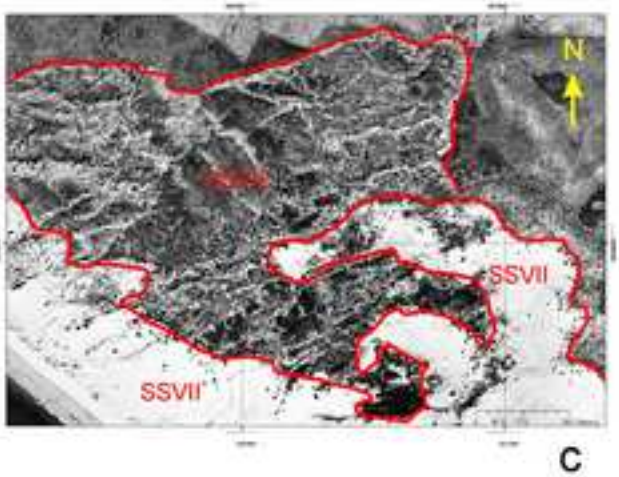

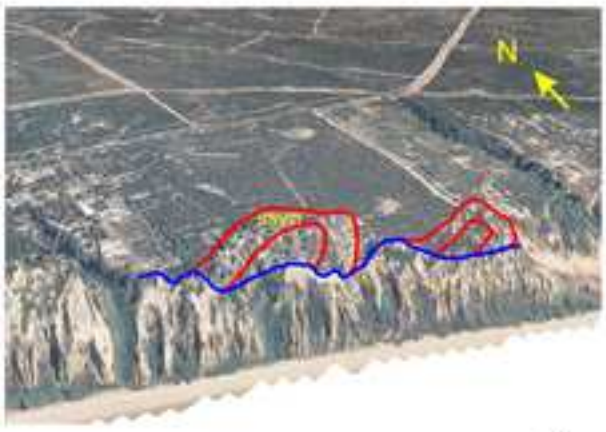

SHEET 3
Active System and Complex System